



Room 14-0551  
77 Massachusetts Avenue  
Cambridge, MA 02139  
Ph: 617.253.5668 Fax: 617.253.1690  
Email: docs@mit.edu  
<http://libraries.mit.edu/docs>

## **DISCLAIMER OF QUALITY**

Due to the condition of the original material, there are unavoidable flaws in this reproduction. We have made every effort possible to provide you with the best copy available. If you are dissatisfied with this product and find it unusable, please contact Document Services as soon as possible.

Thank you.

**Due to the poor quality of the original document, there is some spotting or background shading in this document.**

UNSTEADY THREE-DIMENSIONAL FLOW IN A COMPRESSOR CASCADE  
WITH INLET FLOW DISTORTIONS

by

SAEED FAROKHI

B.S. University of Illinois  
(1975)

S.M. Massachusetts Institute of Technology  
(1976)

SUBMITTED IN PARTIAL FULFILLMENT  
OF THE REQUIREMENTS FOR THE  
DEGREE OF

DOCTOR OF PHILOSOPHY

at the

MASSACHUSETTS INSTITUTE OF TECHNOLOGY

FEBRUARY 1980

© Massachusetts Institute of Technology, 1979

Signature of Author [Signature]  
Department of Aeronautics & Astronautics  
October 3, 1979

Certified by [Signature] Thesis Supervisor

Certified by [Signature] Thesis Supervisor

Certified by [Signature] Thesis Supervisor

Accepted by [Signature] Chairman, Departmental Graduate Committee

Archives  
MASSACHUSETTS INSTITUTE  
OF TECHNOLOGY

SEP 25 1981

LIBRARIES ✓

UNSTEADY THREE-DIMENSIONAL FLOW IN A COMPRESSOR CASCADE  
WITH INLET FLOW DISTORTIONS

by

SAEED FAROKHI

Submitted to the Department of Aeronautics and Astronautics in  
October 1979 in partial fulfillment of the requirements of the Degree  
of Doctor of Philosophy.

ABSTRACT

An unsteady three-dimensional theory is developed to calculate the response of a moving blade row to general inlet flow distortions. The theory is applied to the flow of perfect fluids in a rectilinear cascade, the blades of which are "flat-plates" and are set at the mean-flow incidence angle of zero. For the purpose of linearization, the amplitude of the disturbance velocity field is assumed to be small in comparison to the mean flow speed. Without any loss of generality, the fundamental harmonics of the flow non-uniformities in both pitch and spanwise directions are considered. It is demonstrated that the streamwise component of vorticity in the wakes is responsible for the three-dimensional response of the blades in the presence of the three-dimensional disturbances. The inviscid wakes described above are concentrated in "thin"-sheets, emanating from, and aligned in the direction of, the blades' trailing-edges and are assumed to be convected with the mean flow speed, as part of the linearization procedure. The governing equations are solved via a perturbation analysis. The Clebsch-Hawthorne formulation is utilized to represent the rotational perturbations throughout the flow. The advantages of the Clebsch-Hawthorne representation, instead of the "usual" vector potential approach, are discussed in a separate appendix while the physical arguments, based on the use of the Clebsch-Hawthorne formalism are developed in the analysis of the flow (Section 3.1.2).

Numerical examples are worked out for the unsteady lift coefficient in the limit of two-dimensional flow and the results of the present theory are compared with Whitehead's inlet distortion analysis. Both the magnitude and the phase angle relationship between the present analysis and the Whiteheads' are generally in good agreement. A few examples of low solidity ( $1/2$  and  $1/3$ ) cascades are compared with the isolated airfoil theory developed by von Kármán and Sears. For the reduced frequency range between 1.0 and 2.0, the response of the low-solidity cascades approaches the Sears' results. In the lower range of the reduced frequencies, Sears predicts the isolated-airfoil lift coefficient while the present theory approaches the cascade lift coefficient in quasi-steady flows. The effect of the blade height on the cascade response is studied and a maximum of 15% variation in the magnitude of the force and an average of 25% in the phase

angle are observed between aspect ratios of 3 and  $1/3$ . The magnitude of the response is somewhat damped in the presence of "stronger" three-dimensional flow effects (i.e. the stronger the strength of the trailing streamwise vorticity the weaker the unsteady response of the airfoil). On the other hand, the phase angle of the unsteady component of lift is significantly different, as a result of three-dimensional effects, in the case of aspect ratio of  $1/3$  as compared with  $AR = 3$ .

Thesis Supervisor: James E. McCune

Title: Professor of Aeronautics and  
Astronautics

Thesis Committee

Sir William R. Hawthorne, Professor and Senior Lecturer, Department  
of Aeronautics and Astronautics

Jack L. Kerrebrock, Professor and Head, Department of Aeronautics  
and Astronautics

Steven A. Orszag, Professor of Mathematics

Edward M. Greitzer, Associate Professor of Aeronautics and  
Astronautics

ACKNOWLEDGEMENT

Perhaps the most joyful part of a thesis is acknowledging the help one received from the members of the faculty, his friends, and family. Professor James E. McCune provided the Research Assistantship throughout the duration of my doctoral work at MIT, and most importantly through patience and understanding he implanted some of his brilliant ideas in my mind, for this and the warmth he and his family offered so generously to my family and I, I am most indebted.

Professor Sir William Hawthorne's contribution to this thesis is immeasurable. The analysis in this thesis is a generalization of what Professor Hawthorne proposed, developed, and formulated in an earlier and continuing contribution to unsteady internal fluid mechanics. It was a great honor and joy to be associated with him.

The author benefited from fruitful discussions with other members of his doctoral committee, Professor Jack L. Kerrebrock, Professor Steven A. Orszag, and Professor Edward M. Greitzer, to whom many thanks and appreciations are due.

The many friends and colleagues in the Gas Turbine and Plasma Dynamics Laboratory who provided a conducive atmosphere for working, in particular Dr. Arun Sehra, who helped me start on the CMS and Dr. Choon S. Tan who provided many hours of discussion, to both of them and all of my friends I am grateful. Holly Rathbun accepted the task of typing the manuscript and has performed this work fast and accurately;

Finally, I would like to express my sincere appreciation and thanks to my wife, Mariam, for patience, understanding, and support which was

crucial to the completion of this thesis. Kamelia and Parisa both brought happiness and strengthened the sense of direction in the course of this work.

This thesis is dedicated to my father, Mr. Nasrollah Farokhi, whose dedication to his family through support, encouragement, and love inspired me to pursue a higher education. My family and I owe him all our accomplishments.

This work was supported by AFOSR Contract No. F49620-78-C-0084.

TABLE OF CONTENTS

<u>Chapter No.</u>		<u>Page No.</u>
1	INTRODUCTION	7
2	REVIEW OF LITERATURE	13
3	FLOW ANALYSIS	22
4	EVALUATION OF THE UNSTEADY LIFT	74
5	RESULTS, CONCLUSIONS, AND SUGGESTIONS FOR FUTURE WORK	78
<u>Appendicies</u>		
A	VECTOR IDENTITIES APPLIED TO EQUATION OF MOTION	86
B	ON THE CLEBSCH-HAWTHORNE PARAMETERS AND THE DEGREE OF ARBITRARINESS	89
C	RELATION BETWEEN THE STREAMWISE VORTICITY AND THE SPANWISE DISTRIBUTION OF $\gamma_{\text{BOUND}}$ IN UNSTEADY FLOWS	92
<u>Figures</u>		96
References		111

## CHAPTER I

INTRODUCTION

It is generally recognized by the designers in the field of turbomachinery that the fluid flow phenomena, in such devices, are inherently unsteady. However, the approach to the design and development of turbomachines has always relied heavily on both the use of extensive empirical correlations and the employment of quasi-steady analysis in order to gain some insight to the features, peculiar to the fully unsteady flows.

Some basic problems associated with the unsteady flows, in turbomachines are in the areas of the forced and the self excited vibrations of the compressor blades, which leads to structural failure if left unchecked. A better understanding of those features, of unsteady flow, which contribute to the self-excited instabilities, i.e. flutter, would enable the designer to determine the compressor flutter boundaries more exactly and consequently, could then modify the blade structural requirements (probably relaxing them) to meet the safe operational limit within the stable regime, on the compressor map. Another area of major concern to industrial societies, associated with the unsteady flows, is the problem of noise radiation from operating jet engines. The wakes of the upstream blades, as regions of retarded flow, present the blades with a larger incidence angle than the mean-flow. Thus, the presence of the flow non-uniformities, of the type caused by the stagnation pressure distortions, in the upstream region of any blade row, as in wakes, creates a fluctuating component of the airfoil lift. It is this component of blade force (i.e. fluctuating in time) which acousticians model by pressure dipoles and calculate the radiated sound field from them. The limitations set for the allowable noise radiation



from the jet engines, caused primarily by the rotor-stator interactions in compressors, at present are met by such "fixes" as acoustic liners and other absorbers which significantly increase the weight and the size of the engines, and thus lead to an increase of the fuel consumption rate. Thus, it became clear that the levels of noise radiation can not be effectively reduced, without the penalty of weight and size, until the amplitude and phase of the unsteady lift, in a blade row, as a function of geometrical, i.e. solidity, aspect ratio and stagger, and physical parameters, i.e. reduced-frequency and intra-blade phase angle, are known to the compressor designer, who would then attempt to reduce the radiated noise levels by minimizing the component of fluctuating lift.

The area concerning the impact of the unsteady wakes on the compressor stage efficiency, is somewhat ambiguous. Theoretically the kinetic energy loss in the wake of a two-dimensional non-stationary airfoil in transverse gusts is calculated to be about 1%, by Hawthorne<sup>38</sup> and slightly less by von Kármán and Sears<sup>5</sup>. Based on their results, one may conclude that unsteadiness causes a drop in efficiency. However, a series of experiments were performed and the results of which were reported by Mikolajczak<sup>45</sup> which showed a gain in the adiabatic efficiency with the reduction of the axial distance between succeeding blade rows, which has the effect of strengthening the unsteady wakes, and seems to contradict the above mentioned findings. Therefore the question of efficiency in regard to unsteady effects, inherent in turbomachines, needs to be examined in detail, and with caution. It needs to be stressed, however, that even with "favorable" results reported by Mikolajczak, he has point out,<sup>45</sup> that significant progress in improving the performance and reliability of turbomachines

(in addition to the reducing the development cost), can be made through understanding of the unsteady flows and application of this knowledge to design.

Due to nonlinearity in the governing equations, (analytical) treatment of unsteady flow problems, in practical machines, is beyond the present state of our mathematical capabilities. To simplify the task of analytical development the equations of motion are linearized, via the small-perturbation assumption, i.e. the perturbations produced by the blades in the course of their interactions with non-uniform flow conditions are assumed to be small as compared with the mean (i.e. time-averaged)-flow quantities. This type of idealization inevitably limits the practicality of the problems under consideration. Some common assumptions, in this regard, are two-dimensionality of the flow, inviscidness of the fluid, and small incidence angles (to the blades), which none are satisfied in a practical, present-day, turbomachine. The aircraft industry demand for less weight and compact size, for the jet engines, has decreased the number of compression stages, as a result of which, the load or the pressure ratio per stage has increased tremendously. These high-performance compressors produce bigger compression ratios by essentially higher wheel speeds, larger overall turning angles, and an increase in the incidence angle to the blades. In addition to the above-mentioned performance criteria (which are desirable), some inevitable sources of three-dimensionality are also inherent with those criteria which may affect the performance and reliability of such devices, by a considerable amount. The vortex filaments in the casing boundary layers stretch around the blade-channel-bend and produce a component of streamwise vorticity,

the so-called secondary vorticity, which is responsible for inducing a secondary flow, in the direction of normal to the primary flow direction. There are other sources of three-dimensional flows induced by viscous effects, namely scraping-vortex, from the blade-tip-casing boundary layer interaction, separation of boundary layers caused by adverse pressure gradients or interactions with impinging shock, etc. The inviscid source of three-dimensional flows in turbomachines is clearly demonstrated by the works of McCune and Hawthorne<sup>34</sup>, Chen and McCune<sup>33</sup>, Cheng<sup>37</sup>, Tan<sup>35</sup>, and Adebayo<sup>36</sup> to be due to the presence of trailing vorticity in the wakes of non-uniformly loaded blades; the strength of the wake is proportional to the slope of the circulation variation along the blade span and the axis of the trailing (wake) vorticity is aligned in the streamwise direction.

In this Thesis, we intend to treat the problem of an isolated rotor interacting with general inlet flow non-uniformities, such as caused by total pressure distortions, in both pitch- and spanwise directions, from an analytical point of view. To this end, we have made some simplifying assumptions regarding the compressor geometry and the inlet flow distortions. Compressor cascades of very high hub-to-tip ratio are considered such as to allow the analytical development to be performed and formulated in a rectilinear geometry, as a limiting case of an annular configuration. This assumption, automatically, removes the problems associated with the effect of rotation on the disturbance modes within the compressor, as originally pointed out by Kerrebrock<sup>46</sup>. The blade-setting angle to receive the mean, i.e. time-averaged, flow at zero incidence constitutes our second geometrical assumption, while zero-camber, i.e. flat-blades

restriction provides the last of the geometrical constraints imposed on our cascade. The inlet flow is described by the sum of a uniform-parallel flow and a spatially varying flow of small amplitude (in comparison to the mean) in the pitch and spanwise directions, at large distances from the cascade. Small magnitude of the shear in the upstream region, constitutes our linearizing assumption. The pitchwise component of the inlet flow distortions creates a time-wise fluctuating vorticity to the induced at the position of the blades, while the spanwise shear, in the incoming stream, imposes a spanwise dependence upon the bound-vortices, over the blades. Finally the fluid is assumed to be perfect, i.e. inviscid and incompressible.

Within the limitations described above, we can utilize the linearized small perturbation theory, where in this problem, basically, centers around determination of an unsteady perturbation flow which meets the boundary conditions (i.e. walls and blade surfaces) and satisfy the kinematical as well as dynamical equations of motion. The description of zero-mean-incidence, uniformly determines the nature of the mean-flow throughout the compressor, as being steady-irrotational and exactly defined by the average of the flow at large distances upstream of the cascade. Our assumption of the inviscidness of the fluid in addition to the uniform mean flow "freezes" the vorticity vector to each fluid particle along their trajectories in the flow. Thus, the shear, described at the inlet, is convected towards the cascade, unaltered in magnitude and direction. Thence, the perturbations in the upstream flow are only the potential disturbances caused by the rotor blades plus the original shear introduced at the inlet\*.

---

\*This and other related points are discussed in Chapter 3 in more detail.

The method of splitting a vector field, to analyze its components, is utilized here, but instead of the "usual" vector potential approach, i.e.

$$\underline{V} = \nabla\phi + \underline{A} \quad (1.1)$$

where  $\phi$  describes a potential perturbation and  $\underline{A}$  is the vector potential, which in the classical description is defined as a solenoidal field, we represent the perturbation velocity field by the sum of a potential,  $\Phi$ , and a rotational disturbance,  $\sigma\nabla\tau$ , which was originally suggested by Clebsch<sup>47</sup> and later developed by Hawthorne<sup>41,48</sup>

$$\underline{V} = \nabla\Phi + \sigma\nabla\tau \quad (1.2)$$

The great advantages of the Clebsch-Hawthorne method are physically demonstrated in Section 3.1.3 and Appendix B. The three unknowns in (1.2), i.e.  $\Phi, \sigma$ , and  $\tau$ , are then determined from the continuity of incompressible fluids and the conservation of momentum equations. Finally the response of the blades to the inlet flow distortions is calculated, by the blade surface boundary condition, of no flow penetration into solid surfaces, which determines the strength of the bound-vorticity, i.e. the integral of which over the chord is proportional to the local force.

REVIEW OF LITERATURE

The era of the classical unsteady airfoil theory may be considered to have been started by the analysis of Wagner<sup>1</sup> in 1925. Wagner's analysis concerned the study of the growth of lift of an airfoil set in motion impulsively, in an incompressible fluid, interacting with the starting vortex shed-off its sharp trailing edge in reconciliation of the circulatory flow generated around the airfoil. Wagner's result is expressed in terms of a real function, the argument of which is  $s = Vt/b$  where  $t \equiv$  time,  $v \equiv$  fluid speed, and  $b \equiv$  half-chord length. (N.B. "s" can also be thought of as an inverse-reduced frequency, described later.)

$$L(t) = 2\pi b \rho V W K_1(s) \quad (2.1)$$

In (2.1),  $W \equiv V \sin \alpha$ ,  $\alpha \equiv$  angle of attack, and

$$K_1(s) \equiv \text{Wagner's function} \approx 1 - \frac{2}{4+s} \quad (2.2)$$

An analytic expression for  $K_1(s)$  is not yet known, however to within 2% of the entire range of  $s$ , (2.2) approximates the response function of an airfoil to an impulsive start. In 1929 Glauert<sup>2</sup> published a paper on the forces and moments acting on an oscillating airfoil, which was based primarily on Wagner's analysis. Theodorsen<sup>3</sup> laid the ground work for the general theory of aerodynamic instability and mechanism of flutter, now a famous theory, published originally in a NACA report in 1935. The method he employed drew heavily upon potential theory and, as its tool, conformal transformation. Theodorsen's analysis led to a very simple and compact expression for the unsteady lift and moment generated on an

oscillating airfoil at a small angle of attack with uniform velocity  $V$ , via a complex function,  $C(v)$ , known as Theodorsen's function, (or "circulation function") whose argument is  $v \equiv \frac{\omega b}{V}$ , the so-called "reduced frequency" which is the non-dimensional parameter governing the response of an aerodynamically lifting-surface to unsteadiness in flow conditions or blade vibrations. (N.B.  $v$  is the ratio of two time scales, namely, the fluid convection time over the chord length to the period of oscillatory disturbances.)

$$L(t) = 2\pi b \rho V W(t) C(v) \quad (2.3)$$

where  $W(t)$  denotes an arbitrary motion of an airfoil normal to its flight direction. Küssner<sup>4</sup> studied the response of an airfoil penetrating a region of vertical gust in 1936, however as pointed out by Von Kármán and Sears, Küssner had a (minor) mistake in his analysis due to the sign of  $e^{i\omega t}$  which forced the gust to travel from the trailing edge towards the leading edge of the airfoil, as opposed to the stated problem of an airfoil penetrating into a vertical gust. Another contribution by Küssner may be in his theorem that the line of action of the force, on an airfoil, passes through the quarter-chord point of the airfoil, even in unsteady regimes. Küssner's theorem was later proved to be correct by Von Kármán and Sears<sup>5</sup>, who developed a very systematic approach to the airfoil theory for non-uniform motion, in 1938. Their resulting expression for the lift and moment fluctuations of an airfoil in transverse gusts, of arbitrary shape (including the sharp-edged gust) was elegantly short and compact, involving a complex function, similar to that of Theodorsen's, later known as Sears' function,  $S(v)$

$$L(t) = 2\pi\rho bV W(t) S(v) \quad (2.4)$$

where  $b \equiv$  half-chord,  $W(t) \equiv W e^{i\omega t}$ , transverse-harmonic-gust speed.

The analyses described in the previous paragraph had (or shared) the limitation of two-dimensionality and incompressibility of the fluid. The effects of viscosity and the airfoil camber was also ignored. Their method of analysis relied heavily on the classical potential flow theory and the method of conformal transformation. Furthermore, in view of two-dimensionality of the problems studied, the Biot-Savart law of induction was readily utilized and (provided the "best" (i.e., most convenient) tool for calculation of the vortex-induced velocity field) thus the problem of bounding walls, which provides images for the vortices in the flow, was not encountered. However, the ground work was laid in this period for the application of non-stationary airfoil theory to the analysis of inherently\* unsteady flows in turbomachines.

\*R. C. Dean<sup>28</sup> showed the necessity of unsteady flows in turbomachines, for the transfer of energy ( $\rho(Dh_+ / Dt) = - \partial p / \partial t$ ) from the working blades to the fluid, however by choosing an "appropriate" coordinate system, e.g. in the case of an isolated rotor, operating in uniform flow conditions, in the coordinate fixed to the rotor, the flow is steady, or

$$D' h_+^+ / Dt = 0$$

where  $D' / Dt$  is the Eulerian derivative in relative (rotor-fixed) frame, and  $h_+^+$  is total enthalpy in relative coordinates, and since the flow is steady in the moving coordinates

$$\frac{D'}{Dt} = \frac{\partial}{\partial t} + \underline{W} \cdot \nabla' = \underline{W} \cdot \nabla'$$

or  $\underline{W} \cdot \nabla' h_+^+ = 0$ , which points to the familiar result that  $h_+^+$  is constant along the streamlines of the relative flow. But in the case of inherently unsteady flows, as in the mutual interference problem of neighboring blade rows or blade vibration, etc., the flow remains unsteady as viewed by all observers, moving or stationary.



Kemp and Sears utilized the theory by Kármán and Sears<sup>5</sup>, and Sears<sup>6</sup> in their study of aerodynamic interference between the blade rows in relative motion. Their first paper<sup>7</sup> in 1953 dealt with potential interactions of neighboring blade rows, one stationary and the other moving. The problem of the so-called mutual interference was of sufficient difficulty to exclude three-dimensionality and compressibility, camber and viscosity, at the time when Kemp and Sears undertook its study. The fluctuating lift force, derived by Kemp and Sears was thus expressible in an analytical form, very much similar to the Sears formula, except for the modification of the Sears function  $S(v)$  to  $S(v, \lambda)$  where  $\lambda \equiv k\omega b/\bar{V}$  and  $k \equiv$  characteristic decay parameter of disturbance and  $\bar{V} \equiv$  mean relative speed. However, in view of their use of single-airfoil theory results in cascades, they neglected the effect of the unsteady vortices in the redistribution of the vortices on neighboring blades, i.e., the so-called unsteady blade-to-blade effect was ignored. The second paper by Kemp and Sears<sup>8</sup> attempted in modelling and estimating the unsteady forces due to viscous wakes in turbomachines (1954). It assumed an inviscid-shear flow interacting with a moving blade row where wake-modelling of Silverstein, Katzoff, and Bullivant<sup>9</sup> was utilized in the description of the shear and its tie with the profile drag coefficient of the upstream blade row.

The blade vibration as another prominent source of unsteady flows was treated by Whitehead<sup>10,11,12</sup> extensively and prior to him by a host of investigators like Lane and Wang,<sup>13</sup> Lilley,<sup>14</sup> Sisto,<sup>15</sup> and Eichelbrenner.<sup>16</sup> Whitehead's method of analysis (similar to Lane and Wang's and Lilley's)

distributes vortices on the airfoils and the wakes, where the strength of the vortex sheet is linked to the unsteady behavior of the airfoils (i.e., "bound-vortices") according to the Kelvin's circulation theorem in inviscid flows, and then via Biot-Savart law the appropriate upwash induced by all vortices (to satisfy the blade surface boundary condition) leads to the calculation of the blade forces and moments, from the strength of the bound-vortex distribution. However, the response of the cascade, in Whitehead's analysis, is not expressible in a closed-form, analytical expression as in the Kemp and Sears analysis. This is basically due to the inclusion of unsteady blade-to-blade effect in Whitehead's analysis while Kemp and Sears neglected its contribution in their study. Whitehead's analysis as well as most others before him, shared the same limitations namely two-dimensionality and incompressibility of the fluid.

Horlock<sup>17</sup> shed light upon another aspect of the non-stationary airfoil theory, in his paper of 1968, where he derived the response of an airfoil, at an angle of attack with respect to the undisturbed flow, to chordwise velocity fluctuations. This effect was previously ignored, presuming its negligible contribution to unsteady blade forces in comparison to the transverse gust contributions; but Horlock showed dominant lift and moment fluctuations due to the chordwise gust in low-stagger cascades and vice versa in the case of high-stagger cascades. Thus the additional feature of the gust interactions with cascades of blades was brought into focus by Horlock. Again the expression for lift fluctuations of an airfoil in streamwise gust was represented elegantly via a complex function, similar to Sears' and Theodorsen's, called the Horlock function,  $T(v)$ .

$$L(t) = 2\pi\rho b\bar{V}\alpha\tilde{V} e^{i\omega t} T(v) \quad (2.5)$$

where  $\bar{V} \equiv$  mean flight speed,  $b \equiv$  half-chord length,  $\alpha \equiv$  angle of attack, and  $\tilde{V}$  is defined to be the amplitude of the chordwise gust. In an attempt to apply Horlock's airfoil theory to cascades of airfoils Holmes<sup>18</sup> was able to derive an analytical expression for lift fluctuations in a cascade of flat plates (two-dimensional) interacting with chordwise gust and calculated a cascade response function  $T(v,\lambda)$  which is known as the modified Horlock function, in much similar way as Kemp's cascade response function  $S(v,\lambda)$  to transverse gusts (where  $S(v,\lambda)$  is known as the modified Sears function).

The effect of camber, on the response of single airfoils to chordwise gust was also studied by Holmes, as reported by Horlock<sup>17</sup>. An airfoil of parabolic camber, at zero incidence, with streamwise fluctuation of velocity was considered by Holmes, whose resulting expression for lift fluctuation is in terms of another complex function, named Holmes' function,  $T'(v)$ . The application of cambered-nonstationary-airfoil theory to turbomachines, however was not attempted by Holmes, and Naumann and Yeh<sup>19</sup> were apparently the first to try to apply their single-cambered-airfoil theory in unsteady flows (under periodic gusts, both transverse and chordwise) to the cascades of airfoils, with finite (but small) camber and incidence. However as pointed out by Horlock,<sup>19</sup> the unsteady blade-to-blade effect was neglected in Naumann and Yeh's analysis, thus limiting their results to the cascades of low solidity. Thus as it stands, the full unsteady flow analysis, including the blade-to-blade effect, similar to Whitehead's analysis for flat plates, is still not done for two-

dimensional cascades of cambered airfoils.

The compressibility effect and the influence of three-dimensionality on the flow characteristics and blade response, in unsteady regime, may be considered a modern outlook to the non-stationary flow problems. An early concern on the effects of compressibility was expressed by Lane and Friedman<sup>20</sup> who theoretically investigated the aerodynamic response of a subsonically oscillating blade row, in 1958. A host of authors who investigated subsonic and supersonic unsteady flows through cascades are listed in Carta's<sup>21</sup> Chapter entitled, "Aeroelasticity and Unsteady Aerodynamics," in the "state-of-the-art" publication of the U.S. Airforce, "Aerothermodynamics of Aircraft Gas Turbine Engines," (1977). Also the "classical" work of Bisplinghoff, Ashley, and Hoffman<sup>22</sup> can be sighted as an excellent (and extensive) source of references on all aspects of unsteady aerodynamics. The earliest account on the investigation of the unsteady flows over finite wings, with variations of circulation in spanwise direction, which resulted in the "Prandtl-type" trailing vortices, in addition to the spanwise vortices shed due to local temporal behavior of circulation, seems to be due to Sears<sup>23</sup> in 1938. In this paper, Sears relates the two component of vorticity in the wake to the time and spanwise variation of the bound vortices over the wing. With the inclusion of three-dimensionality, Sears had no longer the power of conformal transformation and thus his expressions for the lift and moment of the finite wing in unsteady flows are in terms of integrals amendable only to numerical evaluation. Perhaps due to this reason, Sears' contribution to non-stationary finite wing theory was never applied to three-dimensional unsteady flows through cascades. As a "substitution" to

fully three-dimensional unsteady flows many recent investigators focussed on the problem of yawed-infinite-airfoils interacting with transverse gusts.<sup>24,25,26</sup> However, the application of such theories to turbomachines would inherently exclude the unsteady blade-to-blade effect, which is an integral part of the cascade flow.

Namba<sup>27</sup> investigated the unsteady compressible flow through annular cascades (of infinite axial extent) with radial variation of inlet flow distortion, from an acoustician's point of view. The blades, in Namba's analysis, are represented by distribution of pressure dipoles (i.e., pressure singularities associated with the pressure field of an elementary horse-shoe vortex of infinitesimal extent); and thus vortices and their induced effect in Namba's analysis are accounted through implicit means (pressure calculations). Aerodynamicists, on the other hand, are interested in tracking wakes of vortices and explicitly relating their strengths to the spatial and temporal behavior of the bound-vortices, and thus derive their insight of the development of the fluid flow phenomenon primarily by the vortex approach.

In recent years a powerful mathematical tool has found its way in the areas of pure and applied sciences which is based on the introduction of a class of functions, called Generalized Functions; originally introduced by Dirac,<sup>29</sup> and later developed by Temple<sup>30</sup> and Lighthill.<sup>31</sup> In the analysis of the flow in turbomachines, the generalized functions were used heavily by McCune<sup>32,33,34</sup> and his students,<sup>35,36,37</sup> who applied its theory to steady and quasi-steady flows through compressor cascades. In applying this relatively modern mathematical tool to the study of the unsteady fluid flow phenomena in turbomachines, Hawthorne<sup>38</sup> is a pioneer.

Hawthorne developed the use of the generalized functions in the analysis of the potential, two-dimensional and incompressible flow past (steady and fluctuating) singularities representing stationary and moving lifting lines (1973). The present work is an extension of Hawthorne's theory from fluctuating lifting lines in two-dimensional flows to lifting surfaces in three-dimensional space, interacting with an inlet flow distortion.

3.1 Analysis of the Flow in the Upstream Region3.1.1 Kinematics

The flow upstream of the cascade is characterized by non-uniform velocity distribution in the span and pitchwise directions.

The description of the flow at distances far upstream of the cascade is known a priori

$$\underline{v}_{-\infty} \equiv \left[ \bar{V} + v(z) e^{ikY} \right] \hat{i} \quad (3.1)$$

where

$\bar{V}$   $\equiv$  tangentially-mean uniform flow speed in the axial (or x) direction, in the absolute frame (i.e. duct-fixed coordinates).

$v(z)$   $\equiv$  small perturbation to the mean absolute flow in the spanwise direction, at  $x = -\infty$ .

$k$   $\equiv$  the wave number of the perturbation flow in the pitchwise direction.

$k$   $\equiv 2\pi/\lambda$ , where  $\lambda$  is the wave length of the inlet flow distortion in the azimuthal direction

$Y$   $\equiv$  the ordinate with the absolute frame (in the pitchwise direction), and

$\hat{i}$   $\equiv$  the unit vector, in the axial direction, in the absolute coordinates.

Mathematically,  $v(z) e^{ikY}$  in (3.1) represents any general perturbation in the z-direction while accounting for only the fundamental harmonic of the distortions in the azimuthal sense. However, due to our

linearizing assumption of

$$\frac{v(z)}{\bar{v}} \ll 1 \quad (3.2)$$

we can superimpose other harmonics of the pitchwise disturbance via Fourier analysis of the inlet distortion flow, and thus (3.1) does not pose as a restriction on our theory. Similarly  $v(z)$  as a general spanwise distribution of perturbation velocity can be harmonically analyzed and, for simplicity, only the fundamental harmonic be kept, knowing well that the effect of all other Fourier components of the radial perturbation can be summed up, in a linearly independent fashion, to represent (or create) a net effect, since the superposition principle in our linear theory holds. Thus, without any lack of generality, we propose the study of the effect of

$$\underline{\tilde{v}}_{-\infty} \equiv v_0 \cos\left(\frac{\pi z}{h}\right) e^{ikY} \quad (3.3)^*$$

as the description of the fundamental harmonic of the inlet flow distortion on the unsteady interactions with a set of moving blade row, where blades are essentially "flat-plates" in relative motion to the inlet flow. In (3.3),  $v_0$  is the small amplitude of the distortion wave and  $h$  is the ratio of the blade height to the chord, which, for normalization purposes, we have defined the chord length to be unity, i.e.

$$C \equiv 1 \quad (3.4)$$

---

\*Vectors are denoted by an underline, e.g.  $\underline{V}$ . All the flow variables with a bar over them, i.e.  $(\bar{\quad})$ , signify the pitchwise-mean flow quantities while  $(\tilde{\quad})$  represents the perturbation component.



and thus

$$h \equiv \frac{\text{blade height}}{\text{blade chord}} \equiv \text{Aspect ratio} \quad (3.5)$$

Associated with (3.1) is the vorticity field described at distances far upstream of the cascade, defined

$$\underline{\underline{\Omega}}_{-\infty} \equiv \text{curl } \underline{\underline{V}}_{-\infty} = \nabla \times \bar{V} \hat{i} + \nabla \times \tilde{V}_{-\infty} \quad (3.6)$$

But since the mean-inlet flow is defined to be uniform, then the mean-inlet vorticity is zero ( $\underline{\underline{\Omega}} \equiv \nabla \times \underline{\underline{V}} = 0$ ) and

$$\tilde{\underline{\underline{\Omega}}}_{-\infty} \equiv \nabla \times \tilde{\underline{\underline{V}}}_{-\infty} = v'(z) e^{ikY} \hat{j} - ikv(z) e^{ikY} \hat{k} \quad (3.7)$$

where  $v'(z) \equiv dv/dz$ , which measures the strength of the spanwise shear in the upstream flow, and  $\hat{j}$  and  $\hat{k} \equiv$  unit vectors in the pitchwise and spanwise directions, in the absolute coordinates, respectively.

From (3.7), the strength of the perturbation vorticity would remain small\* if  $v(z)$  does not undergo an abrupt change in magnitude, in the  $z$ -direction, i.e. where  $dv/dz$  has no singularities. Due to the neglect of viscosity\*\*, the vorticity described by (3.7) is "frozen" to the fluid particles, along their trajectories, in the upstream flow region.

Whence

$$\underline{\underline{\Omega}}^{\text{upstream}} \equiv \underline{\underline{\Omega}}^u = \underline{\underline{\Omega}}_{-\infty} \quad (\text{Zero Viscosity}) \quad (3.8)$$

The total perturbed-velocity field, in the upstream region, can be thought of as being caused by: 1) disturbed shear in the flow, and 2) the

---

\* small vortex strength means: the vorticity-induced velocity is small compared to the mean-flow speed i.e.  $|\underline{\underline{\Omega}}_{-\infty}| \cdot L/\bar{V} \ll 1$ ,  $L \equiv$  characteristic length scale.

\*\*In addition to the mean-flow velocity which is uniform.

potential field induced by the cascade. Since the blades are aligned in the direction of the mean flow, and via (3.2) the distributed shear velocity is prescribed to be of  $O(\epsilon)$ , we can conclude that the interactions of the inlet distortion with the moving blade row only induces a "bound" vortex strength of  $O(\epsilon)$  at the blade locations. Thus, the potential field induced by the cascade has a velocity component of  $O(\epsilon)$ , in comparison to the mean-flow speed, in the upstream region. Hence the description of the inlet flow, in addition to the blade setting angles, enable us to make use of the linear-small perturbation theory. In the "standard" form we can write

$$\underline{V}^u = \underline{\bar{V}} + \underline{\tilde{V}}^u \quad (3.9)$$

where

$$|\underline{\tilde{V}}|/|\underline{\bar{V}}| \ll 1 \quad (\text{Linearizing Assumption}) \quad (3.10)$$

and  $\underline{\bar{V}} \equiv$  the reference, steady, "base" flow, upon which  $\underline{\tilde{V}}^u$  is superimposed. The nature of the perturbation velocity field in the upstream region, as described above, suggests:

$$\underline{\tilde{V}}^u = \nabla \tilde{\phi}^u + \underline{\tilde{A}}^u \quad (3.11)$$

where  $\tilde{\phi}^u \equiv$  upstream, perturbation velocity potential.  $\underline{\tilde{A}}^u \equiv$  the rotational component of the upstream perturbation velocity field, the so-called "vector potential".

In employing the Clebsch-Hawthorne representation of  $\underline{\tilde{A}}^u$ , we introduce two, as yet unknown, scalars  $\sigma^u$  and  $\tau^u$  to, effectively, replace the three components of  $\underline{\tilde{A}}^u$ , i.e. we let

$$\underline{\tilde{A}}^u \equiv \sigma^u \nabla \tau^u \quad (\text{Clebsch-Hawthorne}) \quad (3.12)$$

The operation of "curl" on (3.11) leads to the upstream perturbation vorticity,

$$\underline{\tilde{\Omega}}^u \equiv \text{curl } \underline{\tilde{y}}^u = \nabla \times \underline{\tilde{A}}^u \quad (3.13)$$

or, via (3.12)

$$\underline{\tilde{\Omega}}^u = \nabla \times (\sigma^u \nabla \tau^u) = \nabla \sigma^u \times \nabla \tau^u \quad (3.14)$$

The continuity of the incompressible fluid, in the absence of sources or sinks, demands

$$\nabla \cdot \underline{y}^u = 0 \quad (3.15)$$

Upon substitution of (3.9) in the above equation, we get

$$\nabla \cdot \underline{\tilde{y}}^u = 0 \quad (3.16)$$

Since

$$\nabla \cdot \underline{\tilde{v}}^u \equiv 0 \quad (3.17)$$

Expanding (3.16) in components of  $\underline{\tilde{y}}^u$  as described by (3.11) and (3.12), we arrive at the Poisson equation governing the perturbation potential  $\tilde{\phi}^u$ , i.e.

$$\nabla^2 \tilde{\phi}^u = - \nabla \sigma^u \cdot \nabla \tau^u - \sigma^u \nabla^2 \tau^u \quad (3.18)$$

The "driving" terms in (3.18) are vector operations on the Clebsch-Hawthorne scalar parameters,  $\sigma^u$  and  $\tau^u$ , which are determinable from the dynamical equation of motion, in addition to the description of the up-

stream vorticity field. The physical meaning of the "driving" terms are discussed, at length, in the following section, "Solution of the Poisson equation for  $\tilde{\phi}^u$ ".

### 3.1.2 Dynamics

In the absence of viscosity and body forces, the Euler momentum equation describes the relation between the total fluid particle acceleration and the pressure forces acting on it, in the following form

$$\frac{D\underline{V}}{Dt} = - \frac{1}{\rho} \nabla p \quad (3.19)$$

where

$$\frac{D}{Dt} \equiv \frac{\partial}{\partial t} + \underline{V} \cdot \nabla \quad (3.20)$$

By substituting (3.10) into (3.19) and collecting terms of the same order of magnitude, we get

$$\frac{\partial \underline{V}}{\partial t} + \bar{\underline{V}} \frac{\partial}{\partial x} \underline{V} = - \frac{1}{\rho} \nabla \bar{p} \quad [O(1)] \quad (3.21)$$

and

$$\frac{\partial \tilde{\underline{V}}}{\partial t} + \bar{\underline{V}} \frac{\partial}{\partial x} \tilde{\underline{V}} + \tilde{\underline{V}} \cdot \nabla \bar{\underline{V}} = - \frac{1}{\rho} \nabla \tilde{p} \quad [O(\epsilon)] \quad (3.22)$$

The mean-momentum equation, i.e. (3.21), is identically satisfied by our definition of the mean quantities. However, the perturbation-momentum equation, i.e. (3.22), is as yet unsatisfied. Since our description of  $\tilde{\underline{V}}^u$  involves unknown scalars  $\sigma^u$  and  $\tau^u$ . Expanding (3.22) in  $\tilde{\phi}^u$ ,  $\sigma^u$  and  $\tau^u$  and utilizing some vector identities (given in Appendix A), we get

$$\frac{D_0 \tau^u}{Dt} \nabla \sigma^u - \frac{D_0 \sigma^u}{Dt} \nabla \tau^u = \nabla \left[ \frac{p_0^u - \bar{p}_{0-\infty}}{\rho} + \frac{\partial \tilde{\phi}^u}{\partial t} + \sigma^u \frac{\partial \tau^u}{\partial t} \right] \quad (3.23)$$

where

$$\frac{D_0}{Dt} \equiv \frac{\partial}{\partial t} + \bar{v} \frac{\partial}{\partial x} \quad (\text{mean-Eulerian derivative}) \quad (3.25)$$

and

$$p_0 \equiv p + \frac{1}{2} \rho |\underline{v}|^2 \quad (\text{steady -total pressure}) \quad (3.26)$$

The expression in the bracket, on the r.h.s. of (3.24), resembles a Bernoulli - constant , in this more generalized flow problem, with the inclusion of unsteadiness and the distributed shear. It is this "resemblance" which suggests the following choice for  $\sigma^u$ , eventually leading to the statement of the preservation of  $\sigma^u$  along the mean-fluid paths.\* We can define, without loss of generality

$$\sigma^u \equiv \frac{p_0^u - \bar{p}_0^\infty}{\rho} + \frac{\partial \phi^u}{\partial t} + \sigma^u \frac{\partial \tau^u}{\partial t} \quad (3.27)$$

and (3.24) reduces to

$$\left( \frac{D_0 \tau^u}{Dt} - 1 \right) \nabla \sigma^u - \frac{D_0 \sigma^u}{Dt} \nabla \tau^u = 0$$

Now, a post-cross product of  $\nabla \tau^u$  with (3.28), yields

$$\left( \frac{D_0 \tau^u}{Dt} - 1 \right) \nabla \sigma^u \times \nabla \tau^u = 0 \quad (3.29)$$

(Since  $\nabla \tau^u \times \nabla \tau^u \equiv 0$ ).

We can recognize  $\nabla \sigma^u \times \nabla \tau^u$  as  $\tilde{\underline{\Omega}}^u$ , the magnitude and direction of which is dictated by the geometry of the inlet shear, thus (3.29) is satisfied by

$$\frac{D_0 \tau^u}{Dt} - 1 = 0 \quad (3.30)$$

(Since  $\tilde{\underline{\Omega}}^u \neq 0$ ).

---

\*This choice for  $\sigma^u$ , was originally suggested by Lamb, Hydrodynamics, p. 248-249.

A post-cross product of (3.28) with  $\nabla\sigma^u$  and a similar argument, as presented above, leads to the following governing equation for  $\sigma^u$ ,

$$\frac{D_0\sigma^u}{Dt} = 0 \quad (3.31)$$

The equation (3.30), in the area of fluid mechanics is considered a classical equation which was, originally, solved by Darwin<sup>39</sup>, expounded upon by Lighthill<sup>40</sup> and utilized in the most revealing fashion, in the study of secondary flows, by Hawthorne<sup>41</sup>. The parameter in the Darwin-Lighthill-Hawthorne equation,  $\tau^u$ , is known as the "drift function" and measures the time taken by a fluid element to move (or "drift") from a reference point, in the fluid, to another point along its trajectory. Thus  $\tau^u$  measures an  $O(1)$  quantity. In steady flows, the solution to (3.30) can be written as

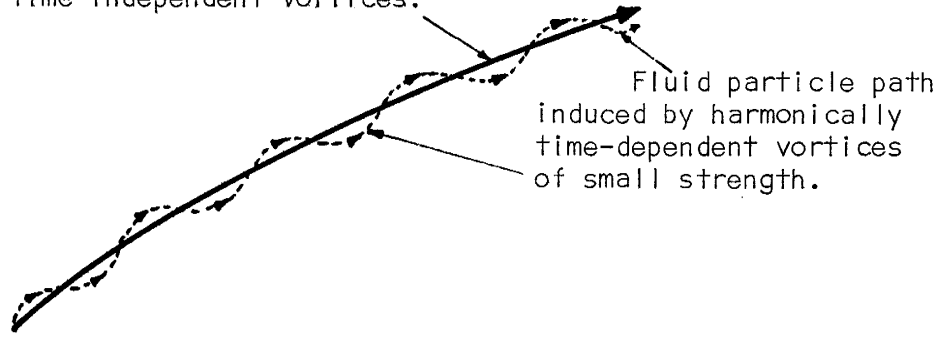
$$\tau_{\text{steady}}^u = \int_{S_{\text{ref}}}^S \frac{d\xi}{|\underline{V}|} = \int_{S_{\text{ref}}}^S \frac{d\xi}{|\bar{\underline{V}}|} + O(\epsilon) \quad *$$
(3.32)

where  $S$  is the coordinate in the tangential direction to the fluid path. However, in the presence of fluctuating vortices in the flow, the strengths of which are of  $O(\epsilon)$ , the fluid particle departs from its steady course and follows a sinusoidal path which winds around the steady course. And since the strength of the bound-fluctuating vortices are of  $O(\epsilon)$ , thus the induced amplitude of the perturbed path is of  $O(\epsilon)$  as well (i.e. compared to other length scales of the problem).

---

\* $O(\epsilon)$  appears since  $|\bar{\underline{V}}|$  has replaced  $|\underline{V}|$  in the denominator of the integrand in (3.32).

Steady fluid path in the presence  
of time-independent vortices.



Thus, we can conclude that in the strictly\*-linearized flow theory

$$\tau_{\text{unsteady}} = \tau_{\text{steady}} + O(\epsilon) \quad (3.33)$$

provided the drift-times are measured with respect to the same reference point (or plane) in the flow field. From (3.32) and (3.33), we deduce

$$\tau^u = \tau_{\text{unsteady}} = \int_{X_{\text{ref}}}^X \frac{d\xi}{\bar{V}} + O(\epsilon) = \frac{X - X_{\text{ref}}}{\bar{V}} + O(\epsilon) \quad (3.34a)$$

and for simplicity we choose  $X_{\text{ref}} \equiv 0$ , i.e. at the face of the cascade,  
or

$$\tau^u = \frac{X}{\bar{V}} + O(\epsilon) \quad (3.34b)$$

From (3.34b) it immediately follows that

$$\frac{\partial \tau^u}{\partial t} = O(\epsilon) \quad (3.35)$$

---

\*Here it applies to the cases where the induced velocities by the "bound" and free vortices are small compared to the mean-inlet flow speed, i.e.  $|\underline{V}_{\text{induced}}|/|\underline{V}| \ll 1$ .

and since  $\sigma^u = O(\varepsilon)$ , according to our description of (3.27), we conclude

$$\sigma^u \frac{\partial \tau^u}{\partial t} = O(\varepsilon^2) \quad (3.36)$$

which is a second order effect and thus, in the linearized sense, is neglected from (3.27), i.e.

$$\sigma^u \approx \frac{p_0 - \bar{p}_{0-\infty}}{\rho} + \frac{\partial \phi}{\partial t} \left( + O(\varepsilon^2) \right) \quad (3.37)$$

which is indeed a constant of the motion according to Kelvin's theorem (or generalized Bernoulli theorem), i.e.  $\sigma^u$  is a preserved quantity for a fluid particle as it moves along its trajectory in an unsteady stream. It is also noted that (3.37) reduces to the more familiar Bernoulli-constant for steady flows. Upon substitution of  $\tau^u$ , from (3.34b), in (3.15) and equating the upstream perturbation vorticity to the known inlet vorticity (at  $X = -\infty$ ), we obtain the following expression for  $\sigma^u$

$$\sigma^u = \bar{V}_V(z) e^{ikY} = \bar{V}_V^0 \cos \left( \frac{\pi z}{h} \right) e^{ikY} \quad (3.38)$$

(note that  $\sigma^u = O(\varepsilon)$ ).

Now, to Order  $\varepsilon$ , the dynamical equation of motion is satisfied and we have determined the Clebsch-Hawthorne parameters in the upstream flow region. Therefore, the Poisson equation for  $\tilde{\phi}^u$  (resulted from the kinematics) can now be solved with the description of  $\sigma^u$  and  $\tau^u$ .

### 3.1.3 Solution of the Poisson Equation for $\tilde{\phi}^u$

It will prove advantageous to solve the governing equation for the upstream perturbation potential,  $\tilde{\phi}^u$ , in the moving (i.e. relative) frame, as we have to match the upstream flow with the flow inside the moving cascade in order to achieve a unified flow picture. The relationship



between the moving frame attached to the cascade, in the direction of and normal to the blades and the stationary frame the axes of which are rotated in the clockwise direction by the angle of blade setting  $\alpha$  (i.e. stagger angle) are as follows:

$$Y = y - Ut \quad (3.39)$$

$$y = x' \sin \alpha + y' \cos \alpha \quad (3.40)$$

$$x = x' \cos \alpha - y' \sin \alpha \quad (3.41)$$

$$t = t'$$

where

$U \equiv$  blade speed, in the pitchwise direction

$Y \equiv$  coordinate in the gapwise direction in absolute frame

$x \equiv$  coordinate in the axial direction in absolute frame

$y \equiv$  coordinate in the pitchwise direction in relative frame

$x' \equiv$  coordinate along the reference blade chord in relative frame

$y' \equiv$  coordinate normal to reference blade chord in relative frame

$\alpha \equiv$  blade setting angle, or cascade stagger angle

$t \equiv$  time measured in absolute frame (=  $t'$  in relative frame)

The upstream velocity field, expressed in the relative (blade-fixed) frame is

$$\underline{W}^u = \underline{\bar{W}} + \nabla' \tilde{\phi}'^u + \sigma' \nabla' \tau'^u \quad (3.43)*$$

where, we have fixed the blade speed (or the blade setting angle,  $\alpha$ ) such that the mean-relative velocity,  $\underline{\bar{W}}$ , is aligned in the direction of the

---

\*All dashed-quantities, i.e.  $(\ )'$ , express those quantities in the relative (blade-fixed) frame.

chord line, i.e. the blades receive the mean-flow at zero incident angle, thus

$$\underline{\bar{W}} = \bar{V} \hat{i} + U \hat{j} \quad (3.44)$$

and

$$W \equiv \bar{V} \sec \alpha \hat{e}_x, \quad (3.45)$$

In (3.43),

$$\nabla' \equiv \hat{e}_x' \frac{\partial}{\partial x'} + \hat{e}_y' \frac{\partial}{\partial y'} + \hat{k} \frac{\partial}{\partial z} \quad (3.46)$$

$$\sigma'^u = \bar{V} \tilde{v}_0 \cos \left( \frac{\pi z}{h} \right) \exp[ik (\sin \alpha x' + \cos \alpha y' - Ut)] \quad (3.47)$$

and

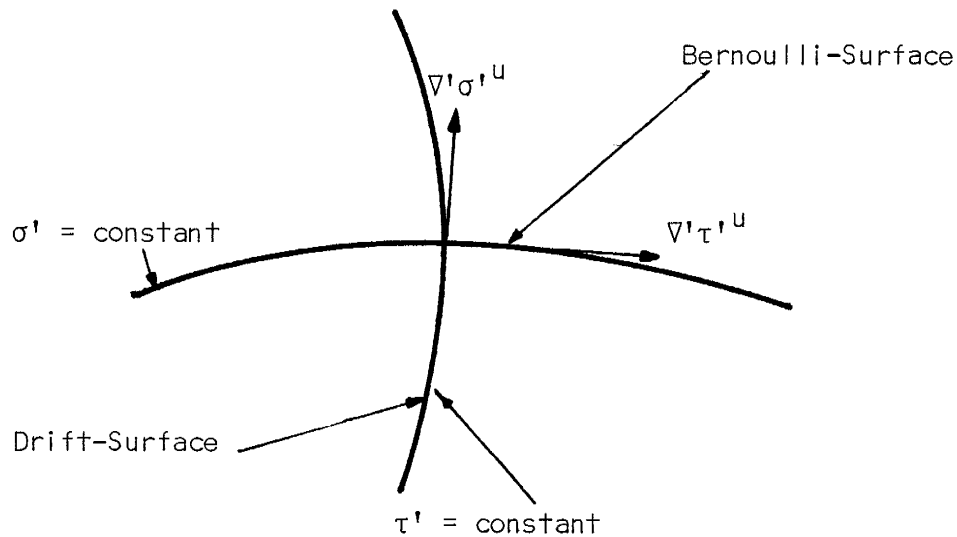
$$\tau'^u = \frac{x'}{\bar{W}} - \frac{\tan \alpha}{\bar{W}} y' + O(\epsilon) \quad (3.48)$$

The governing equation for the  $\tilde{\phi}'^u$  can be written via the application of continuity of mass flow equation (in the absence of sources and sinks) to (3.44), i.e.

$$\nabla'^2 \tilde{\phi}'^u = -\nabla' \sigma'^u \cdot \nabla' \tau'^u - \sigma'^u \nabla'^2 \tau'^u \quad (3.49)$$

By applying (3.46), (3.47), and (3.48) to (3.49), we can show mathematically, that the r.h.s. of the Poisson equation governing  $\tilde{\phi}'^u$ , (3.49), identically vanishes and thus reduces to Laplace's equation for  $\tilde{\phi}'^u$ . The physics behind this "drastic" reduction (from Poisson's to Laplace's) is quite interesting and can be explained in two ways, 1) due to our description of the perturbation velocity field, the shear in the upstream velocity is purely convected by the mean flow and hence there are no regions of concentrated vorticity so as to create a net induced velocity

field contributing to  $\tilde{\phi}'^u$ , i.e. the inlet shear does not "enhance" the perturbation potential in the upstream region, but rather accompanies it in an independent manner, 2)  $\sigma'^u = \text{constant}$  depicts a generalized Bernoulli-surface initially starting as planes parallel to the hub and casing at distances far upstream, to the cascade, and  $\nabla'\sigma'^u$  is a normal vector to that surface.  $\tau'^u = \text{constant}$ , on the other hand, depicts a "drift" surface which to  $O(\varepsilon)$  is convected by the mean flow and  $\nabla'\tau'^u$  is a normal to the "drift-surface".



Initially,  $\sigma'^u = \text{constant}$  and  $\tau'^u = \text{constant}$  (i.e. at  $x' = -\infty$ ) are orthogonal to each other, i.e.  $\nabla'\sigma'^u \cdot \nabla'\tau'^u \equiv 0$  at  $x' = -\infty$ . However, the perturbations to the Bernoulli-surfaces, as they approach the cascade of blades, are of  $O(\varepsilon)$ , i.e. proportional to the strength of the bound-vorticity. While  $\tau'^u$  maintains its shape to  $O(\varepsilon)$  as well, thus the angle between  $\nabla'\tau'^u$  and  $\nabla'\sigma'^u$  differs from  $\pi/2$  by  $\varepsilon$ , thence

$$\begin{aligned}
\nabla^i \sigma^i{}^u \cdot \nabla^i \tau^i{}^u &= |\nabla^i \sigma^i{}^u| |\nabla^i \tau^i{}^u| \cos \left( \frac{\pi}{2} \pm \varepsilon \right) \\
&= |\nabla^i \sigma^i{}^u| |\nabla^i \tau^i{}^u| (\mp \sin \varepsilon) \\
&= |\nabla^i \sigma^i{}^u| |\nabla^i \tau^i{}^u| \left( \mp \varepsilon \pm \frac{\varepsilon^3}{3!} \mp \dots \right) = O(\varepsilon^2) \quad (3.50)
\end{aligned}$$

and as a second order effect, it is neglected in our linearized theory. Again, by constructing arguments based on the geometry and kinematics of the flow-surfaces, we can identify the reason for zero contribution of  $\sigma^i{}^u \nabla^i{}^2 \tau^i{}^u$  to the perturbation potential  $\tilde{\phi}^i{}^u$ . We note that

$$\begin{aligned}
\nabla^i{}^2 \tau^i{}^u = \nabla^i \cdot (\nabla^i \tau^i{}^u) &\equiv \text{Efflux of } \nabla^i \tau^i{}^u\text{-vector from any control} \\
&\text{volume in the (upstream) flow} \quad (3.51)
\end{aligned}$$

which according to our theory,  $\tau^i{}^u = \text{constant}$  surfaces are convected by the mean-flow to  $O(\varepsilon)$ , thence  $\nabla^i \tau^i{}^u$ , as a normal vector to  $\tau^i{}^u = \text{constant}$  surface, always maintains its magnitude and direction to  $O(\varepsilon)$ , thus "accumulation" of  $\tau^i{}^u$ -surfaces (i.e. drift surfaces) in any control volume, completely submerged in the upstream flow, would be of  $O(\varepsilon)$ , the contribution of which to "driving" the  $\tilde{\phi}^i{}^u$  is measured by

$$\sigma^i \nabla^i{}^2 \tau^i{}^u = O(\varepsilon^2) \quad (3.52)$$

which again is neglected in our linearized theory.

It is important to note here that the second physical expansion offered for the reduction of the Poisson's equation as governing the perturbation potential, in the upstream region, to the Laplace's equation was only made possible by the use of the Clebsch-Hawthorne methodology.

Thus the governing equation for  $\tilde{\phi}'^u$  is

$$\nabla'^2 \tilde{\phi}'^u = 0 \quad (3.53)$$

The solution to the above equation, in terms of Fourier series can be written, in the moving frame attached to the reference blade, as

$$\tilde{\phi}'^u = \sum_{m=-\infty}^{+\infty} C_m^u e^{\lambda_m x'} \cdot e^{i(2m\pi + \beta)y'/s'} \cdot \cos\left(\frac{\pi z}{h}\right) \cdot e^{i\omega t} \quad (3.54)$$

where

$C_m^u \equiv$  Fourier coefficients in the upstream region

$$\lambda_m \equiv \sqrt{\left(\frac{2m\pi + \beta}{s'}\right)^2 + \left(\frac{\pi}{h}\right)^2} = \text{Axial decay parameter} \quad (3.55)$$

$$\beta \equiv \text{Inter-blade phase angle} = \frac{2\pi s}{\lambda} \quad (3.56)$$

$$\omega \equiv \text{Angular velocity of fluctuations} = \frac{2\pi U}{\lambda} \quad (3.57)$$

$$s' \equiv s \cos \alpha, \text{ the normal distance between adjacent blades} \quad (3.58)$$

with the following considerations:

1.  $\tilde{\phi}'^u$  decays to zero as  $x' \rightarrow -\infty$  ("Elliptic-field" solution)
2.  $\tilde{\phi}'^u$  is phased-periodic in the  $y'$ -direction
3.  $\tilde{\phi}'^u$  is harmonic in time, with the frequency of the blade interactions, with the inlet flow distortion,  $U/\lambda$
4.  $\partial \tilde{\phi}'^u / \partial z$  vanishes at both inner and outer shrouds to satisfy the solid wall boundary condition.

The decaying nature of  $\tilde{\phi}'^u$  is demanded by the governing partial differential equation, which is elliptic, and requires the disturbances to decay at distances far from the "source". The phased periodicity of  $\tilde{\phi}'^u$  is expected due to the nature of the driving-sources, i.e. the vortex distribution on the blades are different from one another by a

common phase angle  $2\pi s/\lambda$ . We further expect all perturbation quantities (including  $\tilde{\phi}'^u$ ) to be harmonic functions of time with the frequency of the blade interactions with the inlet flow distortions. And finally the solid wall boundary condition, i.e. of no fluid penetration,

$$\underline{W} \cdot \nabla' \psi' \Big|_{\text{hub,tip}} = 0 \quad (3.59)$$

where  $\psi' \equiv$  the relative stream function, in our problem  $\psi' = \psi'(x', y', z, t)$ , and  $\nabla' \psi'$  depicts the normal vector to the stream surfaces and at hub and tip,

$$\frac{\nabla' \psi'}{|\nabla' \psi'|} = \hat{e}_z \quad \text{at } z = 0 \text{ and } h \quad (3.60)$$

demands

$$W_z = \tilde{W}_z = \frac{\partial \tilde{\phi}'^u}{\partial z} \equiv 0 \quad \text{at } z = 0 \text{ and } h \quad (3.61)$$

which is identically satisfied by (3.54). The Fourier coefficients,  $C_m^u$  will be determined by matching the perturbation flows of the upstream and the inter-blade region at their common plane of interface.

## 3.2 Analysis of the Flow Inside the Blade Row

### 3.2.1 Kinematics

In this region besides the convected upstream vorticity, which is of distributed nature, vortex sheets of "bound" and free kind also exist periodically representing blades and their wakes. Interaction of the disturbed-inlet flow with the cascade of blades induces "bound"-vortex sheets at the location of the blades. Due to the relative motion of the blades with respect to the inlet flow distortion, the induced "bound"-

vorticity fluctuates, in its strength, harmonically in time. Furthermore, due to spanwise dependence of the inlet disturbances, the induced "bound"-vorticity exhibits a spanwise (or radial) dependence as well. Thus, it may be concluded that in the region within and including the blades, besides the upstream convected vorticity, "bound"-vorticity is induced at the location of the blades, the strength of which is both a function of time (harmonic) and the spanwise location. It is classically known that such a "bound"-vortex structure sheds free-vorticity in the spanwise direction, due to its temporal behavior, and also a wake of trailing vortices in the streamwise direction as a result of its spanwise dependence. These results concerning the wakes of free-vortices are both observed via fluid mechanical experiments and also their existence are proved, theoretically, by invoking Kelvin's circulation theorem for inviscid-barotropic fluids, and Helmholtz vortex theorems.

To describe the induced effect of these complexly-structured vortices, we again utilize the linear-small perturbation theory, with the rotational contribution of the perturbation term represented by the Clebsch-Hawthorne scalars  $\sigma$  and  $\tau$ , in  $\sigma\nabla\tau$  format, i.e.

$$\underline{w}^i = \underline{\bar{w}}^i + \underline{\tilde{w}}^i, \quad |\underline{\tilde{w}}^i|/|\underline{\bar{w}}^i| \ll 1 \quad (3.62)$$

where

$$\underline{\bar{w}}^i \equiv \bar{v}\hat{i} + U\hat{j} \quad (\equiv \underline{\bar{w}}^u), \quad \text{mean-relative velocity} \quad (3.63)$$

and

$$\underline{\tilde{w}}^i \equiv \nabla^i \tilde{\phi}^i + \sigma^u \nabla^i \tau^u + \sigma^i \nabla^i \tau^i \quad (3.64)$$

where

$\tilde{\phi}^i \equiv$  the perturbation potential inside the blade row,

$\sigma^u \nabla' \tau^u$   $\equiv$  the convected-inlet disturbance velocity (known from the upstream field), and

$\sigma^i \nabla' \tau^i$   $\equiv$  the rotational-perturbation inside the blade row.

However, due to distinctly different origins for the concentrated vortices in the sheets, it is found desirable to represent their rotational-induced effects by two different terms in the Clebsch-Hawthorne transformation, i.e. we propose to employ a multiple Clebsch-Hawthorne representation.

$$\underline{\tilde{W}}^i \equiv \nabla' \tilde{\phi}^i + \sigma^u \nabla' \tau^u + \sigma^i \nabla' \tau^i + s^i \nabla' \Gamma^i \quad (3.65)$$

where

$\sigma^i \nabla' \tau^i$   $\equiv$  the rotational contribution of the "bound" and free-vortices in the spanwise direction, to the perturbation velocity field inside the blade row.

$s^i \nabla' \Gamma^i$   $\equiv$  the rotational contribution of the free-streamwise vortices, to the perturbation velocity field inside the blade row.

The prevailing vorticity field within and including the blades can be represented in terms of the Clebsch-Hawthorne parameters as follows:

$$\underline{\Omega}^i \equiv \text{curl} \underline{W}^i = \text{curl} \underline{\bar{W}}^i + \text{curl} \underline{\tilde{W}}^i \quad (3.66)$$

where

$$\underline{\bar{\Omega}}^i \equiv \text{curl} \underline{\bar{W}}^i \equiv 0, \text{ via (3.63)} \quad (3.67)$$

and

$$\underline{\tilde{\Omega}}^i \equiv \text{curl} \underline{\tilde{W}}^i = \nabla' \sigma^u \times \nabla' \tau^u + \nabla' \sigma^i \times \nabla' \tau^i + \nabla' s^i \times \nabla' \Gamma^i \quad (3.68)$$

From the above description, we intend to represent the "bound" and free-vorticity, in the spanwise direction, by  $\nabla' \sigma^i \times \nabla' \tau^i$  and the free-streamwise vorticity via  $\nabla' s^i \times \nabla' \Gamma^i$  and the upstream-distributed vorticity, as



it convects inside the blade channel, by  $\nabla' \sigma'^u \times \nabla' \tau'^u$ . Recalling the neglect of viscosity in our analysis, the free-vortices over the blades, remain inside the plane of the blades and thus remain undiffused, in "thin"-sheets, eventually emanating from the blades' trailing-edges as inviscid-wakes.

As the lifting characteristics of the blades in the cascade are of interest to us in this analysis, the problem of thickness, which involves distribution of mass-sources and sinks, is then neglected when we apply the law of conservation of mass flow, to the region within the blade row, i.e.

$$\nabla' \cdot \underline{w}^i = 0 \quad (\text{incompressible fluid}) \quad (3.69)$$

Via substitution of (3.62) and (3.65) in (3.69), we get

$$\nabla' \cdot \underline{\bar{w}}^i \equiv 0, \quad \text{mean-incompressible flow} \quad (3.70)$$

and

$$\begin{aligned} \nabla'^2 \tilde{\phi}^i &= -\nabla' \sigma'^u \cdot \nabla' \tau'^u - \sigma'^u \nabla'^2 \tau'^u - \nabla' \sigma'^i \cdot \nabla' \tau'^i - \sigma'^i \nabla'^2 \tau'^i \\ &\quad - \nabla' s^i \cdot \nabla' \Gamma^i - s^i \nabla'^2 \Gamma^i \end{aligned} \quad (3.71a)$$

Since the contribution of the first two terms on the r.h.s. of (3.71a) is shown to be of order  $\epsilon^2$ , in Section 3.1.3, then (3.71a) reduces to

$$\nabla'^2 \tilde{\phi}^i = -\nabla' \sigma'^i \cdot \nabla' \tau'^i - \sigma'^i \nabla'^2 \tau'^i - \nabla' s^i \cdot \nabla' \Gamma^i - s^i \nabla'^2 \Gamma^i \quad (3.71b)$$

where we observe that the perturbation potential  $\tilde{\phi}^i$  is driven by the free and "bound" vortex sheets, the contributions of which appear on the

r.h.s. of (3.71b). However, the Clebsch-Hawthorne scalars in the Poisson equation (3.71b) are as yet undefined and thus we propose to determine their description by applying the dynamical equation of motion to the fluid inside the blade row, including the effect of the blades, i.e. concentrated force fields.

### 3.2.2 Dynamics

The region, within and including the blades, is dynamically characterized by the presence of continuous and discontinuous pressure fields. The discontinuity of the pressure is sustained by the "bound" vortex sheets, while the continuous pressure field prevails over the fluid elements (potential and rotational) in the region in between the blades. Thus, the inviscid momentum equation (i.e. Euler's equation) with the blades' forces expressed in terms of body-force singularities, now represents the governing dynamical equation, to be satisfied in the interblade region, i.e.

$$\frac{D'W^i}{Dt} = - \frac{1}{\rho} \nabla' p^i + \frac{F^i}{\rho} \quad (3.72)$$

where

$$\frac{D'}{Dt} \equiv \frac{\partial}{\partial t} + \underline{W}^i \cdot \nabla', \quad \text{Eulerian derivative in relative} \quad (3.73)$$

frame

and

$$\underline{F}^i = \text{the blade force} \quad (3.74)$$

The perturbation analysis of (3.72) leads to

$$\frac{\partial \bar{w}^i}{\partial t} + \bar{w}^i \frac{\partial}{\partial x^r} \bar{w}^i = -\frac{1}{\rho} \nabla^r \bar{p}^i + \frac{\bar{F}^i}{\rho} \quad (3.75)$$

and

$$\frac{\partial \tilde{w}^i}{\partial t} + \bar{w}^i \frac{\partial}{\partial x^r} \tilde{w}^i + (\tilde{w}^i \cdot \nabla^r) \bar{w}^i = -\frac{1}{\rho} \nabla^r \tilde{p}^i + \frac{\tilde{F}^i}{\rho} \quad (3.76)$$

The equation (3.75) is the mean-momentum equation which is identically satisfied, since  $\bar{w}^i$  is time and space invariant thus the left-hand-side of (3.75) identically vanishes and similarly  $\bar{p}^i$  is space invariant, by definition, therefore its gradient is null, and finally  $\bar{F}^i$  defining the mean-specific blade force is zero since the blades are "set" at zero-mean angle of attack (or incidence),

$$\bar{F}^i \equiv 0 \quad (3.77)$$

Expanding the perturbation momentum equation, i.e. (3.76), in the Clebsch-Hawthorne scalars and  $\tilde{\phi}^i$ , we get\*

$$\begin{aligned} & \frac{D^r \tau^i u}{Dt} \nabla^r \sigma^i u - \frac{D^r \sigma^i u}{Dt} \nabla^r \tau^i u + \frac{D^r \tau^i}{Dt} \nabla^r \sigma^i - \frac{D^r \sigma^i}{Dt} \nabla^r \tau^i + \frac{D^r \Gamma^i}{Dt} \nabla^r s^i - \frac{D^r s^i}{Dt} \nabla^r \Gamma^i \\ & = \nabla^r \left[ \frac{p_0 - \bar{p}_{0-\infty}}{\rho} + \frac{\partial \tilde{\phi}^i}{\partial t} + \sigma^i u \frac{\partial \tau^i u}{\partial t} + \sigma^i \frac{\partial \tau^i}{\partial t} + s^i \frac{\partial \Gamma^i}{\partial t} \right] - \frac{\tilde{F}^i}{\rho} \end{aligned} \quad (3.78)$$

From the knowledge of the kinematics of the upstream flow,

$$\frac{D^r \sigma^i u}{Dt} = \frac{D^r \tau^i u}{Dt} - 1 = 0$$

and

---

\*Vector identities utilized in this derivation are summarized in Appendix A.

$$\sigma^i u \frac{\partial \tau^i u}{\partial t} = O(\epsilon^2)$$

Thus (3.78) simplifies to

$$\begin{aligned} \nabla^i \sigma^i u + \frac{D^i \tau^i}{Dt} \nabla^i \sigma^i - \frac{D^i \sigma^i}{Dt} \nabla^i \tau^i + \frac{D^i \Gamma^i}{Dt} \nabla^i s^i - \frac{D^i s^i}{Dt} \nabla^i \Gamma^i = \\ \nabla^i \left[ \frac{p_0^i - \bar{p}_{0-\infty}^i}{\partial t} + \frac{\tilde{\phi}^i}{\partial t} + \sigma^i \frac{\partial \tau^i}{\partial t} + s^i \frac{\partial \Gamma^i}{\partial t} \right] - \frac{\tilde{F}^i}{\rho} \end{aligned} \quad (3.79)$$

It is important to point out, briefly here, that one of the Clebsch-Hawthorne scalars, in a  $\sigma \nabla \tau$  type of presentation, can be chosen, based on the physical arguments to simplify the dynamical equation of motion, without any loss of generality so long as  $\nabla \sigma \times \nabla \tau$  represents the prevailing vorticity field in the flow, or in our multiple Clebsch-Hawthorne representation  $\nabla \sigma \times \nabla \tau$  must be able to represent a component of the prevailing vorticity in the flow. Appendix B deals with this concern in detail.

Since, we wish to represent the streamwise vorticity by  $\nabla^i s^i \times \nabla^i \Gamma^i$  and  $\nabla^i s^i$ , mathematically, represents a normal to the surface  $s^i =$  constant, then if we imagine that the time-dependent streamwise vortices lie on the mean (i.e. time-averaged) Bernoulli-surfaces, where steady-streamwise vortices lie, to  $O(\epsilon)$ , then

$$s^i = z + O(\epsilon) \quad (3.80)$$

since the mean-Bernoulli-surfaces\* are  $z = \text{constant}$  planes parallel to the hub and tip casing. In Appendix C, by invoking Helmholtz vortex theorems, we have shown that the strength of the trailing vorticity, in the wake, is related to the spanwise gradient of the "bound"-vortex distribution via the following relation

$$\gamma_{x'} = - \int_0^{x'} \frac{\partial \gamma_B}{\partial z} (\xi, z, t) \Big|_{t=t-(x'-\xi)/\bar{W}} d\xi \quad (3.81)$$

where  $(x'-\xi)/\bar{W}$  is the "convection-time" for any free vortex element generated at the chordwise station  $\xi$ . From (3.80) and (3.81), we can deduce that

$$\Gamma^i = \frac{\partial}{\partial z} \int_0^{x'} \gamma_B(\xi, z) e^{i\omega(t-(x'-\xi)/\bar{W})} d\xi H_p(y') \quad (3.82)$$

where  $\omega \equiv$  the angular velocity of fluctuations,  $2\pi U/\lambda$  and,  $H_p(y')$  the periodic-Heaviside function, "jumping" in steps of unity at the blade locations (see Figure 9).

Incorporating (3.80) into (3.79), we get

$$\begin{aligned} \nabla'^i \sigma'^u + \frac{D'^i \tau^i}{Dt} \nabla'^i \sigma^i - \frac{D'^i \sigma^i}{Dt} \nabla'^i \tau^i + \frac{D'^i \Gamma^i}{Dt} \hat{e}_z = \\ \nabla'^i \left[ \frac{p_0^i - \bar{p}_{0-\infty}^i}{\rho} + \frac{\partial \tilde{\phi}^i}{\partial t} + \sigma^i \frac{\partial \tau^i}{\partial t} + s^i \frac{\partial \Gamma^i}{\partial t} \right] - \frac{F^i}{\rho} \end{aligned} \quad (3.83)$$

From the description of  $\sigma'^u$  we can transform (3.83) into the following

---

\*A Bernoulli-surface, in a steady flow, is any fluid surface where  $(p/\rho + V^2/2)$  takes on a constant value, the so-called Bernoulli constant. A generalized Bernoulli-surface which includes the effect of unsteadiness in the flow is defined here as any fluid surface upon which  $(p/\rho + V^2/2 + \partial\phi/\partial t)$  remains constant.

$$\begin{aligned} \frac{D'\tau^i}{Dt} \nabla'\sigma^i - \frac{D'\sigma^i}{Dt} \nabla'\tau^i + \frac{D'\Gamma^i}{Dt} \hat{e}_z = \\ \nabla' \left[ \frac{(p_0^i - p_0^u)}{\rho} + \frac{\partial}{\partial t} (\tilde{\phi}^i - \tilde{\phi}^u) + \sigma^i \frac{\partial \tau^i}{\partial t} + s^i \frac{\partial \Gamma^i}{\partial t} \right] - \frac{\tilde{r}}{\rho} \end{aligned} \quad (3.84)$$

Note that  $(p_0^i - p_0^u)$  is also a perturbation quantity, i.e.  $O(\epsilon)$  since

$$p_0^i = \bar{p}_{0-\infty} + \tilde{p}_0^i, \quad \tilde{p}_0^i / \bar{p}_{0-\infty} \ll 1$$

$$p_0^u = \bar{p}_{0-\infty} + \tilde{p}_0^u, \quad \tilde{p}_0^u / \bar{p}_{0-\infty} \ll 1$$

Due to the presence of the solid surfaces, represented by "bound"-vortices, we expect the perturbation pressure field to exhibit a continuous behavior in the blade-core flow region and a discontinuous behavior at the position of the blades, i.e. lifting surfaces, this can mathematically be represented as:

$$p^i - p_{-\infty} = p_c^i - p_{-\infty} + \overline{\Delta p} H_p(y') \quad (3.85)$$

where

$p_c^i \equiv$  the continuous pressure field

$\overline{\Delta p} \equiv$  the amplitude of the pressure discontinuity.

From (3.84)

$$p_0^i - \bar{p}_{0-\infty} = p^i - p_{-\infty} + \rho \bar{w} \tilde{\phi}_{x'}^i + O(\epsilon^2) = p_c^i - p_{-\infty} + \rho \bar{w} \tilde{\phi}_{x'}^i + \overline{\Delta p} H_p(y') \quad (3.86)$$

where

$$\tilde{\phi}_{x'}^i \equiv \frac{\partial}{\partial x'} \tilde{\phi}^i$$

We can also choose either  $\sigma^i$  or  $\tau^i$ , as expressed before, without any loss of generality, so long as  $\nabla^i \sigma^i \times \nabla^i \tau^i$  represents the "appropriate" vorticity component in the flow. Due to the nature of the freely-convected shed vortices, we expect  $\tau^i$  to depict the drift-time associated with the motion of the spinning-fluid particles in the interblade region, i.e.

$$\frac{D^i \tau^i}{Dt} = 1 \quad (3.87)$$

or

$$\tau^i = \frac{x^i}{\bar{W}} + O(\varepsilon), \quad \text{on the reference blade} \quad (3.88)$$

Substitution of (3.86), (3.87), and (3.88) into (3.84) yields

$$\begin{aligned} \nabla^i \sigma^i - \frac{D^i \sigma^i}{Dt} \frac{\hat{e}_{x^i}}{\bar{W}} + \frac{D^i \Gamma^i}{Dt} \hat{e}_z = \nabla^i \left[ \frac{p_c^i - p^u}{\rho} + \frac{\overline{\Delta p}}{\rho} H_p(y^i) + \rho \bar{W} (\tilde{\phi}_{x^i}^i - \tilde{\phi}_{x^i}^u) \right. \\ \left. + \frac{\partial}{\partial t} (\tilde{\phi}^i - \tilde{\phi}^u) + s^i \frac{\partial \Gamma^i}{\partial t} \right] - \frac{\tilde{F}}{\rho} \end{aligned} \quad (3.89)$$

The  $y^i$ -component of (3.89) is

$$\frac{\partial \sigma^i}{\partial y^i} = \frac{\partial}{\partial y^i} \left[ \frac{p_c^i - p^\infty}{\rho} + \frac{\overline{\Delta p}}{\rho} H_p(y^i) + \rho \bar{W} \tilde{\phi}_{x^i}^i + \frac{\partial \tilde{\phi}^i}{\partial t} + s^i \frac{\partial \Gamma^i}{\partial t} \right] - \frac{\tilde{F}}{\rho} \quad (3.90)$$

where

$$p_c \equiv p_c^i - p^u \quad (3.91)$$

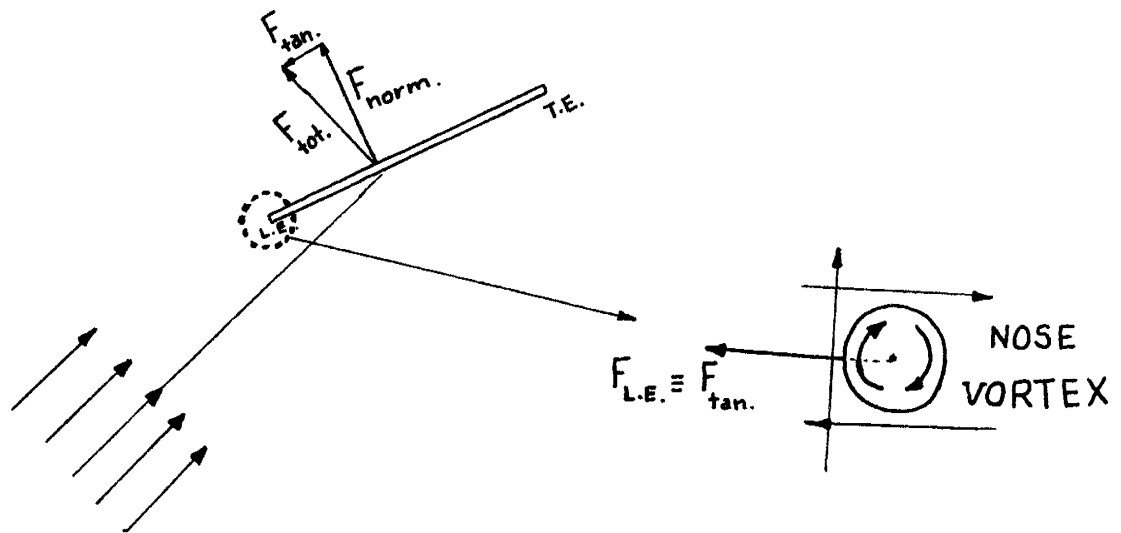
and

$$\tilde{\phi}^i \equiv \tilde{\phi}^i - \tilde{\phi}^u \quad (3.92)$$

and have recognized

$$\underline{F} = \tilde{F} \hat{e}_{y^i} + O(\varepsilon^2) \hat{e}_{x^i} \quad (3.93)$$

In the limit of negligible fluid viscosity, the streamwise component of the blade force is negligible (identically zero, for inviscid fluids, D'Alembert's paradox), but however a second order tangential force exists due to the presence of the finite leading-edge vortex, ("nose"-vortex), the so-called leading-edge suction force, to render the total inviscid-force acting on the blade, normal to the incoming stream.



Furthermore we recognize that the component of force normal to the blade surface is created by the "jumping" behavior of the pressure across the blade and in fact identically balances the jump of fluid pressure across its pressure and suction surfaces, i.e.

$$\bar{F} \hat{e}_{y'} = \overline{\Delta P} \delta_P(y') \hat{e}_{y'} \quad (3.94)$$

Note that (3.94) is dimensionally consistent, remembering

$$[\delta_P(y')] = \left[ \frac{1}{L} \right] \quad \text{and} \quad [\overline{\Delta P}] = \left[ \frac{F}{L^2} \right], \quad [\overline{\Delta P} \delta_P(y')] = \left[ \frac{F}{L^3} \right],$$



i.e. force density, consistent with the dimension of the l.h.s. of (3.94). Substitution of (3.94) into (3.92) identically cancels one term in the bracket, reducing (3.92) to

$$\frac{\partial \sigma^i}{\partial y^i} = \frac{\partial}{\partial y^i} \left[ \frac{p_c - p_{-\infty}}{\rho} + \bar{w} \tilde{w}'_{x^i} + \frac{\partial \tilde{\phi}^i}{\partial t} + s^i \frac{\partial \Gamma^i}{\partial t} \right] \quad (3.95)$$

where upon integration in  $y^i$ -direction, we get

$$\sigma^i = \frac{p_c - p_{-\infty}}{\rho} + \bar{w} \tilde{w}'_{x^i} + \tilde{\phi}'_t + s^i \Gamma^i_t + g(x^i, z, t) \quad (3.96)$$

where  $g(x^i, z, t)$  is a general function as a result of partial integration of (3.95). However, since we intend to determine the vorticity field exclusively by  $s^i$ ,  $\Gamma^i$ ,  $\sigma^i$ , and  $\tau^i$ , thus any general function can be ignored since its combined effect may be assumed to have been included in the perturbation potential  $\tilde{\phi}^i$ , i.e.

$$\sigma^i = \frac{p_c - p_{-\infty}}{\rho} + \bar{w} \tilde{w}'_{x^i} + \tilde{\phi}'_t + s^i \Gamma^i_t \quad (3.97)$$

Comparison of the  $x^i$ -derivative of (3.97) with the  $x^i$ -component of (3.92) results in

$$\frac{\partial \sigma^i}{\partial x^i} + \frac{1}{\bar{w}} \frac{\partial \sigma^i}{\partial t} = - \frac{\partial}{\partial x^i} \left( \frac{\overline{\Delta P}}{\rho \bar{w}} \right) H_p(y^i) \quad (3.98)$$

where

$$\frac{\overline{\Delta P}}{\rho \bar{w}} = \frac{F}{\rho \bar{w}} \equiv \gamma_{\text{BOUND}}(x^i, z, t) = \gamma_B(x^i, z) e^{i\omega t} \quad (3.99)$$

and  $\gamma_B \equiv$  the strength of the "bound"-vortex sheet.

The solution of (3.98), in terms of  $\gamma_B$ , can be written as:

$$\sigma^i = -\bar{W} \frac{\partial}{\partial x'} \left[ \int_0^{x'} \gamma_B(\xi, z) e^{i\omega(t - (x' - \xi)/\bar{W})} d\xi \right] H_p(y') \quad (3.100)$$

or via Leibniz-rule

$$\sigma^i = -\bar{W} \left[ \gamma_B(x', z) e^{i\omega t} - i \frac{\omega}{\bar{W}} e^{i\omega(t - x'/\bar{W})} \int_0^{x'} \gamma_B(\xi, z) e^{i(\omega\xi)/\bar{W}} d\xi \right] H_p(y') \quad (3.101)$$

The vorticity field inside and including the blades is now known to

be

$$\underline{\tilde{\Omega}}^i = \underline{\tilde{\Omega}}^u + \underline{\tilde{\Omega}}_{\text{blade}}^i \quad (3.102)$$

where

$$\underline{\tilde{\Omega}}^u = \nabla' \sigma'^u \times \nabla' \tau'^u$$

and

$$\begin{aligned} \underline{\tilde{\Omega}}_{\text{blade}}^i &= \nabla' \sigma'^i \times \nabla' \tau'^i + \nabla' s'^i \times \nabla' \Gamma'^i \Rightarrow \\ \underline{\tilde{\Omega}}_{\text{ref. blade}}^i &= \left[ \gamma_B(x', z) e^{i\omega t} - \frac{i\omega}{\bar{W}} e^{i\omega(t - x'/\bar{W})} \int_0^{x'} \gamma_B(\xi, z) e^{i(\omega\xi)/\bar{W}} d\xi \right] \delta(y') \hat{k} \\ &\quad - e^{i\omega(t - x'/\bar{W})} \frac{\partial}{\partial z} \int_0^{x'} \gamma_B(\xi, z) e^{i(\omega\xi)/\bar{W}} d\xi \delta(y') \hat{e}_x, \quad (3.103) \end{aligned}$$

The first term on the r.h.s. of (3.103) is the fluctuating "bound"-vorticity, concentrated at the reference blade, the axis of which points in the spanwise direction. The second term in the bracket in (3.103), is the freely-convected shed vorticity in the spanwise direction. These two

terms are consistent with the classical results, with the exception that the "bound" and free shed vorticity here are functions of span as well. The last term on the r.h.s. of (3.103) is indeed generated due to the spanwise dependence of the "bound"-vorticity and depicts the trailing vorticity strength in the streamwise direction, the strength of which is proportional to  $\partial\gamma_B/\partial z$ .

The vorticity induced on the  $m$ -th blade possesses a phase relation with respect to the reference blade, via a constant intra-blade phase angle,  $\beta$ , i.e.

$$\tilde{\Omega}_m = \tilde{\Omega}_{\text{ref}} \cdot e^{im\beta} \quad (3.104)$$

where

$$\beta = \frac{2\pi s}{\lambda} \quad (3.105)$$

(3.104) and (3.105) imply that the vorticity distribution on two adjacent blades would be in phase only if the blade spacing is an integer multiple of the disturbance wave length, or

$$s = k\lambda, \quad k = 1, 2, 3, \dots$$

With the introduction of the generalized coordinates  $x'_m$  and  $y'_m$  we can write  $\tilde{\Omega}_m$  as follows:

$$\begin{aligned} \tilde{\Omega}_m = & \left[ \gamma_B(x'_m, z) e^{i\omega t} - \frac{i\omega}{\bar{W}} e^{i\omega(t - x'_m/\bar{W})} \int_0^{x'_m} \gamma_B(\xi_m, z) e^{i\omega/\bar{W} \xi_m} d\xi_m \right] \delta(y'_m) \hat{k} \\ & - e^{i\omega(t - x'_m/\bar{W})} \frac{\partial}{\partial z} \int_0^{x'_m} \gamma_B(\xi_m, z) e^{i\omega/\bar{W} \xi_m} d\xi_m \delta(y'_m) \hat{e}_{x'} \end{aligned} \quad (3.106)$$

where

$$x'_m \equiv x' - ms'', \quad s'' \equiv s \sin \alpha \quad (3.107)$$

and

$$y'_m \equiv y' - ms', \quad s' \equiv s \cos \alpha \quad (3.108)$$

It is interesting to note that by modifying the perturbation potential, in the manner described as follows, we can reduce the multiple Clebsch-Hawthorne representation of the rotational perturbations in a single representation of the same type. This reduction simplifies the mathematical analysis of the Poisson equation considerably. First, making use of the following vector identity

$$\nabla'(s^i \Gamma^i) \equiv s^i \nabla' \Gamma^i + \Gamma^i \nabla' s^i \quad (3.109)$$

we can define a new potential  $\phi^i$ , where

$$\phi^i \equiv \tilde{\phi}^i + s^i \Gamma^i \quad (3.110)$$

and re-express the perturbation velocity field in terms of the newly defined potential as follows:

$$\underline{w}^i = \nabla' \phi^i + \sigma'^u \nabla' \tau'^u + \sigma^i \nabla' \tau^i - \Gamma^i \nabla' s^i \quad (3.111)$$

From our previous description of the Clebsch-Hawthorne scalars  $\sigma^i$ ,  $\tau^i$ ,  $s^i$ , and  $\Gamma^i$ , we note that

$$\begin{aligned} \sigma^i \nabla' \tau^i - \Gamma^i \nabla' s^i &= -H_p(y') \left[ \hat{e}_{x'} \frac{\partial}{\partial x'} + \hat{k} \frac{\partial}{\partial z} \right] \left[ \int_0^{x'_m} \gamma_B(\xi_m, z) e^{i\omega(t - \frac{x'_m - \xi_m}{\bar{w}})} d\xi_m \right] \\ &= H_p(y') \nabla' Q_m^i \end{aligned} \quad (3.112)$$

where

$$Q_m^i \equiv - \int_0^{x'_m} \gamma_B(\xi_m, z) e^{i\omega(t - (x'_m - \xi_m)/\bar{w})} d\xi_m \quad (3.113a)$$

or

$$Q_m^i \equiv - \int_0^{x'_m} \gamma_B(\xi, z) e^{i\omega(t - (x' - \xi)/\bar{w})} d\xi \cdot e^{im\beta} \quad (3.113b)$$

Thus, the perturbation velocity field is now expressible as

$$\underline{\tilde{w}}^i = \nabla' \phi^i + \sigma'^u \nabla' \tau'^u + H_p(y') \nabla' Q_m^i \quad (3.114)$$

Now, via the application of the continuity of the mass flow equation, for incompressible fluids, to (3.114) we get the Poisson's equation governing the perturbation potential  $\phi^i$

$$\nabla'^2 \phi^i = - \nabla' \sigma'^u \cdot \nabla' \tau'^u - \sigma'^u \nabla'^2 \tau'^u - H_p(y') \cdot \nabla' Q_m^i - H_p(y') \nabla'^2 Q_m^i \quad (3.115)$$

But, we have shown in the previous section that the first two terms on the r.h.s of (3.115) are of second order, and presented physical arguments for the mathematical elimination of these terms. Therefore, (3.115) reduces to

$$\nabla'^2 \phi^i = - \nabla' H_p(y') \cdot \nabla' Q_m^i - H_p(y') \nabla'^2 Q_m^i \quad (3.116)$$

Again, by modifying the potential  $\phi^i$ , via the following definition

$$\tilde{\Phi}^i \equiv \phi^i + Q_m^i H_p(y') \quad (3.117)$$

(3.116) transforms to

$$\begin{aligned}\nabla'^2 \tilde{\Phi}^i &= \nabla'^2 \Phi^i + Q_m^i \nabla'^2 H_p(y') + H_p \nabla'^2 Q_m^i \\ &= -\nabla' H_p(y') \cdot \nabla' Q_m^i + Q_m^i \nabla'^2 H_p(y')\end{aligned}\quad (3.118)$$

The first term on the r.h.s. of (3.118) is the scalar (dot) product of two orthogonal vectors, having zero-projection upon each other thence,

$$\nabla'^2 \tilde{\Phi}^i = Q_m^i \delta_p^i(y') \quad (3.119)$$

where

$$\nabla'^2 H_p(y') \equiv \delta_p^i(y') \equiv \frac{d}{dy'} [\delta_p(y')] \quad (3.120)$$

In terms of the new perturbation potential  $\tilde{\Phi}^i$ , the disturbance velocity field is then written as

$$\underline{\tilde{W}}^i = \nabla' \tilde{\Phi}^i + \sigma^{\tau u} \nabla' \tau^{\tau u} - Q_m^i \nabla' H_p(y') \quad (3.121)$$

### 3.2.3 Solution of the Poisson Equation for $\tilde{\Phi}^i$

The complete solution for the perturbation potential  $\tilde{\Phi}^i$ , in (3.119), is composed of a homogeneous solution,  $\tilde{\Phi}_h^i$ , satisfying the Laplace's equation

$$\nabla'^2 \tilde{\Phi}_h^i = 0 \quad (3.122)$$

and a particular solution,  $\tilde{\Phi}_{inhomogeneous}^i$ , which satisfies the Poisson's equation, (3.119), identically. The homogeneous contribution to the perturbation potential  $\tilde{\Phi}^i$ , in terms of Fourier series can be written as

$$\tilde{\Phi}_h^i = \sum_{m=-\infty}^{+\infty} C_{m_1}^i e^{-\lambda_m x'} + C_{m_2}^i e^{\lambda_m (x'-1)} e^{i(2m\pi+\beta)y'/s'} \cos\left(\frac{\pi z}{h}\right) e^{i\omega t} \quad (3.123)$$

where  $C_{m_1}^i$  and  $C_{m_2}^i$  are Fourier coefficients, and  $\lambda_m$  is the axial decay parameter  $\equiv \sqrt{\left(\frac{2m\pi+\beta}{s'}\right)^2 + \left(\frac{\pi}{h}\right)^2}$ .

In attempting to "guess" an inhomogeneous solution to (3.119) it will prove useful to Fourier analyze its "driving"-term, i.e.

$$\begin{aligned} \text{r.h.s. of (3.119)} &= Q_m^i \delta_p'(y') = \\ & x' \\ & - \int_0^{\infty} \gamma_B(\xi) e^{i\nu\xi} d\xi \cdot e^{-i\nu x'} \cdot e^{i\omega t} \cdot \cos\left(\frac{\pi z}{h}\right) \cdot \sum_{m=-\infty}^{+\infty} e^{im\beta} \delta'(y'-ms') \end{aligned} \quad (3.124)$$

where

$$\nu \equiv \frac{\omega}{\bar{W}} \quad (3.125)$$

is the reduced frequency, a nondimensional parameter controlling the response of the blades to unsteadiness in the flow, as will be shown in this section. Note that all lengths are nondimensionalized with respect to the chord,  $C \equiv 1$ , therefore  $\nu \equiv \omega/\bar{W}$  is the ratio of two time scales, one, the period of oscillation,  $T = 2\pi/\omega$  and two, the mean-particle-convection time over the blade chord,  $C/\bar{W}$ . The right-hand-side of (3.124) is written, making use of the following relation

$$\gamma_B(\xi_m, z) = \gamma_B(\xi, z) e^{im\beta} = \gamma_B(\xi) \cdot \cos\left(\frac{\pi z}{h}\right) e^{im\beta} \quad (3.126)$$

The series in (3.124) is summed over all the phased-periodic singularities, i.e. vortex sheets in the cascade. By utilizing the following Fourier expansions<sup>38,31</sup>

$$\sum_{m=-\infty}^{+\infty} e^{im\beta} \delta'(y' - ms') = \frac{d}{dy'} \left[ e^{i\beta y'/s'} \sum_{m=-\infty}^{+\infty} \delta(y' - ms') \right] \quad (3.127)$$

and

$$\sum_{m=-\infty}^{+\infty} \delta(y' - ms') = \frac{1}{s'} \sum_{m=-\infty}^{+\infty} e^{i2m\pi y'/s'} \quad (3.128)$$

The series on the r.h.s. of (3.124) can be written as

$$\sum_{m=-\infty}^{+\infty} e^{im\beta} \delta'(y' - ms') = \frac{i}{s'^2} \sum_{m=-\infty}^{+\infty} e^{i(2m\pi + \beta)y'/s'} \quad (3.129)$$

It is important to note that the convergence of the above series is only in the sense of the generalized functions, i.e., the series "converge" to the generalized functions they represent, but otherwise by "classical" tests for convergence of series, the above summations are divergent. However, we note that Dirac's delta-function is characterized by a singularity in the space and all of its derivatives are higher order singularity-functions in the space. Thence, it is only in the sense of these singularities that the above summations do converge.

The inhomogeneous solution to (3.119) can now be assumed to have the following form:

$$\tilde{\Phi}_i = \sum_{m=-\infty}^{+\infty} D_m e^{i(2m\pi + \beta)y'/s'} \cdot \cos\left(\frac{\pi z}{h}\right) \cdot f_m(x') \cdot e^{i\omega t} \quad (3.130)$$

via substitution of (3.130) into (3.119), we get

$$D_m = -i(2m\pi + \beta)/s'^2 \quad (3.131)$$

and



$$f_m''(x') - \lambda_m^2 f_m(x') = e^{-i\nu x'} \int_0^{x'} \gamma_B(x') e^{i\nu\xi} d\xi \equiv F(x') \quad (3.132)$$

The method of variation of parameter can be employed to arrive at

$$f_m(x') = e^{-\lambda_m x'} \int_{-\infty}^{x'} \frac{F(\xi)}{W} e^{\lambda_m \xi} d\xi - e^{\lambda_m x'} \int_{-\infty}^{x'} \frac{F(\xi)}{W} e^{-\lambda_m \xi} d\xi \quad (3.133)$$

where

$$W = \text{the Wronskian} = -2\lambda_m \quad (3.134)$$

and  $F(\xi)$  is defined in (3.132). Therefore

$$f_m(x') = -\frac{1}{2\lambda_m} \left\{ e^{-\lambda_m x'} \int_{-\infty}^{x'} F(\xi) e^{\lambda_m \xi} d\xi + e^{\lambda_m x'} \int_{x'}^{\infty} F(\xi) e^{-\lambda_m \xi} d\xi \right\} \quad (3.135)$$

Now, the total perturbation potential inside the blade row is the linear sum of the homogeneous,  $\tilde{\Phi}_h^i$ , and inhomogeneous,  $\tilde{\Phi}_i^i$ , solutions, i.e.

$$\tilde{\Phi}^i = \sum_{-\infty}^{+\infty} \left\{ \left[ C_{m_1}^i e^{-\lambda_m x'} + C_{m_2}^i e^{\lambda_m (x'-1)} \right] - \frac{i(2m\pi+\beta)}{2s'^2 \lambda_m} F_m(x') \right\} e^{i(2m\pi+\beta) y'/s'} \cdot \cos\left(\frac{\pi z}{h}\right) \cdot e^{i\omega t} \quad (3.136)$$

### 3.2.4 "Bound"-Vortex Distribution and the Kutta Condition

For the chordwise distribution of "bound"-vorticity, we follow the classical Glauert's method applied to thin airfoils, i.e.

$$\gamma_B(\theta) = a_0 \cot \frac{\theta}{2} + \sum_{r=1}^{\infty} a_r \sin r\theta \quad (3.137)$$

where

$$\theta \equiv \cos^{-1} (1-2x') \quad (3.138)$$

The first term in the Glauert's expansion, i.e.  $a_0 \cot \theta/2$ , represents the "bound"-vorticity distribution on a flat-airfoil inclined at a small angle of attack with respect to the stream. At the position of the leading-edge, i.e.  $\theta = 0$ , cotangent diverges, depicting the leading-edge singularity associated with the nose-vortex of a flat airfoil at an incidence. The series summation in Glauert's expansion represents the strength of a cambered vortex sheet at zero inclination (or incidence) with respect to the stream. The linearly combined vortex sheet strengths represents the "bound"-vortex distribution on a cambered airfoil at an angle of attack. The representation of (3.137) can still be applied to the nonstationary thin airfoils of zero-camber via the following rationale. An airfoil in a periodic gust experiences a fluctuating incidence angle, thus the instantaneous "bound"-vortex distribution creates a leading edge singularity, and in addition satisfies the Kutta condition, stated as the continuity of the static pressure at the trailing edge. These requirements are both met by the first term of the Glauert's expansion. Furthermore, the airfoil in disturbed stream experienced an up and down wash convected over its chord, posing as an "effective"-camber to the

airfoil, and thus the necessity of the series summation of the Glauert's method.

As stated above, the Kutta condition is the statement of the continuity of static pressure at the trailing edge of an airfoil, in both steady and unsteady streams. We have related the pressure "jump" across the cascade blades to the strength of the "bound"-vortex sheet via

$$\frac{\overline{\Delta p}}{\rho \bar{W}}(x', z) = \gamma_B(x', z)$$

At the trailing edge, i.e.  $x' = 1$ , or  $\theta = \pi$ , Kutta condition may be expressed as

$$\left. \frac{\overline{\Delta p}}{\rho \bar{W}} \right|_{\text{T.E.}} \equiv 0 \quad (3.139)$$

Thence

$$\left. \gamma_B \right|_{\text{T.E.}} \equiv 0 \quad (3.140)$$

which is noted to be satisfied in (3.137).

### 3.3 Analysis of the Flow Downstream of the Cascade

#### 3.3.1 Kinematics

The region downstream of the cascade is kinematically characterized by the presence of periodic wakes, emanating from the blades' trailing-edges. The neglect of viscosity, in our analysis, forces the wakes to remain in thin sheets, with zero lateral diffusion. The absence of body forces, in the downstream region, facilitates the free-convection of the shed vortices into the wakes. The shear in the upstream region is super-

imposed upon the potential region in between the vortex sheets. The vorticity vector in the wake can be decomposed into two different components, each arising from distinctly different origins, namely temporal behavior and spatial dependence of the "bound"-vorticity causes the span and streamwise vortices to be shed, in the wakes, respectively. Even though, the vortex structure in the downstream region, being made of free vortices, is simpler to physically model and to mathematically represent than the region within the cascade, yet we propose to formulate the downstream problem, both kinematically and dynamically, in the same manner as described in the blade-channel region. Small perturbation method is utilized to linearize the governing equations of motion, and thus the relative velocity field is assumed to be representable as:

$$\underline{w}^d = \underline{\bar{w}}^d + \underline{\tilde{w}}^d, \quad |\underline{\tilde{w}}^d|/|\underline{\bar{w}}^d| \ll 1 \quad (3.141)$$

where

$$\underline{\bar{w}}^d \equiv \bar{v}\hat{i} + U\hat{j} \quad (\equiv \underline{\bar{w}}^i \equiv \underline{\bar{w}}^u) \quad (3.142)$$

and

$$\underline{\tilde{w}}^d \equiv \nabla' \phi^d + \sigma'^u \nabla' \tau'^u + \sigma^d \nabla' \tau^d + s^d \nabla' \Gamma^d \quad (3.143)$$

where

$\phi^d \equiv$  the perturbation potential in downstream region

$\sigma'^u \nabla' \tau'^u \equiv$  the convected-upstream distortion velocity field

$\sigma^d \nabla' \tau^d \equiv$  the rotational contribution of the free-spanwise vorticity in the wake to the perturbation velocity field.

$s^d \nabla' \Gamma^d \equiv$  the rotational contribution of the free-stream vorticity in the wake to the perturbation velocity field.

The application of the incompressible-continuity equation to the fluid downstream of the cascade results in the Poisson's equation for the perturbation potential  $\tilde{\phi}^d$  where the Clebsch-Hawthorne parameters do contribute to  $\tilde{\phi}^d$  appearing as the driving-terms of the Poisson's equation, i.e.

$$\nabla' \cdot \underline{\tilde{W}}^d = 0 \quad (3.144)$$

(incompressible fluid in source-less flow)

or

$$\nabla' \cdot \underline{\tilde{W}}^d \equiv 0 \quad (\text{by definition}) \quad (3.145)$$

Thence

$$\nabla' \cdot \underline{\tilde{W}}^d = 0 \quad (3.146)$$

or

$$\nabla'^2 \tilde{\phi}^d = -\sigma^d \nabla'^2 \tau^d - \nabla' \sigma^d \cdot \nabla' \tau^d - s^d \nabla'^2 \Gamma^d - \nabla' s^d \cdot \nabla' \Gamma^d \quad (3.147)$$

The contributions of the upstream-distributed-shear to the perturbation potential is null, as was shown in Section 3.2.3, both mathematically and physically. The nature of the driving-terms in (3.147) are determined by the dynamics of the downstream flow.

### 3.3.2 Dynamics

The Euler momentum equation, with no body forces, represent the governing flow equation, in the dynamical sense, in the downstream region, i.e.

$$\frac{D' \underline{W}^d}{Dt} = -\frac{1}{\rho} \nabla' p^d \quad (3.148)$$

which upon linearization yields

$$\frac{\partial \bar{w}^d}{\partial t} + \bar{w}^d \frac{\partial}{\partial x'} \bar{w}^d = - \frac{1}{\rho} \nabla' \bar{p}^d \quad (3.149)$$

$$\frac{\partial \bar{w}^d}{\partial t} + \bar{w}^d \frac{\partial}{\partial x'} \tilde{w}^d + \tilde{w}^d \cdot \nabla' \bar{w}^d = - \frac{1}{\rho} \nabla' \tilde{p}^d \quad (3.150)$$

The mean-inviscid-momentum equation, (3.149), is identically satisfied, since  $\bar{w}^d$  is both space and time invariant and furthermore  $\bar{p}^d$ , by definition is independent of space. The perturbation momentum equation is, however, as yet unsatisfied. We propose to proceed, in solving (3.150), in the same manner as in the blade-channel region, except for the change in the behavior of the pressure field, namely the static pressure exhibits a continuous variation in the downstream region, as opposed to the "jumping"-characteristic of the static pressure field inside the blade row.

Mean-Bernoulli surfaces in the downstream region continue to be

$$z = \text{constant}$$

planes, thus in the same spirit as in the bladed region, we suggest

$$s^d \equiv z + O(\epsilon) \quad (3.151)$$

and from the strength of the free-streamwise vorticity in the reference wake

$$\gamma_{x'}^d = - \frac{\partial}{\partial z} \int_0^l \gamma_B(\xi, z) e^{i\nu\xi} d\xi \cdot e^{i\omega(t - x'/\bar{w})} \quad (3.152)$$

we can deduce

$$\Gamma_{\text{ref.}}^d = \frac{\partial}{\partial z} \int_0^l \gamma_B(\xi, z) e^{i\nu\xi} d\xi \cdot e^{i\omega(t - x'/\bar{w})} H(y') \quad (3.153)$$

while a generalized  $\Gamma^d$ , i.e.  $\Gamma_m^d$  on the m-th wake with respect to the reference wake, is

$$\Gamma_m^d = \Gamma^d \cdot e^{im\beta} H(y' - ms') \quad (3.154)$$

Vector operations, given in Appendix A, performed on the perturbation-momentum equation yields

$$\frac{D'\tau^d}{Dt} \nabla'\sigma^d - \frac{D'\sigma^d}{Dt} \nabla'\tau^d + \frac{D'\Gamma^d}{Dt} \hat{e}_z = \nabla' \left[ \frac{p^d - p_\infty}{\rho} + \rho W \tilde{\phi}_{x'} + \tilde{\phi}_t + s^d \Gamma_t^d \right] \quad (3.155)$$

From (3.153),

$$\frac{D'\Gamma^d}{Dt} = 0 \quad (3.156)^*$$

which is the statement of the Kelvin's Circulation Theorem for inviscid-barotropic fluids.

From the  $y'$ -component of (3.155), we get

$$\frac{\partial}{\partial y'} \sigma^d = \frac{\partial}{\partial y'} \left[ \frac{p^d - p_\infty}{\rho} + \bar{W} \tilde{\phi}_{x'} + \tilde{\phi}_t + s^d \Gamma_t^d \right] \quad (3.157)$$

where we have assumed that,  $\tau$ , in the downstream region continues to depict the drift-time of the fluid particles, i.e.

$$\frac{D'\tau^d}{Dt} = 1 \quad (3.158)$$

or to  $O(\epsilon)$

$$\tau^d = \frac{x'}{\bar{W}} \quad (3.159)$$

( $x'$ -reference is taken at the  $x' = 0$  plane).

\*Note that (3.156), due to the presence of "bound"-vortices, does not hold in the bladed region, i.e.  $D'\Gamma^d/Dt \neq 0$ .

Integration of (3.157) along  $y'$ -axis, results in

$$\sigma^d = \frac{\tilde{p}-p_{-\infty}}{\rho} + \bar{W}\tilde{\phi}_{x'} + \tilde{\phi}_t + s_{\Gamma_t}^d + h(x', z, t)$$

where  $h(x', z, t)$  is a general function, we can assume the contribution of which is "lumped" with the perturbation potential as explained in Section 3.2.2, i.e.

$$\sigma^d = \frac{\tilde{p}-p_{-\infty}}{\rho} + \bar{W}\tilde{\phi}_{x'} + \tilde{\phi}_t + s_{\Gamma_t}^d \quad (3.160)$$

Comparison of  $x'$ -derivative of (3.160) with the  $x'$ -component of (3.155) results in

$$\sigma_{x'}^d + \frac{1}{\bar{W}}\sigma_t^d = 0 \quad (3.161)$$

the general solution of which is

$$\sigma^d = \sigma^d(x' - \bar{W}t) \quad (3.162)$$

But, however, by drawing analogy with the blade-channel flow we can deduce that

$$\begin{aligned} \sigma^d &= -\bar{W} \frac{\partial}{\partial x'} \left[ \int_0^l \gamma_B(\xi, z) e^{i\omega(t - (x' - \xi)/\bar{W})} d\xi \right] H_p(y') \\ &= i\omega e^{i\omega(t - x'/\bar{W})} \int_0^l \gamma_B(\xi, z) e^{i\nu\xi} d\xi H_p(y') \end{aligned} \quad (3.163)$$

and note that it satisfies the property of the general solution (3.162) by





The Libraries  
Massachusetts Institute of Technology  
Cambridge, Massachusetts 02139

Institute Archives and Special Collections  
Room 14N-118  
(617) 253-5688

This is the most complete text of the  
thesis available. The following page(s)  
were not included in the copy of the  
thesis deposited in the Institute Archives  
by the author: p 6-1

which trails downstream of the reference blade) and

$$\frac{\tilde{\Omega}^d}{m} = \frac{\tilde{\Omega}^d}{\text{ref}} \cdot e^{im\beta} \delta(y' - ms') \quad (3.170)$$

Again, as in the bladed region, we can reduce the multiple Clebsch-Hawthorne formulation of the perturbation velocity field, to the single representation of the same type, by modifying the perturbation potential, details given in Section 3.2.2. We finally arrive at

$$\underline{w}^d = \nabla' \tilde{\Phi}^d + \sigma'^u \nabla' \tau'^u - Q_m^d \nabla' H_p(y') \quad (3.171)$$

where

$$Q_m^d = \int_0^l \gamma_B(\xi, z) e^{i\omega(t - (x' - \xi)/\bar{W})} d\xi \cdot e^{im\beta} \quad (3.172)$$

The Poisson's equation, governing the perturbation potential  $\tilde{\Phi}^d$ , is now expressible as

$$\nabla'^2 \tilde{\Phi}^d = Q_m^d \delta_p'(y') \quad (3.173)$$

### 3.3.2 Solution of the Poisson's Equation For $\tilde{\Phi}^d$

Due to the similarity of the governing equations for  $\tilde{\Phi}^d$  and  $\tilde{\Phi}^i$ , we propose to utilize the same technique in representing the perturbation potential  $\tilde{\Phi}^d$  as that which was developed, in detail, in Section 3.2.3. Thus the total solution is the linear sum of the homogeneous and particular (or inhomogeneous) parts i.e.

$$\tilde{\Phi}^d = \tilde{\Phi}_h^d + \tilde{\Phi}_i^d \quad (3.174)$$

where

$$\nabla'^2 \tilde{\phi}_h^d \equiv 0 \quad (3.175)$$

and

$$\nabla'^2 \tilde{\phi}_i^d = Q_m^d \delta_p'(y') \quad (3.176)$$

The solution to (3.175), in terms of the Fourier series representation,

is

$$\tilde{\phi}_h^d = \sum_{m=-\infty}^{+\infty} C_m^d e^{-\lambda_m(x'-1)} e^{i(2m\pi+\beta)y'/s'} \cdot \cos\left(\frac{\pi z}{h}\right) \cdot e^{i\omega t} \quad (3.177)$$

where

$$C_m^d \equiv \text{Fourier Coefficients}$$

and

$$\lambda_m \equiv \sqrt{\frac{2m\pi+\beta}{s'}^2 + \left(\frac{\pi}{h}\right)^2}, \text{ the axial decay parameter}$$

The "guess" at the inhomogeneous solution is facilitated by the Fourier series expansion of the periodic-generalized function, on the r.h.s. of (3.176), details of which is given in Section 3.2.3. Thus, without repetition, we can write

$$\tilde{\phi}_i^d = \sum_{m=-\infty}^{+\infty} \frac{i(2m\pi+\beta)\tilde{\Gamma}}{s'^2(\lambda_m^2+v^2)} e^{-ivx'} \cdot e^{i(2m\pi+\beta)y'/s'} \cdot \cos\left(\frac{\pi z}{h}\right) \cdot e^{i\omega t} \quad (3.178)$$

where

$$\tilde{\Gamma} \equiv \int_0^1 \gamma_B(\xi) e^{iv\xi} d\xi \quad (3.179)$$

and the total perturbation-potential in the downstream region is

$$\tilde{\phi}^d = \sum_{m=-\infty}^{+\infty} \left[ C_m^d e^{-\lambda_m (x'-1)} + \frac{i(2m\pi+\beta) \tilde{\Gamma}}{s'^2 (\lambda_m^2 + v^2)} e^{-ivx'} \right] e^{i(2m\pi+\beta) y'/s'} \cos\left(\frac{\pi z}{h}\right) \cdot e^{i\omega t} \quad (3.180)$$

### 3.4 Matching Conditions

The disturbance velocity fields in the upstream, within the blade row, and the downstream regions are not yet fully determined, as the Fourier coefficients in the descriptions of the perturbation potentials are as yet unknown. A set of compatibility conditions, stemming from the kinematics and dynamics of the fluid flow, are to be imposed at the planes of the interfaces, in order to establish a unified flow field.

One of the compatibility conditions to be imposed is

$$\tilde{W} \cdot \hat{e}_{x'} \Big|_{\text{interface}^-} = \tilde{W} \cdot \hat{e}_{x'} \Big|_{\text{interface}^+} \quad (3.181)$$

which is the statement of the continuity of the mass flow at the interface ( $x'=0$  and  $1$ ), a kinematical condition.

The condition (3.182) requires

$$\tilde{\phi}_{x'}^u \Big|_{x'=0} = \tilde{\phi}_{x'}^i \Big|_{x'=0^+} \quad (3.182)$$

and

$$\tilde{\phi}_{x'}^i \Big|_{x'=1^-} = \tilde{\phi}_{x'}^d \Big|_{x'=1^+} \quad (3.183)$$

The other matching condition at the interfaces is the continuity of the spanwise velocity, since the radial component of the blade

forces, in axial turbomachines in general, is negligibly small (due to nearly radial blade shapes), and in our problem, in particular, is identically zero, (3.93), i.e.

$$(F_{blade})_z \equiv 0 \quad (3.184)$$

Thus, via dynamical considerations, we impose the continuity of the radial velocity perturbations at the interfaces, i.e.

$$\tilde{W} \cdot \hat{r} \Big|_{\text{interface}^-} = \tilde{W} \cdot \hat{k} \Big|_{\text{interface}^+} \quad (3.185)$$

which again implies

$$\tilde{\Phi}_z^u \Big|_{x'=0^-} = \tilde{\Phi}_z^d \Big|_{x'=0^+} \quad (3.186)$$

and

$$\tilde{\Phi}_z^i \Big|_{x'=1^-} = \tilde{\Phi}_z^d \Big|_{x'=1^+} \quad (3.187)$$

The relations (3.182), (3.183), (3.186), and (3.187) provide the, kinematical and dynamical, linkage between different regions of the flow field. In two-dimensional problems, involving vortices, the application of the Biot-Savart law of induction, which integrates over all vorticity fields does not divide the space into subspaces and thus the compatibility conditions are not needed. However, in three-dimensional problems, where vortices are encountered in confined spaces, the strict application of the Biot-Savart law leads to paramount difficulties.\* Thus, since in our

---

\*Since each vortex produces images with respect to the bounding walls, and in turn those images produce further images, ad infinitum.

method of analysis, we have to divide the flow space into three characteristically distinct regions, and solve the governing equations regionally, each solution still remains "unaware" of other solutions, until the regions are communicated both kinematically and dynamically via the compatibility conditions. This is basically due to the fact that the potential regions in any part (say, within the blade row) are partially driven by the distant vortex fields (outside the designated region) and the necessity of the communication is apparent.

The application of (3.182), (3.183), (3.186), and (3.187) yields the following Fourier coefficients and thus render our solution completely known in terms of the "bound"-vortex distribution,

$$C_m^u = \frac{(2m\pi + \beta)}{2s^{\prime 2}} \left[ \frac{\tilde{\Gamma} e^{-i\nu}}{\lambda_m^2 + \nu^2} \left( \frac{\nu}{\lambda_m} + i \right) + \frac{i\bar{F}_2}{\lambda_m^2} \right] e^{-\lambda_m} - \frac{i(2m\pi + \beta)}{2s^{\prime 2} \lambda_m^2} \bar{F}_1 \quad (3.188)$$

where

$$\bar{F}_1 \equiv -\frac{1}{2} \int_0^l F(\xi) e^{-\lambda_m \xi} d\xi \quad (3.189)$$

and

$$\bar{F}_2 \equiv -\frac{e^{-\lambda_m}}{2} \int_0^l F(\xi) e^{\lambda_m \xi} d\xi \quad (3.190)$$

$$C_{m_1}^i = 0 \quad (3.191)$$

$$C_{m_2}^i = \frac{2m\pi + \beta}{2s^{\prime 2}} \left[ \frac{\tilde{\Gamma} e^{-i\nu}}{\lambda_m^2 + \nu^2} \left( \frac{\nu}{\lambda_m} + i \right) + \frac{i\bar{F}_2}{\lambda_m^2} \right] \quad (3.192)$$

and finally,

$$C_m^d = \frac{2m\pi + \beta}{2s^{\prime 2}} \left[ \frac{\tilde{\Gamma} e^{-i\nu}}{\lambda_m^2 + \nu^2} \left( \frac{\nu}{\lambda_m} - i \right) \right] \quad (3.193)$$

### 3.5 Boundary Condition On the Solid Surfaces

At the position of solid surfaces, i.e. inner and outer shrouds, and the blades, the condition of no fluid penetration, in general, is expressible mathematically as

$$\frac{Df}{Dt} \equiv \frac{\partial f}{\partial t} + (\underline{V} \cdot \nabla) f = 0 \quad (3.194)$$

where

$$f(x,y,z,t) = \text{constant} \quad (3.195)$$

represents the equation of solid surfaces, as a function of space and time, in the same frame of reference in which  $D/Dt$  of (3.194) is expressed. The equations of the hub and tip surfaces, in our problem, are

$$z = 0 \quad (3.196)$$

and

$$z = h(= \text{constant}) \quad (3.197)$$

and thus (3.194) demands that

$$\underline{W} \cdot \hat{k} = 0 \quad \text{on } z = 0 \text{ and } h \quad (3.198)$$

which implies\* that the normal component of the relative perturbation velocity field is zero at the casings, i.e.

$$\underline{\tilde{W}} \cdot \hat{k} = 0 \quad \text{on } z = 0 \text{ and } h \quad (3.199)$$

The consequence of (3.199) is

---

\*Since, the mean-flow has no component in the z-direction, i.e.

$$\underline{W} \cdot \hat{k} \equiv 0$$

$$\frac{\partial \tilde{\phi}^{u,i,d}}{\partial z} + \sigma^{i,u} \frac{\partial \tau^{i,u}}{\partial z} - Q_m^{i,d} \frac{\partial}{\partial z} H_p(y^i) = 0 \quad \text{on } z = 0 \text{ and } h \quad (3.200)$$

in which

$$\frac{\partial \tau^{i,u}}{\partial z} \equiv 0$$

and

$$\frac{\partial}{\partial z} H_p(y^i) \equiv 0$$

Thence

$$\left. \tilde{\phi}_z^{u,i,d} \right|_{z=0 \text{ and } h} = 0 \quad (3.201)$$

which is identically satisfied by the perturbation potentials described in the up, within and downstream of the cascade, i.e., since

$$\tilde{\phi}^{u,i,d} \sim \cos\left(\frac{\pi z}{h}\right) \quad (3.202)$$

then

$$\left. \tilde{\phi}_z^{u,i,d} \right|_{z=0 \text{ and } h} \equiv 0 \quad (3.203)$$

The equations of the blade surfaces in the moving frame, attached to the referenced blade, are\*

$$y^i = ms^i, \quad m = 0, \pm 1, \pm 2, \dots \quad (3.204)$$

where  $m = 0$  depicts the reference blade. Thus application of (3.194) and (3.204) to the flow in the bladed region yields

---

\*Note that the blade surface equations are time-independent in the rotor frame due to the non-vibrating nature of the blades in this problem. However, in general,  $y^i = y^i(t) = ms^i$ , where  $y^i(t)$  describes the displacement of the blades' vibrational mode as a function of time in the relative frame.



$$\underline{w}^i \cdot \hat{e}_{y_I} = 0 \quad \text{on } y' = ms' \quad (3.205)$$

or

$$\underline{\tilde{w}}^i \cdot \hat{e}_{y_I} = 0 \quad \text{on } y' = ms' \quad (3.206)$$

(Since  $\underline{\bar{w}}^i \cdot \hat{e}_{y_I} \equiv 0$ ).

We apply the condition (3.206) to (3.114) i.e.

$$\frac{\partial \phi^i}{\partial y'} + \sigma'^u \frac{\partial \tau'^u}{\partial y'} + H_p(y') \frac{\partial Q_m^i}{\partial y'} = 0 \quad \text{on } y' = ms'$$

Since the last term, i.e.

$$H_p(y') \frac{\partial Q_m^i}{\partial y'}$$

identically vanishes, due to  $Q_m^i \neq Q_m^i(y')$ . Thus

$$\frac{\partial \phi^i}{\partial y'} = - \sigma'^u \frac{\partial \tau'^u}{\partial y'} \quad \text{on } y' = ms' \quad (3.207)$$

The right-hand-side of (3.207) acts as the driving -source and is the normal downwash component of the inlet flow distortion, convected through the bladed region by the mean-flow. The left-hand-side of (3.207) is the normal velocity field, in the upwash direction, induced by the vortex sheets, to render the solid surfaces impenetrable.

Equation (3.207) is the basis for determination of strength of the "bound"-vortex sheets, as explained in the next Chapter, on the evaluation of the unsteady lift.

EVALUATION OF THE UNSTEADY LIFT4.1 Expression In Terms of the Bound-Vorticity

The theoretical analysis presented in Chapter 3 describes the static pressure (or the velocity) field inside the blade row as the sum of a continuous and a discontinuous field. The jump in the static pressure (or the velocity) field within the bladed region occurs at the blade locations, where the bound-vortices represent this character of the static pressure and the velocity fields. It is however the discontinuous behavior of the pressure, across the blades which generates a net resultant force, in the direction of the normal to the blade surfaces, which is related to the bound-vortex structure via (3.100),

$$\overline{\Delta P}(\xi, z, t) = \rho \bar{w} \gamma_B(\xi, z) e^{i\omega t}$$

on the reference blade. The integration of  $\overline{\Delta P}(\xi, z, t)$  over the blade chord yields the unsteady fluctuating force, as a function of span and time, i.e.

$$\underline{F}(z, t) = F(z, t) \hat{e}_y, \quad (4.1)$$

and

$$\begin{aligned} F(z, t) &= - \int_0^l \overline{\Delta P}(\xi, z, t) d\xi \\ &= - \rho \bar{w} \int_0^l \gamma_B(\xi, z) d\xi \cdot e^{i\omega t} \end{aligned} \quad (4.2)^*$$

---

\*Our definition of the bound-vorticity is in the clockwise sense which makes a positive pressure jump from the pressure to suction side,  $[\overline{\Delta P} H_p(y!)]$ , (as opposed to a negative-step in that direction). Thence, the sign in (4.2) stems from our convention (or definition) of the bound-vorticity.

The unsteady lift is thus expressible in terms of the bound-vortex structure on the blades, via (4.2), but however the  $\gamma$ -Bound as expressed by the Glauert's expansion series (3.138)

$$\gamma_B(\theta) = a_0 \cot \frac{\theta}{2} + \sum_{r=1}^{\infty} a_r \sin r\theta$$

where

$$\theta \equiv \cos^{-1} (1-2x')$$

possesses unknown coefficients,  $a_0, a_1, a_2, \dots, a_r, \dots$ . The method for their determination is presented in the following section.

#### 4.2 Determination of the Glauert-Coefficients

As explained in the section on the solid-surface boundary-conditions, 3.5, the condition of no flow through the blade surface requires that, {via (3.207)}

$$\frac{\partial \phi^i}{\partial y'} = -\sigma' u \frac{\partial \tau' u}{\partial y'}, \quad y' = ms'$$

which is a balance between the convected downwash, from the upstream distorted velocity field, and the vorticity-induced upwash at the blade surfaces. By satisfying the blade surface boundary condition at  $R$  points, along the chord, we will generate a matrix equation in  $R$  unknowns in the Glauert coefficients as,  $a_0, a_1, a_2, \dots, a_R$ , which provides an  $R$ -term approximation to the infinite series describing the bound-vorticity. It was originally shown by Whitehead that a six-term truncation of the Glauert series approximates the unknown coefficients to within four-digit accuracy, unless for the cascades of high solidity which the convergence rate

was poor. Whitehead equally spaced the six points along the reference blade chord, including the leading and trailing edges; and then evaluated the lift by the application of the trapezoidal-rule to the points midway in between the six points which satisfied the blade surface boundary conditions. The numerical evaluation of the Glauert coefficients in our analysis was formulated on the IBM 370/168, in the Information Processing Center of M.I.T., and utilized LEQTIC, a highly accurate subroutine in the IMSL (International Mathematical and Statistical Library) which inverted the complex coefficient matrix and produced a set of the Glauert-solutions. In the examples studied, the convergence of the coefficients to within three-digits accuracy was accomplished with an eight-term expansion of the series solution. The first point along the blade chord, in our numerical evaluation was slightly removed from the leading-edge position, since the L.E. is located on the boundary dividing the upstream and the bladed region (a singular point). However, the convergence rate of the perturbation potentials improves exponentially as the point of interest is removed further from the singularity. A sensitivity study was performed on the value of the force coefficients (defined in the following section) resulting from varying the position of the leading point, and a reasonable accuracy\* was obtained by positioning the first point, on the chord, at 5% of the leading-edge. Other points were equally spaced from each other along the chord and the last point was positioned at the trailing-edge.

---

\*It should be noted that points closer to the leading-edge, say within 1% of it, even though they predict the unsteady lift to a better accuracy but however require an unreasonable number of terms in the summation of the perturbation potential series.

### 4.3 Unsteady Force Coefficient

We have defined a complex force (or lift) coefficient as

$$C_F \equiv \frac{F}{\pi \rho C \bar{W} \tilde{W}_d e^{i\omega t}} \quad (4.3)$$

where

$F$   $\equiv$  the complex, reference blade force, and

$\tilde{W}_d$   $\equiv$  the amplitude of the inlet-convected downwash.

Dimensionally,  $C_F$  has the units of force per unit spanwise length and it thus represents a two-dimensional lift coefficient, normalized in the classical manner.

The magnitude of the force coefficient is defined as

$$|C_F| \equiv \frac{1}{\pi \rho C \bar{W} \tilde{W}_d} \left( F_{\text{REAL}}^2 + F_{\text{IMAG.}}^2 \right)^{1/2} \quad (4.4)$$

while the phase angle between the lift and the disturbance velocity field at the leading-edge is

$$\phi \equiv \tan^{-1} (F_{\text{IMAG.}}/F_{\text{REAL.}}) \quad (4.5)$$

and the phase angle between the unsteady lift and the steady response of the cascade to inlet distortions is

$$\tilde{\phi}_{\text{L.E.}} = \phi - \pi \quad (4.6)$$

---

\*Since there is a  $\pi$ -phase lag between the steady lift and the disturbance velocity field at the L.E.

The purpose of normalization of the blade force by  $\pi\rho C\bar{W} \tilde{W}_d e^{i\omega t}$  stems from our desire to compare the present theory results to well-established, two-dimensional, theoretical results, namely Whitehead's and Von Kármán - Sears. The results of the comparisons, including some three-dimensional study in the aspect ratios are discussed in the following Chapter.

RESULTS, CONCLUSIONS, AND SUGGESTIONS FOR FUTURE WORK5.1 Results and Conclusions

An unsteady, three-dimensional vortex theory is developed in Chapters 3 and 4 to calculate the component of unsteady lift in compressor cascades, with inlet flow distortions. The results of these calculations are reported and briefly discussed in this section, while suggestions for future work are given in the latter part of this Chapter.

Some numerical examples are worked out in the limit of infinite aspect ratio ( $h \rightarrow \infty$  while  $C$  remains constant,  $C \equiv 1$ ) as a check on validity of our numerical results versus the well-established two-dimensional theories. The theory by Whitehead, on the force and moment calculations for a vibrating cascade, has the capability of predicting unsteady response of rigid blades to inlet flow distortions, which we have utilized for the purpose of two-dimensional cascade comparisons. The theory developed by von Karman and Sears to treat the interaction of an isolated airfoil with transverse gust is used for the purpose of comparison between the low-solidity cascade results of the present theory and the isolated airfoil theory. In order to achieve a meaningful comparison between different theoretical results, we have non-dimensionalized\* the unsteady response of the blade force,  $F_{2D}(t)$ , by a group of parameters commonly accepted in the literature on unsteady flows, namely  $\pi\rho C\bar{W} \tilde{W}_d e^{i\omega t}$ , where  $\tilde{W}_d$  is the amplitude of the convected-downwash in the incoming stream. In Figure 11 we have represented the magnitude of the unsteady lift coefficient,

---

\*The  $(C_{F_{2D}})$  is the value of the force coefficient per unit span.

$|C_F|_{2D}$ , versus the reduced frequency,  $\nu$ , ranging from  $\nu \rightarrow 0$  to  $\nu = 2.0$ .

In approaching the  $\nu \rightarrow 0$  limit, we have kept the ratio of the inter-blade phase angle to the reduced frequency constant, i.e.,  $\beta/\nu = \text{constant}$ , as proposed by Horlock et al<sup>43</sup> as the "proper" approach to  $\nu \rightarrow 0$ , in the analysis of inlet-distortion problems. The example of Figure 11 considers a cascade of unit solidity (i.e.  $C/s \equiv 1$ ) and the blade setting or stagger angle of  $45^\circ$ , as typical values for compressor cascades. The present theory predicts the results of Whitehead reasonably well. There is a, generally, a difference of 7.5% between the theoretical predictions of Whitehead and the present theory. The small discrepancy between the two results is believed to be caused by the numerical evaluation of the unsteady response in the present theory, which neglected the contribution of the leading-edge in the calculation of the unsteady lift. In evaluating the lift, the lower limit of the integral over the bound-vorticity distribution was set at five percent - chord position downstream of the leading-edge\*, i.e.  $x' = 0.05$ , since the potential, i.e. the homogeneous part of the, solution of the Poisson's equation, in both the bladed and upstream regions diverge at the position of  $x' = 0$ ,\*\* i.e. at the boundary dividing the regions. In order to avoid this problem, one method is to take the principal-value (P.V.), or the average of the disturbances "just"-upstream (i.e.  $x' = -\epsilon$ ,  $0 < \epsilon \ll 1$ ) and immediately downstream, i.e.  $x' = +\epsilon$ , of the boundary point. This method effectively removes the singularity, i.e.

---

\*A sensitivity study was carried out for positioning the leading point along the blade chord and 5% proved a sensible choice. This point is discussed in more detail in Chapter 4.

\*\*See Eqs. (3.54) and (3.123). Both homogeneous solutions show decaying characteristics up- and downstream of  $x'=0$  point respectively and diverge at  $x'=0$  identically.



at  $x' = 0$ . The second method is to evaluate the disturbance a finite, but small, distance downstream of the point of singularity, i.e. where the solutions decay. The second method is less exact, but simpler than the first technique, in application, as far as the numerical evaluations are concerned. We have chosen the latter, more approximate, method, since the purpose of cross-checking the two theories has been in assessing the validity of our numerical calculations (and not necessarily on "perfect" matching of the two theories); and we believe Figure 11 alludes to this point. At the lower half of Figure 11 the phase angle between the unsteady component and the steady lift\* is plotted versus the reduced frequency. A fairly good agreement, in the phase angle, is observed between Whitehead's results and the present theory.

The response of a rectilinear cascade of solidity 0.5, or gap-to-chord ratio of 2.0, and the blade setting or stagger angle of  $45^\circ$ , to inlet disturbances is plotted versus the reduced frequency, in Figure 12. The results of the present theory approaches Whitehead's in the range of  $0 < v < 1.1$  and approaches the Sears theory for  $v > 1.1$ . The behavior of approaching the isolated-airfoil result (i.e. Sears  $S/c = \infty$ ) by the low-solidity cascades is expected since the aerodynamic interference, between the blades, or equivalently the blade-to-blade effect is reduced as the ratio of gap-to-chord is increased. At  $v = 0$ , Sears result predicts the classical isolated-airfoil lift coefficient in steady flows (i.e. Sears result reduces to  $C_L = 2\pi i$ , where  $i \equiv$  angle of attack for a zero-camber airfoil inclined at an angle  $i$  with respect to the stream), while both

---

\*The phase angle between the steady component of lift and the inlet disturbance velocity field is  $\pi$  ( $180^\circ$ ), thus

$$\tilde{\phi}_{L.E.} = \tan^{-1}[F_{imag}/F_{real}] - 180^\circ$$

Whitehead's and the present theory's results approach the quasi-steady cascade lift coefficient, which has the same magnitude as the steady lift coefficient for cascades, but its phase angle lags the steady lift by nearly  $45^\circ$ <sup>42,43</sup>. The comparison of the phase angles in Figure 12 is, otherwise good over the range of the plotted reduced frequencies, (i.e. good except for  $\nu \rightarrow 0$ ).

In Figure 13, two gap-to-chord ratios of 2.0 and 3.0 are compared with the isolated-airfoil theory of Sears. Within the reduced-frequency range of 1.0 to 2.0, the three results approach each other considerably (i.e. in the fully-unsteady regime), while maximum deviation occurs at reduced frequencies corresponding to quasi-steady limit. The phase angle plot shows that the cascade solidity of 1/2 compares closer to the isolated airfoil case for  $\nu > 0.85$ , while for the reduced frequencies up to nearly 0.85, the lower solidity cascade (i.e.  $S/c = 1/3$ ) compares better with Sears phase angle.

The comparison of the cascade response in different gap-to-chord ratio configurations (in the two-dimensional limit) suggests<sup>44</sup> that at lower solidities the magnitude of the unsteady lift undergoes a more noticeable variation, while in the higher solidity cascades the response is somewhat less noticeably varying, with respect to the reduced-frequency. The implication of this result finds immediate use in simplifying the analysis of the problems involving the interaction of high-solidity cascades with inlet disturbances, which allows for a quasi-steady analysis to be performed (i.e.  $\nu \rightarrow 0$  and  $\beta/\nu = \text{constant}$ ), with the condition of constant leaving angle imposed at the cascade trailing-edge.

The effect of the aspect ratio is studied in Figure 14. Three

examples are worked out for the cascade solidity of one and stagger angle of  $45^\circ$  (as "typical" cascade parameters) with three different blade heights, keeping the chord length constant ( $\Xi 1$ ). We have plotted the magnitude and the phase angle response (of the blades) versus the reduced-frequency in Figure 14. The magnitude of the unsteady lift, for all examined aspect ratios, (i.e.  $AR = 1/3, 1$  and  $3$ ), in general, run parallel to each other. The magnitude of  $C_F$  is slightly damped as the aspect ratio is decreased from the cases studied. A maximum difference of nearly 15% between the aspect ratios of  $1/3$  and  $3$  can be observed, while only 6% difference between aspect ratios of  $1$  and  $3$  exists. An explanation offered<sup>44</sup> for the minuteness of the magnitude change of the blade response, due to three-dimensional effects, which suggests that the change of the blade height (i.e.  $h$ ) even though changes the strength of the shear in the upstream flow, locally, and consequently the strength of the streamwise vorticity in the blade wakes (i.e. in the downstream region), it yields the same integrated effect, induced over the blades by, the trailing vortex sheets. This is, basically due to the fact that the functional form of the inlet spanwise disturbance is kept fixed in all cases  $\sim \cos(\pi z/h)$ . The minor change in the magnitude of the response is, however, caused by the invariance of the blade chord length, in the cases of different aspect ratio studies, which effectively displaces the trailing wakes either closer to the blades (high AR) or removes them further from the blades, in the case of low AR. The plot of the phase angle in Figure 14 shows small deviation between AR of  $3$  and  $1$ , while the aspect ratio of  $1/3$  differs by nearly  $10^\circ$  (or 25%) with respect to the phase angle corresponding to  $AR = 3$ . In order to view the

complex blade response at different blade heights, in a unified manner, we have plotted the real component of  $C_F$  versus its imaginary component in a phase-diagram, Figure 15. In this Figure, we can observe a general (and gradual) migration of the response-loops from higher  $(C_F)_{\text{imag.}}$  components towards lower  $(C_F)_{\text{imag.}}$  levels as the blade height-to-chord ratio is decreased. The implication of this trend of migration, points to the importance of three-dimensional effects on the development of the phase angle and to its rather minimal (or unimportant) contribution to the magnitude of the three-dimensional unsteady lift coefficient, as the response loops maintain their range over the real axis.

The conclusions reached in this analysis, regarding the two- and three-dimensional response of cascades to inlet flow distortions, can now be summarized as follows:

i) The three-dimensional effects are most pronounced and important in changing the phase angle of the unsteady lift.

ii) The three-dimensional effects are minimal, as far as the magnitude of three-dimensional response is concerned, within the assumptions of the present theory (the most important of which, zero-loading and small shear).

iii) The lower solidity cascades develop a wider response to the inlet flow non-uniformities and thus unsteady analyses should be performed in estimating the fluctuating lift coefficient for such configurations.

iv) The higher solidity cascades tend to behave more according to the quasi-steady limit, even in the upper ranges of the reduced-frequency. Therefore a quasi-steady analysis with the constant-cascade-leaving-angle

assumption provides adequate approximation for the force coefficient.

## 5.2 Suggestions for Future Work

The development of the present theory, hopefully, has demonstrated new potentials for the analytical formulation of the more difficult, i.e. the more practical, problems in the unsteady flows in turbomachines.

A few of the following suggestions, however, are immediately in the light of the present theory, namely, the study of the three-dimensionally vibrating blades driven into self-induced instabilities by the working fluid, i.e. flutter, within the same limitations as the present theory. We believe the conclusion (i) reached in the last section, (the rather large change of the three-dimensional unsteady phase angle response to inlet disturbances, may have important effects in altering the compressor stage flutter boundaries, by sufficient margins, as to warrant a fully three-dimensional study (as opposed to the currently used Strip-theory). This problem of vibrating blades (with common intro-blade phase angle) of general mode shape is analytically formulated by the author and will undergo numerical studies shortly.

In order to isolate the effect of three-dimensionality, and study its effect, we need to compare the results of the present theory with the Strip-theory. In both the above mentioned suggestions the higher solidity as well as the larger stagger angles to the cascades need to be studied in detail.

As explained in the Introductory Chapter, the aim of the present theory has been in developing a rather "unfamiliar" and yet very powerful method of analysis which allows for the eventual generalization to the problems of practical importance. To this end, new parameter spaces need

to be explored, with emphasis on the finite-blade-camber and large, overall, turning cascades, first in the rectilinear geometries. Then by imposing a "gravitational-type" acceleration field,<sup>45</sup> as a function of blade span, try to simulate some of the effects of annular geometry.

Finally, the compressibility of the fluid needs to be taken into account, however it doesn't seem to be of immediate concern. It is more desirable to remove the small-inviscid-shear assumption from the present theory and explore the problems with inlet flow distortions described by i) large-inviscid-shear, ii) small-viscous-shear, and iii) larger-viscous shear. However, it is believed that exploring new parameter spaces, as diversified as described above, require ingenuity and by no means they are achieved by straight forward application of the present theory.

VECTOR IDENTITIES APPLIED TO EQUATION OF MOTION

One of the major steps in our analysis is the vector manipulation of the dynamical equation of motion, which lead to derivation of key equations (3.23) and (3.78). In this Appendix the vector identities and operations are listed according to the order in which they are used in the following derivation.

The inviscid-momentum equation

$$\frac{D\underline{V}}{Dt} = -\frac{1}{\rho} \nabla p + \frac{\underline{F}}{\rho} \quad (\text{A.1})$$

can be written as

$$\frac{\partial \underline{V}}{\partial t} + (\underline{V} \cdot \nabla) \underline{V} = -\frac{1}{\rho} \nabla p + \frac{\underline{F}}{\rho} \quad (\text{A.2})$$

via vector identity

$$(\underline{V} \cdot \nabla) \underline{V} \equiv \nabla \frac{V^2}{2} - \underline{V} \times (\nabla \times \underline{V}) \quad (\text{A.3})$$

(A.2) becomes

$$\frac{\partial \underline{V}}{\partial t} - \underline{V} \times \underline{\Omega} = -\nabla \left\{ \frac{p}{\rho} + \frac{V^2}{2} \right\} + \frac{\underline{F}}{\rho} \quad (\text{A.4})$$

Now, upon linearization of (A.4), via

$$\underline{V} = \bar{\underline{V}} + \tilde{\underline{V}}, \quad |\tilde{\underline{V}}| / |\bar{\underline{V}}| \ll 1 \quad (\text{A.5})$$

$$p = \bar{p} + \tilde{p}, \quad \tilde{p}/\bar{p} \ll 1 \quad (\text{A.6})$$

$$\underline{\Omega} = \bar{\underline{\Omega}} + \tilde{\underline{\Omega}} \quad (\text{A.7})$$

$$\underline{F} = \underline{\bar{F}} + \underline{\tilde{F}} \quad (\text{A.8})$$

where

$\underline{\bar{V}} \equiv$  mean-velocity field, in our problem  $\underline{\bar{V}}$  is steady and irrotational, i.e.  $\underline{\bar{\Omega}} \equiv 0$ , and

$$\underline{\tilde{V}} = \nabla\phi + \sigma\nabla\tau \quad (\text{A.9})$$

we get

$$\frac{\partial \underline{V}}{\partial t} - \underline{\bar{V}} \times \underline{\tilde{\Omega}} = -\nabla\left(\frac{p}{\rho} + \underline{\bar{V}}\underline{\tilde{V}}\right) + \frac{\underline{\tilde{F}}}{\rho} + O(\epsilon^2) \quad (\text{A.10})$$

where

$$\underline{\tilde{\Omega}} \equiv \text{curl } \underline{\tilde{V}} = \nabla\sigma \times \nabla\tau \quad (\text{A.11})$$

By making use of the following vector identity

$$\underline{A} \times (\underline{B} \times \underline{C}) \equiv (\underline{A} \cdot \underline{C})\underline{B} - (\underline{A} \cdot \underline{B})\underline{C} \quad (\text{A.12})$$

we can write

$$\underline{\bar{V}} \times \underline{\tilde{\Omega}} = \underline{\bar{V}} \times (\nabla\sigma \times \nabla\tau) \equiv (\underline{\bar{V}} \cdot \nabla\tau)\nabla\sigma - (\underline{\bar{V}} \cdot \nabla\sigma)\nabla\tau \quad (\text{A.13})$$

Furthermore

$$\frac{\partial \underline{V}}{\partial t} = \frac{\partial}{\partial t} (\nabla\phi + \sigma\nabla\tau) \equiv \nabla\left(\frac{\partial\phi}{\partial t}\right) + \frac{\partial}{\partial t} (\sigma\nabla\tau) \quad (\text{A.14})$$

and

$$\frac{\partial}{\partial t} (\sigma\nabla\tau) \equiv \frac{\partial\sigma}{\partial t} \nabla\tau - \frac{\partial\tau}{\partial t} \nabla\sigma + \nabla\left(\sigma \frac{\partial\tau}{\partial t}\right) \quad (\text{A.15})$$

Thence



$$\frac{\partial \tilde{Y}}{\partial t} = \nabla \left( \frac{\partial \tilde{\phi}}{\partial t} \right) + \frac{\partial \sigma}{\partial t} \nabla \tau - \frac{\partial \tau}{\partial t} \nabla \sigma + \nabla \left( \sigma \frac{\partial \tau}{\partial t} \right) \quad (\text{A.16})$$

The inclusion of (A.13) and (A.16) into (A.10) yields

$$\begin{aligned} \nabla \left( \frac{\partial \tilde{\phi}}{\partial t} \right) + \frac{\partial \sigma}{\partial t} \nabla \tau - \frac{\partial \tau}{\partial t} \nabla \sigma + \nabla \left( \sigma \frac{\partial \tau}{\partial t} \right) - (\underline{\tilde{V}} \cdot \nabla \tau) \nabla \sigma + (\underline{\tilde{V}} \cdot \nabla \sigma) \nabla \tau = \\ - \nabla \left( \frac{\tilde{p}}{\rho} + \tilde{V} V \right) + \frac{\tilde{F}}{\rho} + O(\epsilon^2) \end{aligned} \quad (\text{A.17})$$

Rearranging (A.17) results in

$$\left( \frac{\partial \sigma}{\partial t} + \underline{\tilde{V}} \cdot \nabla \sigma \right) \nabla \tau - \left( \frac{\partial \tau}{\partial t} + \underline{\tilde{V}} \cdot \nabla \tau \right) \nabla \sigma = - \nabla \left[ \frac{\tilde{p}}{\rho} + \tilde{V} V + \frac{\partial \tilde{\phi}}{\partial t} + \sigma \frac{\partial \tau}{\partial t} \right] + \frac{\tilde{F}}{\rho} + O(\epsilon^2)$$

By recognizing the terms in the parentheses as the Eulerian derivative of  $\sigma$  and  $\tau$  (in the linearized sense) we conclude that (A.1) is reducible to

$$\frac{D_0 \sigma}{Dt} \nabla \tau - \frac{D_0 \tau}{Dt} \nabla \sigma = - \nabla \left[ \frac{\tilde{p}}{\rho} + \tilde{V} V + \frac{\partial \tilde{\phi}}{\partial t} + \sigma \frac{\partial \tau}{\partial t} \right] + \frac{\tilde{F}}{\rho} + O(\epsilon^2) \quad (\text{A.18})$$

where

$$\frac{D_0}{Dt} \equiv \frac{\partial}{\partial t} + \underline{\tilde{V}} \cdot \nabla$$

## APPENDIX B

ON THE CLEBSCH-HAWTHORNE PARAMETERS AND THE DEGREE OF ARBITRARINESS

The idea of representing a vector field by the sum of a potential and a solenoidal field is a sound mathematical idea which has found extensive use in the classical field theory, and more recently in fluid flow problems with vorticity.

In the same spirit, we decompose the velocity field, inside a turbomachine, into a potential and a "rotational" contribution, where the vector operation of "curl" on the rotational term(s) describes the pertaining vorticity field in the flow, i.e.,

$$\underline{V} = \nabla\phi + \underline{A} \quad (\text{B.1})$$

where

$$\underline{\Omega} \equiv \text{curl } \underline{V} = \nabla \times \underline{A} \quad (\text{B.2})$$

But, however, we note that the governing equations of motion, i.e. linear-momentum equations, continuity of the mass flow, the energy equation and the equation of the state, are unable to fully determine the velocity field represented by (B.1). Since the system of equations, i.e. three momentum, one continuity, one energy and one state equation, can simultaneously be solved for six unknowns, in general, while the number of unknowns, with (B.1) representation of the velocity field, is seven, i.e.  $\phi$ ,  $A_x$ ,  $A_y$ ,  $A_z$ ,  $p$ ,  $\rho$ , and  $T$ . However, if  $\underline{A}$  were to be described as a solenoidal field, then

$$\nabla \cdot \underline{A} \equiv 0 \quad (\text{B.3})$$

which would have supplied the seventh equation.

The Clebsch-Hawthorne formulation of the rotational perturbation term

$$\underline{A} = \sigma \nabla \tau \quad (\text{B.4})$$

reduces the number of unknowns in  $\underline{A}$  from three to two unknowns  $\sigma$  and  $\tau$ , i.e. via the Clebsch-Hawthorne technique, we no longer need to specify that the non-potential perturbation is solenoidal. However, if we wish to represent the rotational perturbation term by multiple Clebsch-Hawthorne type contributions, as we did in Section 3.2, then we have introduced more parameters than the governing equations can determine, which leaves a degree of arbitrariness in choosing certain parameters of the rotational perturbation. For example, in the bladed-region or downstream of the cascade, we represented the perturbation velocity field by

$$\underline{\tilde{V}} = \nabla \phi + \sigma \nabla \tau + S \nabla \Gamma + \sigma^u \nabla \tau^u \quad (\text{B.5})$$

which had a total of five (5) unknowns,\* instead of the three components of  $\underline{\tilde{V}}$ , i.e. in order to determine the three components of  $\underline{\tilde{V}}$ , we need to calculate five parameters  $\phi$ ,  $\sigma$ ,  $\tau$ ,  $S$ , and  $\Gamma$ . Therefore, in rendering the problem solvable, we choose to specify  $S$  and  $\tau$ , based on the physical arguments, to represent the mean-Bernoulli and "drift"-surfaces, in the flow, respectively. It is clear however that why our choice is limited to one parameter from each Clebsch-Hawthorne perturbations as opposed to choosing both parameters from the same Clebsch-Hawthorne perturbation. The latter choice, even though leads to a dynamically consistent flow, but  $\sigma^u$  and  $\tau^u$  were known from the upstream flow

however the flow structure may be kinematically inconsistent, since

$$\underline{\Omega}_{\text{blade}} \equiv \nabla\sigma \times \nabla\tau + \nabla S \times \nabla\Gamma \quad (\text{B.6})$$

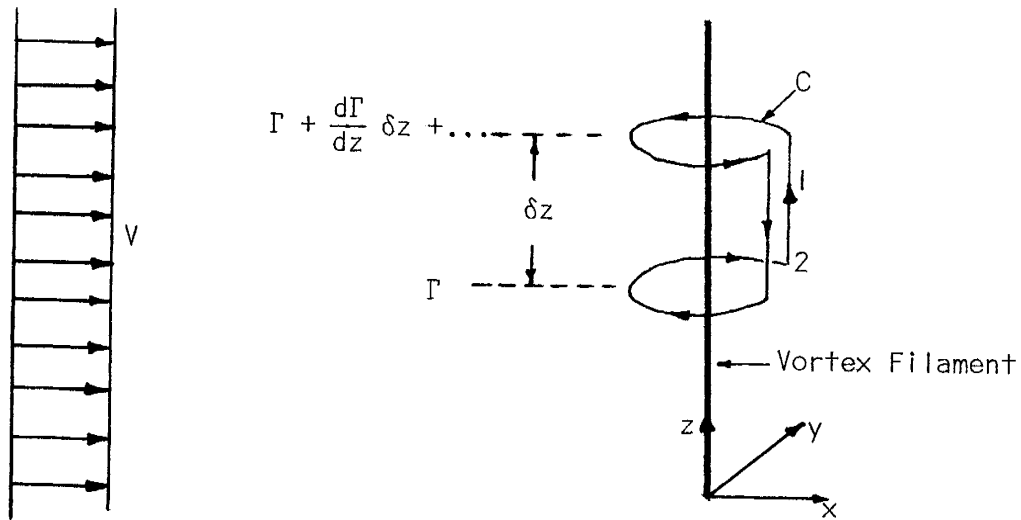
and our choice of  $\sigma$  and  $\tau$  (or  $S$  and  $\Gamma$ ) may produce an "extraneous" component for the blade vorticity.

Thus, it may be concluded that, in a double Clebsch-Hawthorne presentation of the rotational perturbations we have the freedom of choosing a single parameter from each Clebsch-Hawthorne perturbation, provided that our choice does not lead to a kinematically inconsistent flow, or in other words (B.6) should only contain the components of vorticity dictated by the nature of the flow problem.

## APPENDIX C

RELATION BETWEEN THE STREAMWISE VORTICITY AND THE  
SPANWISE DISTRIBUTION OF  $\gamma_{\text{BOUND}}$  IN UNSTEADY FLOWS

Consider a bound-vortex filament in a steady flow. If the strength of this vortex tube varies along its axis, then by considering the following contour wrapped around the filament, we can deduce that a shear flow along the axis of the tube exists, downstream of the filament.

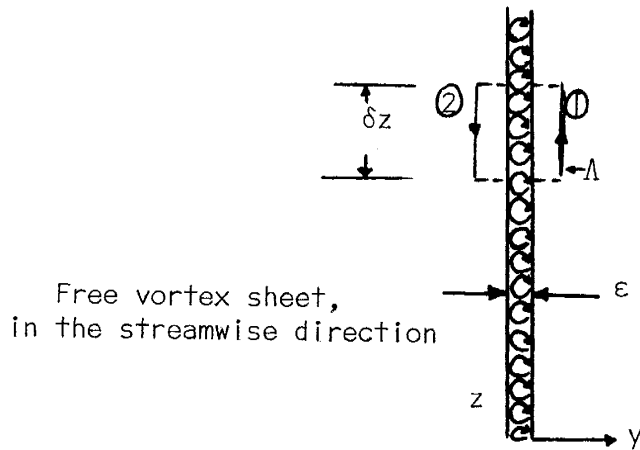


$$\oint_C \underline{y} \cdot d\underline{l} = 0 \quad (\text{C.1})$$

$$\Gamma + \frac{d\Gamma}{dz} \delta z - \Gamma + (v_1 - v_2) \delta z = 0 \quad (\text{C.2})$$

$$\frac{d\Gamma}{dz} = - (v_1 - v_2) \quad (\text{C.3})$$

From the kinematics of free-vortex sheets, the local jump in the tangential velocity is equal to the strength of the sheet



From identity,

$$\oint \frac{\mathbf{v}}{\Lambda} \cdot d\mathbf{l} \equiv -\Omega \cdot \delta z \cdot \epsilon \quad (\text{C.4})$$

we get

$$(v_1 - v_2) \delta z = -\Omega \cdot \delta z \cdot \epsilon$$

and

$$-\Omega \cdot \epsilon \equiv \gamma_{\text{sheet}} \Big|_{\text{in the clockwise direction}} \quad (\text{C.5})$$

thus

$$v_1 - v_2 = \gamma_{\text{sheet}} \quad (\text{C.6})$$

From (C.3) and (C.6), we can deduce that

$$\frac{d\Gamma}{dz} = -\gamma_{\text{sheet}} \quad (\text{C.7})^*$$

and since the axis of the trailing vortex sheet is in the x-direction we can rewrite (C.7) as

---

\*Note that the minus sign signifies an inverse relationship between the slope of  $\Gamma(z)$  and the direction of the axis of the trailing vorticity, i.e. if

$$\frac{\Delta\Gamma}{\Delta z} \equiv \frac{\Gamma(z+\Delta z) - \Gamma(z)}{\Delta z} > 0$$

then the streamwise vorticity points in the negative x-direction and viceversa.

$$\frac{d\Gamma}{dz} = - (\gamma_x)_{\text{sheet}} \quad (\text{C.8})$$

Now, we can replace the circulation around the vortex filament,  $\Gamma$ , by the integral of the elemental circulations around a distribution of bound vortices (say, over the chord length,  $C$ )

$$\Gamma = \int_0^C \gamma_B(\xi, z) d\xi \quad (\text{C.9})$$

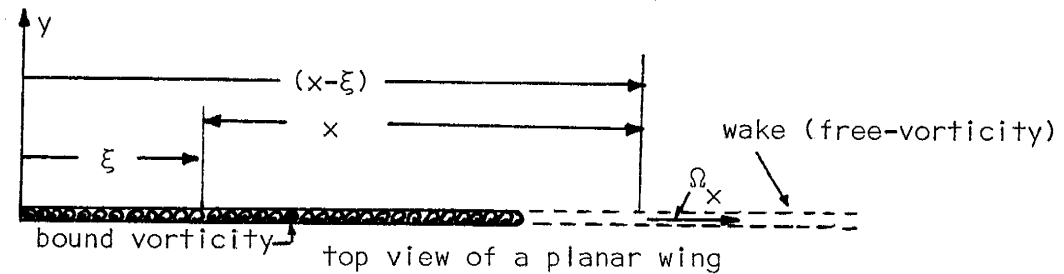
Thus the strength of the trailing vortex sheet via (C.8) and (C.9) can be written as

$$(\gamma_x)_{\text{sheet}} = - \frac{d}{dz} \int_0^C \gamma_B(\xi, z) d\xi = - \int_0^C \frac{\partial \gamma_B}{\partial z}(\xi, z) d\xi \quad (\text{C.10})$$

(differentiation via Leibniz rule).

The shear in the downstream region, created by the trailing vortex sheet, is convected by the mean flow; and associated with this convection, there is a finite time for an element of free-streamwise vorticity to move from its point of creation,  $\xi$  on the chord, to any point in the wake,  $x$ , that is

$$\text{Free Convection - Time} = \frac{x - \xi}{V} \quad (\text{C.11})$$



Since the mechanism for generating the Prandtl-type streamwise vorticity is totally based on the variation of bound-vorticity strength along its axis, the temporal behavior of  $\gamma_B$  enters (C.10) by introducing the convection-time lag of (C.11) i.e.

$$\gamma_x(x,t) \Big|_{\text{wake}} = - \int_0^C \frac{\partial \gamma_B}{\partial z} (\xi, z, t) \Big|_{t=t - (x-\xi)/\bar{V}} d\xi \quad (\text{C.12})$$

If the point  $x$  is located on the chord, then

$$\gamma_x(x,t) \Big|_{\text{blade}} = - \int_0^x \frac{\partial \gamma_B}{\partial z} (\xi, z, t) \Big|_{t=t - (x-\xi)/\bar{V}} d\xi \quad (\text{C.13})$$

And finally for a harmonic fluctuation of  $\gamma_B$  in time, i.e.

$$\gamma_B(\xi, z, t) = \gamma_B(\xi, z) e^{i\omega t} \quad (\text{C.14})$$

$$\gamma_x(x,t) \Big|_{\text{wake, blade}} = - \int_0^{C,x} \frac{\partial \gamma_B}{\partial z} (\xi, z) e^{i\omega(t - (x-\xi)/\bar{V})} d\xi \quad (\text{C.15})$$



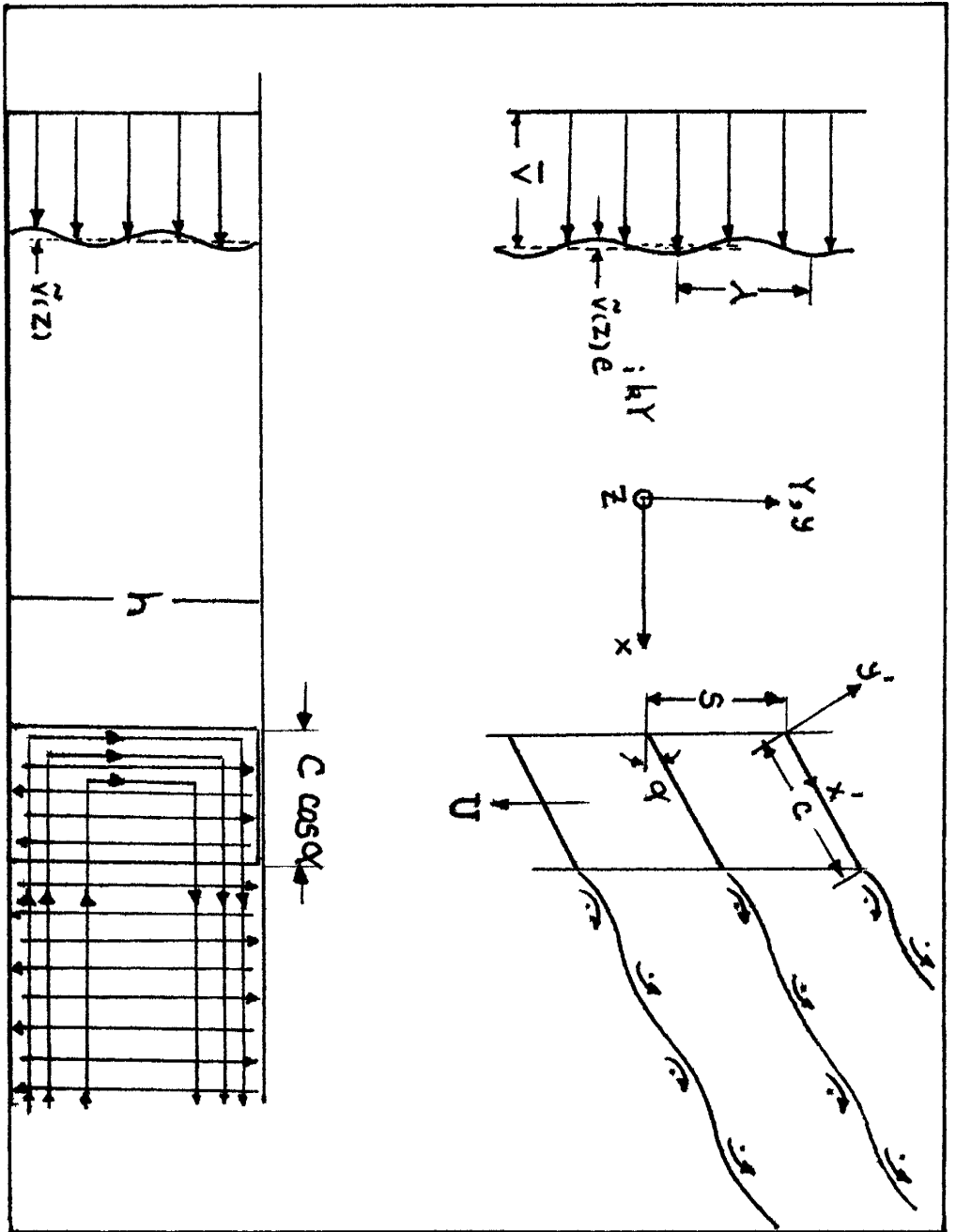


Figure 1. Schematic of the fundamental harmonics of the pitch- and spanwise inlet flow distortions, and the unsteady wakes.

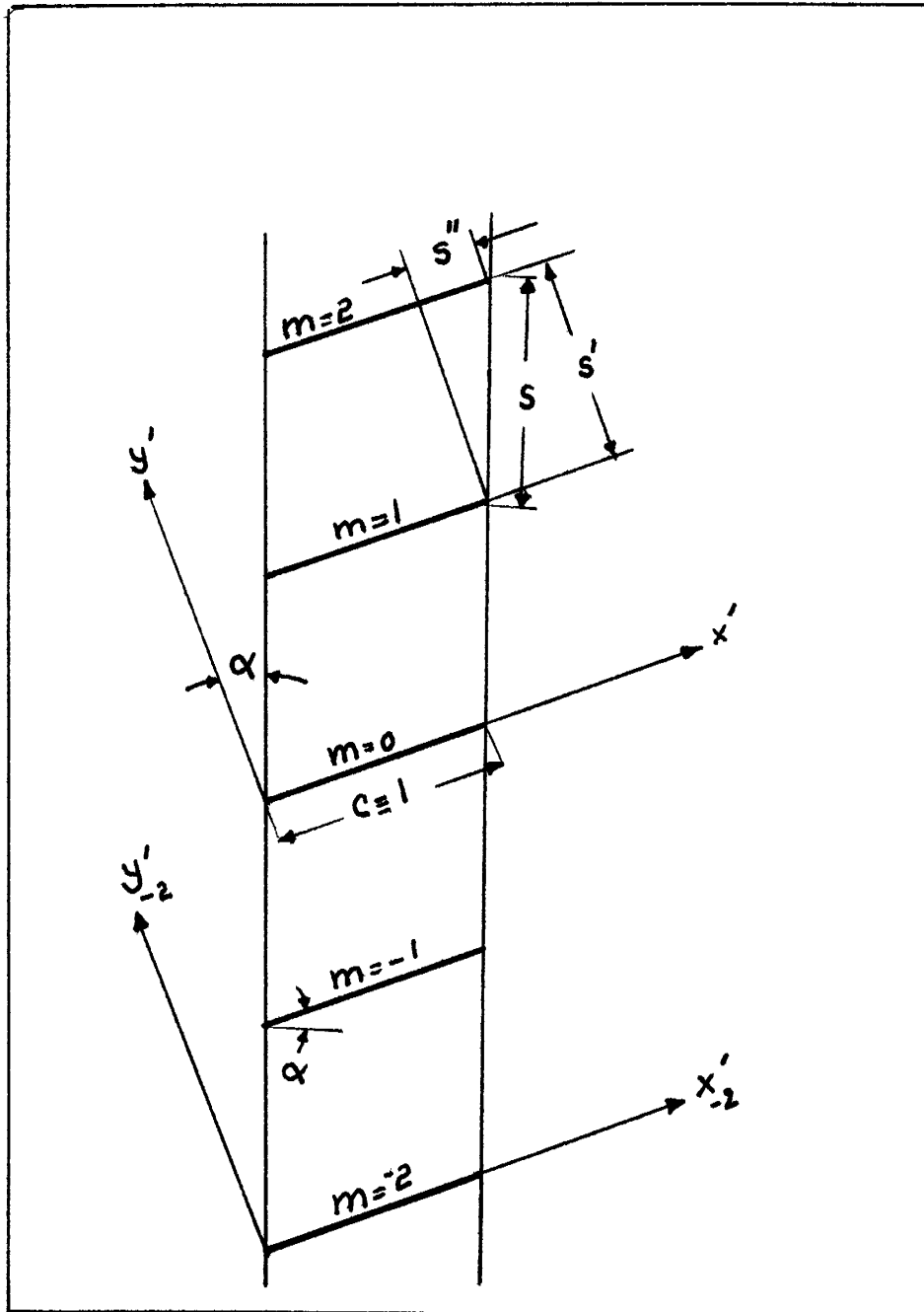


Figure 2. Cascade nomenclature and the generalized coordinates.

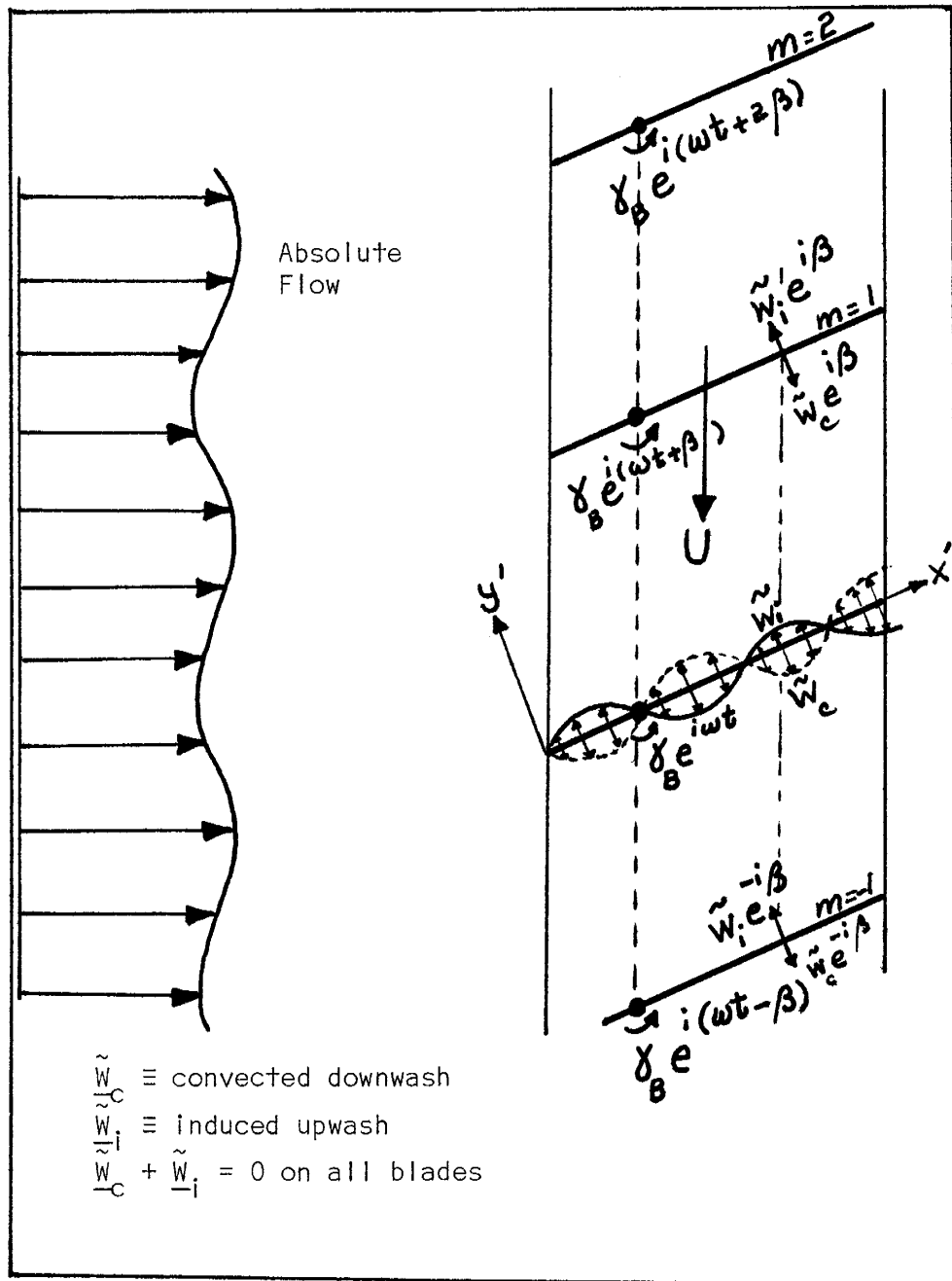


Figure 3. Schematic of the blade surface boundary condition.

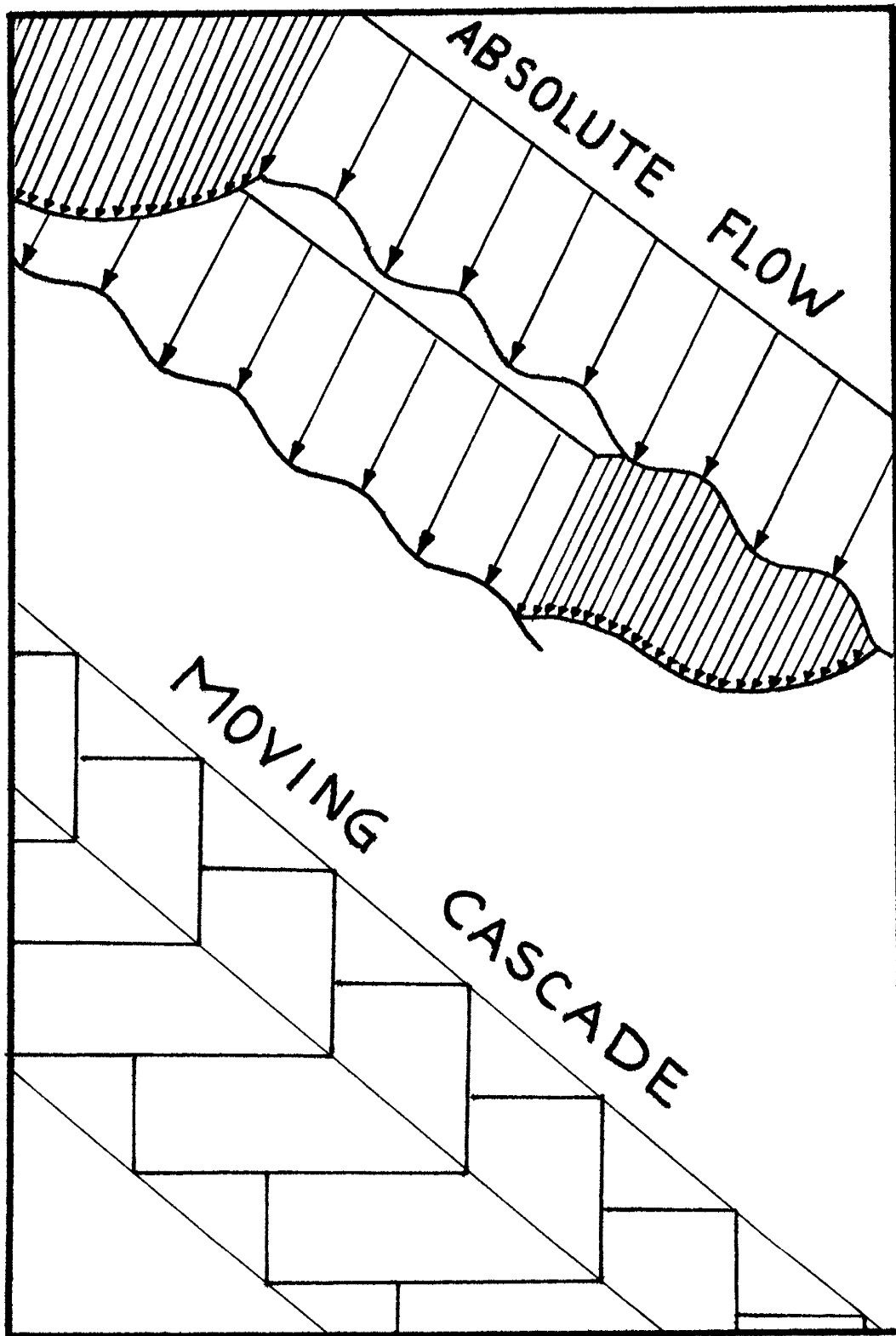


Figure 4. Three-dimensional view of inlet flow distortions and the moving cascade.

# SPANWISE SHEAR AT THE INLET

# TRAILING VORTEX FILAMENTS

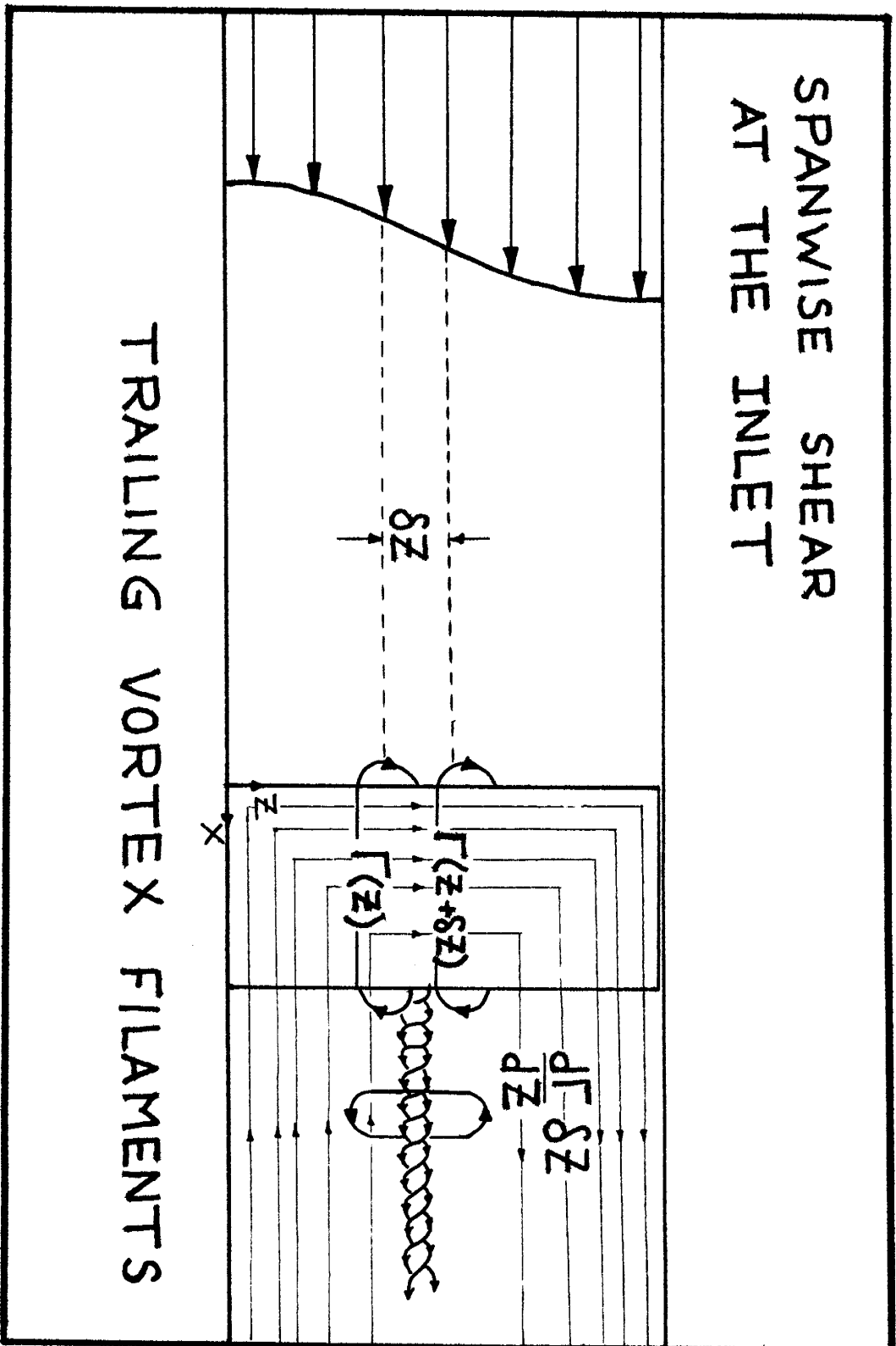


Figure 5. Interaction of a spanwise shear with a blade row, in steady flows.

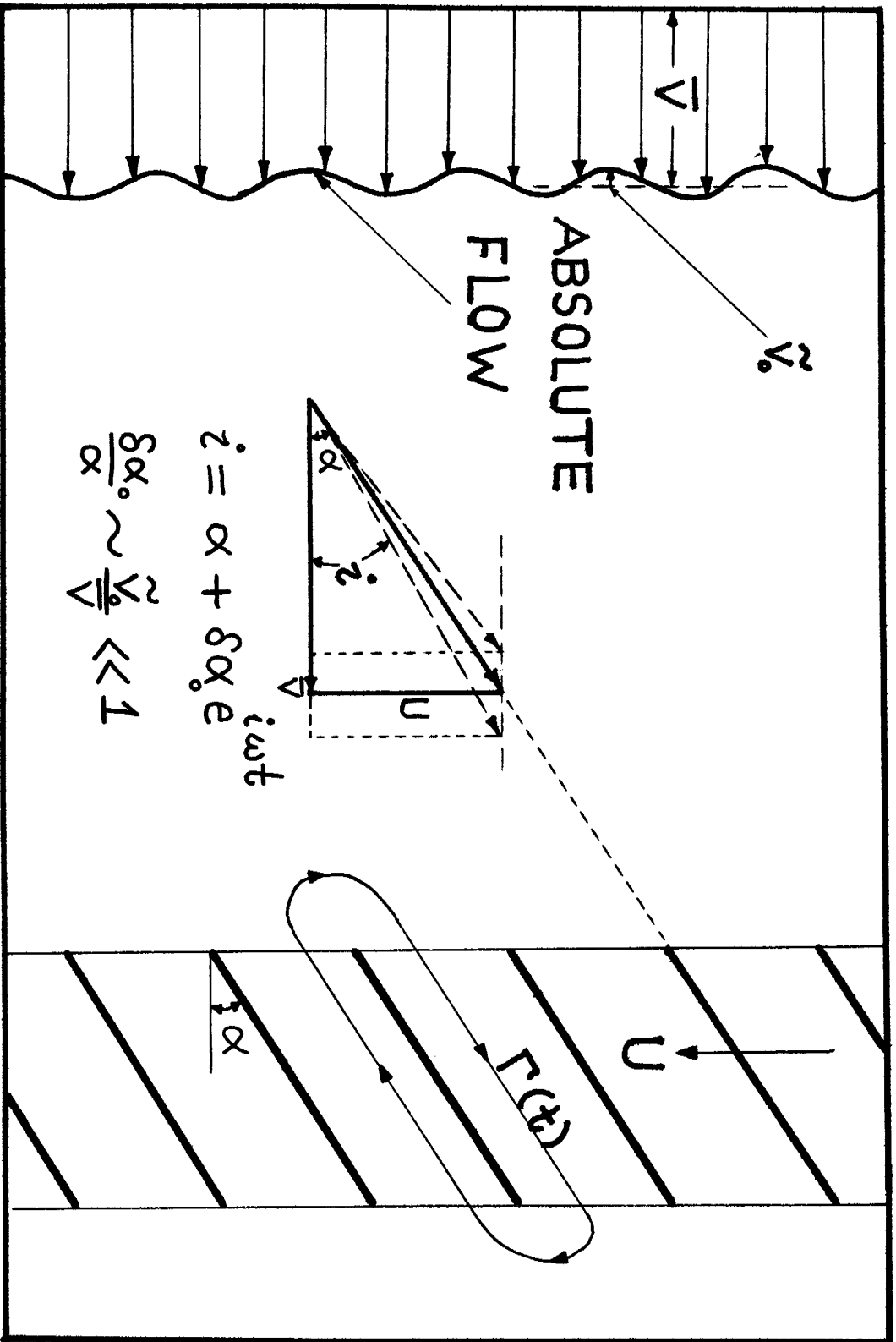


Figure 6. Interaction of pitchwise flow distortion with two-dimensional cascades.

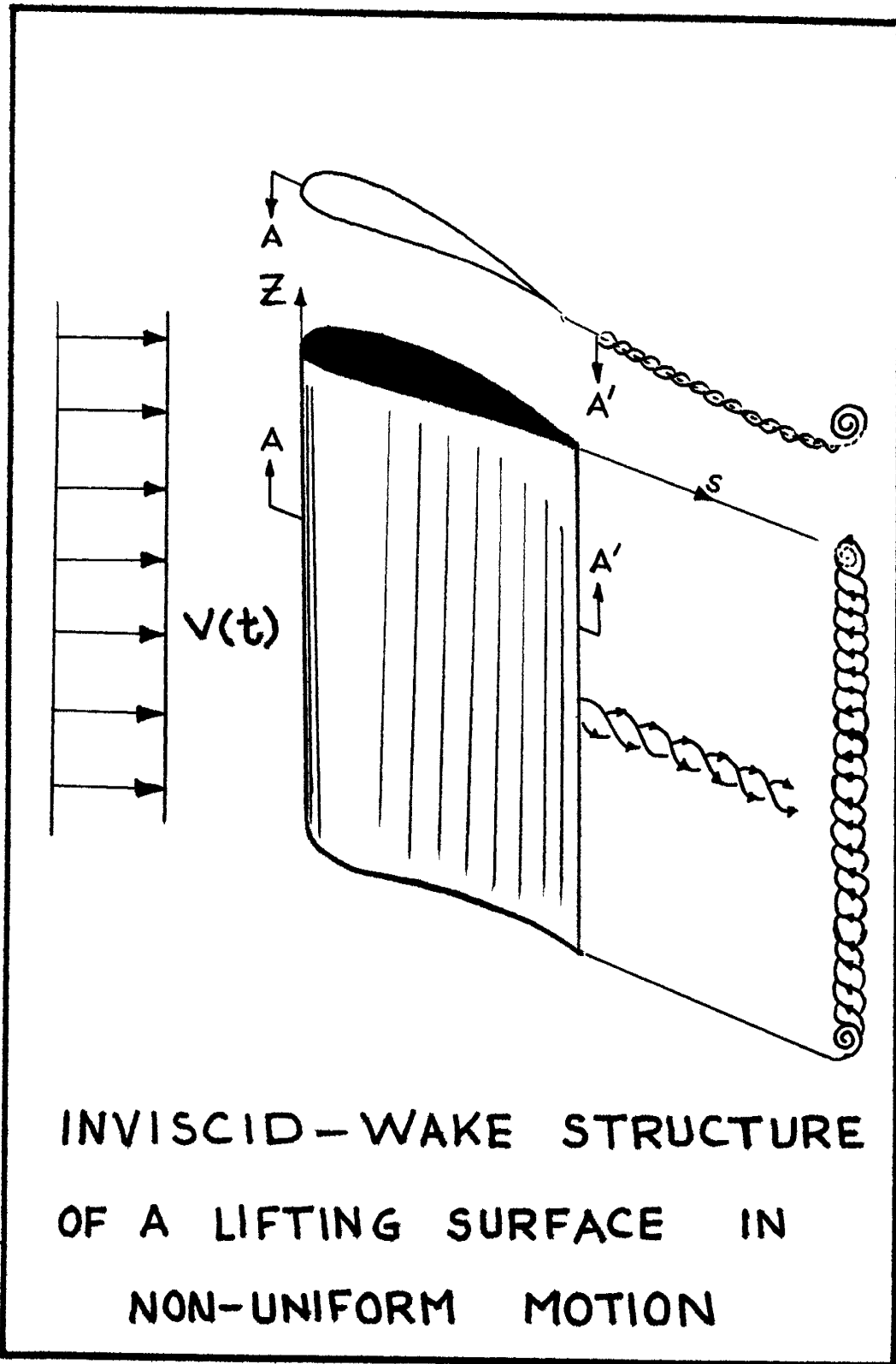


Figure 7. Schematic of inviscid wake structure downstream of a non-stationary finite wing.

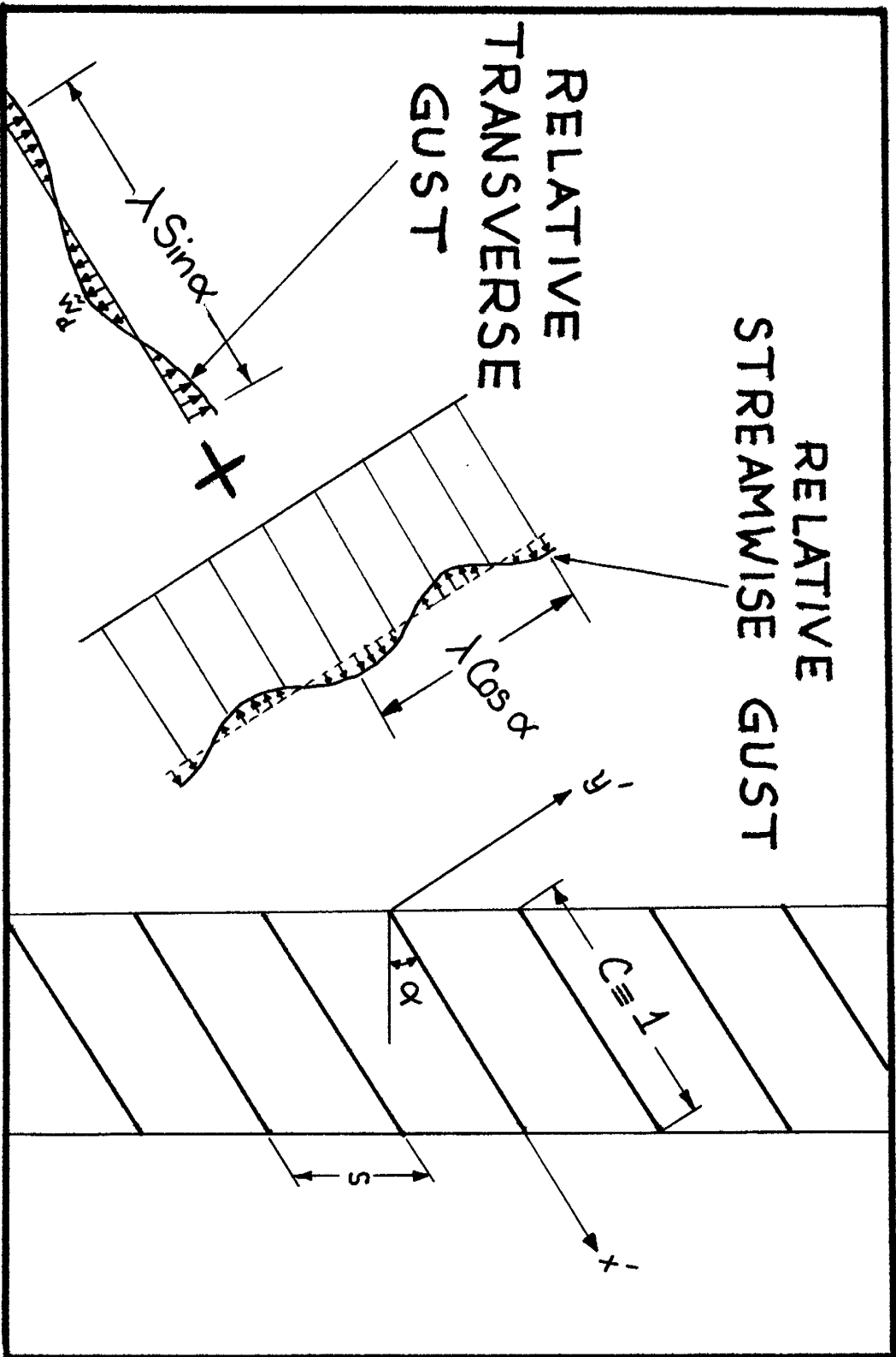


Figure 8. Decomposition of azimuthal inlet flow distortion in transverse and streamwise directions to the cascade.



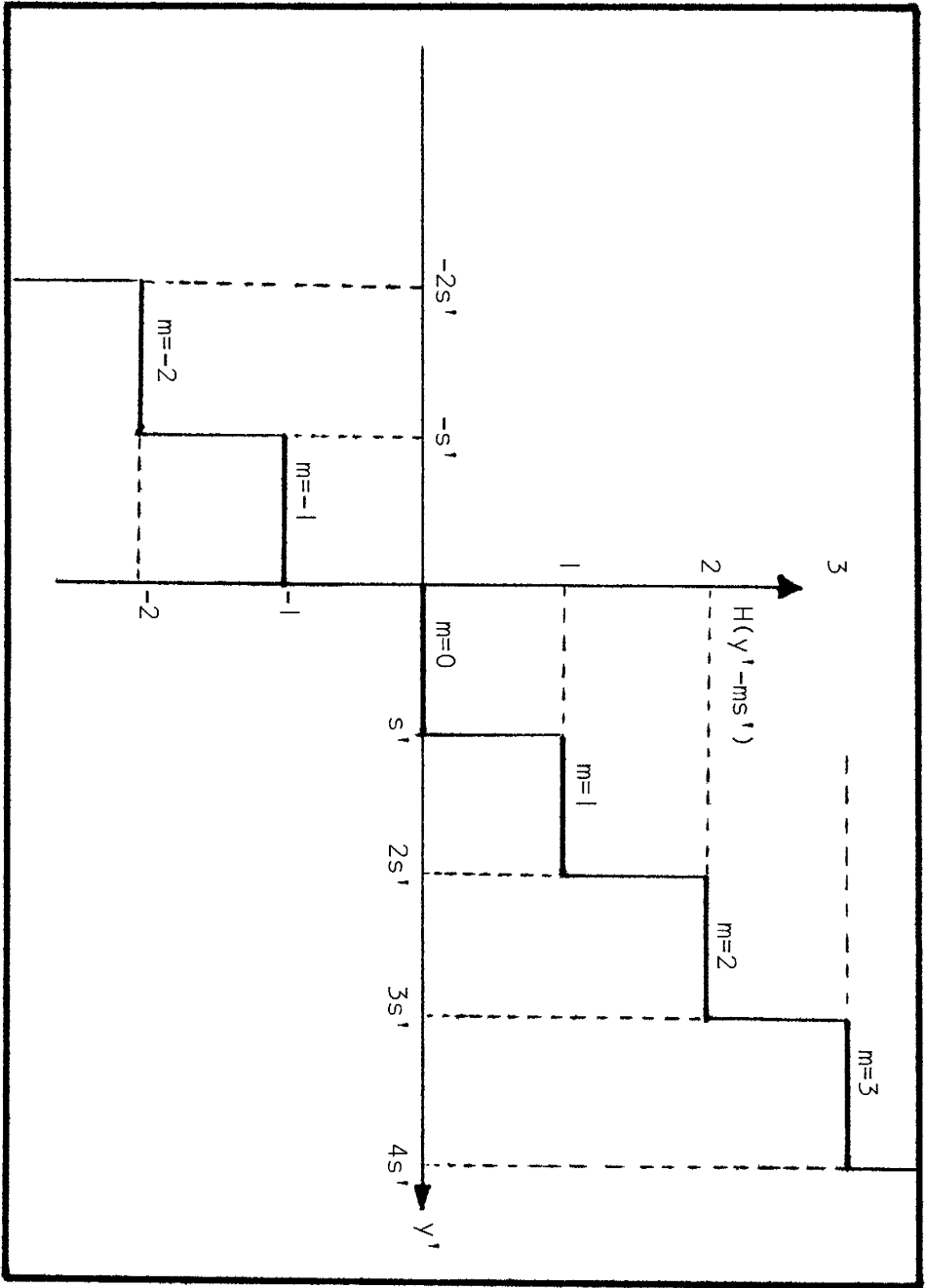


Figure 9. Heaviside Step-Function.

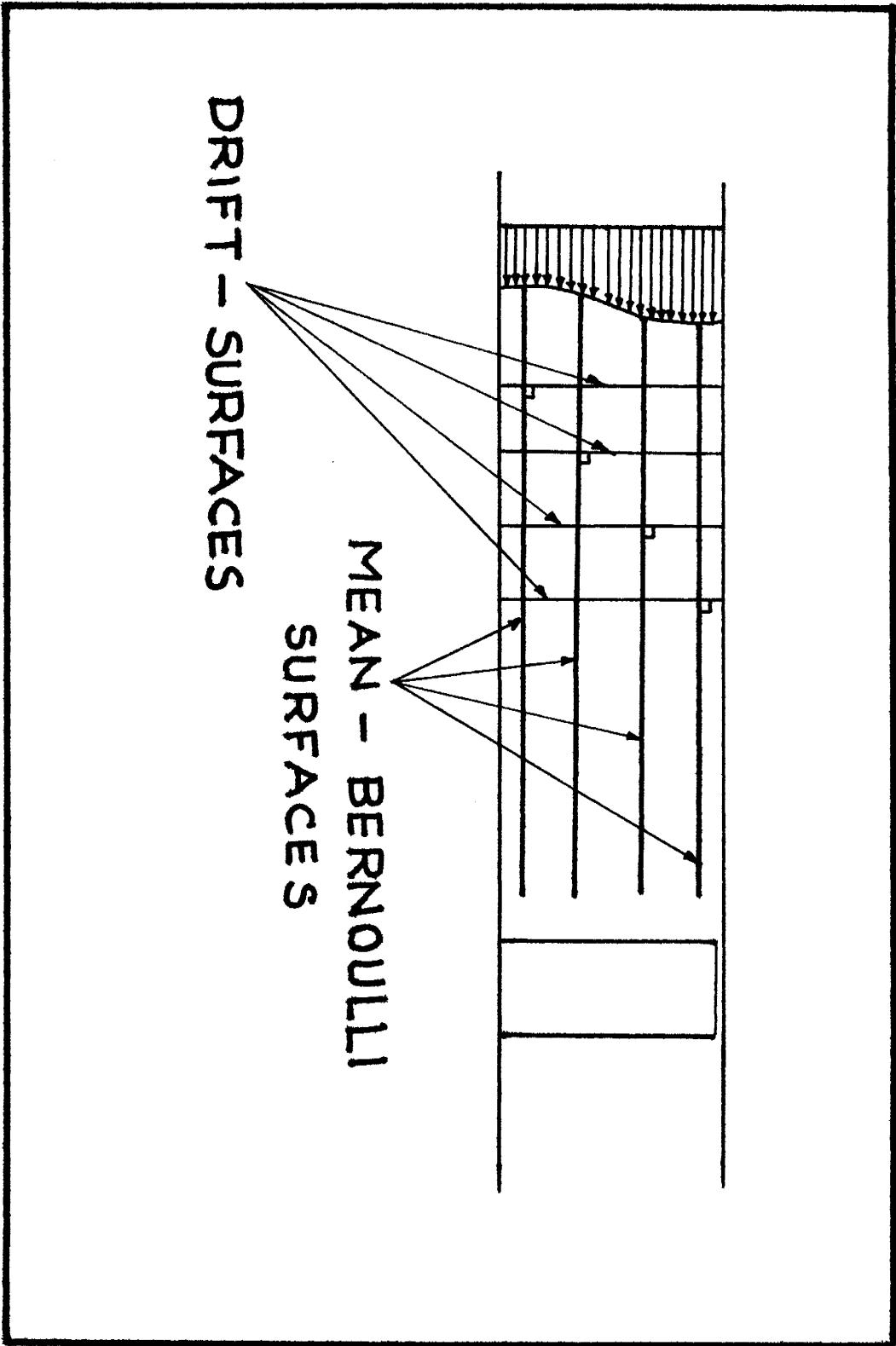


Figure 10. Schematic of drift and mean-Bernoulli surfaces upstream of the cascade.

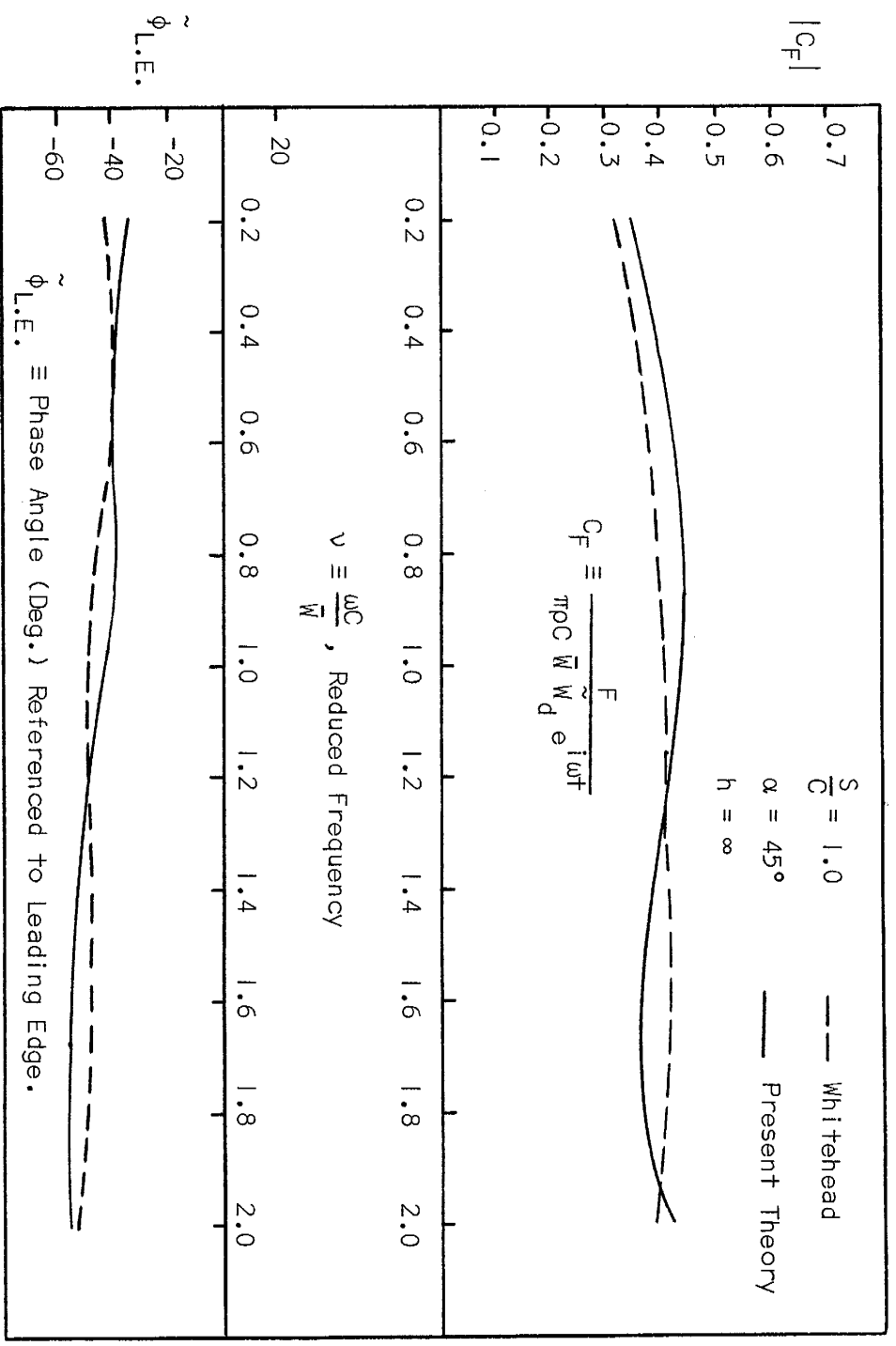


Figure 11. Comparison of predicted two-dimensional unsteady lift.

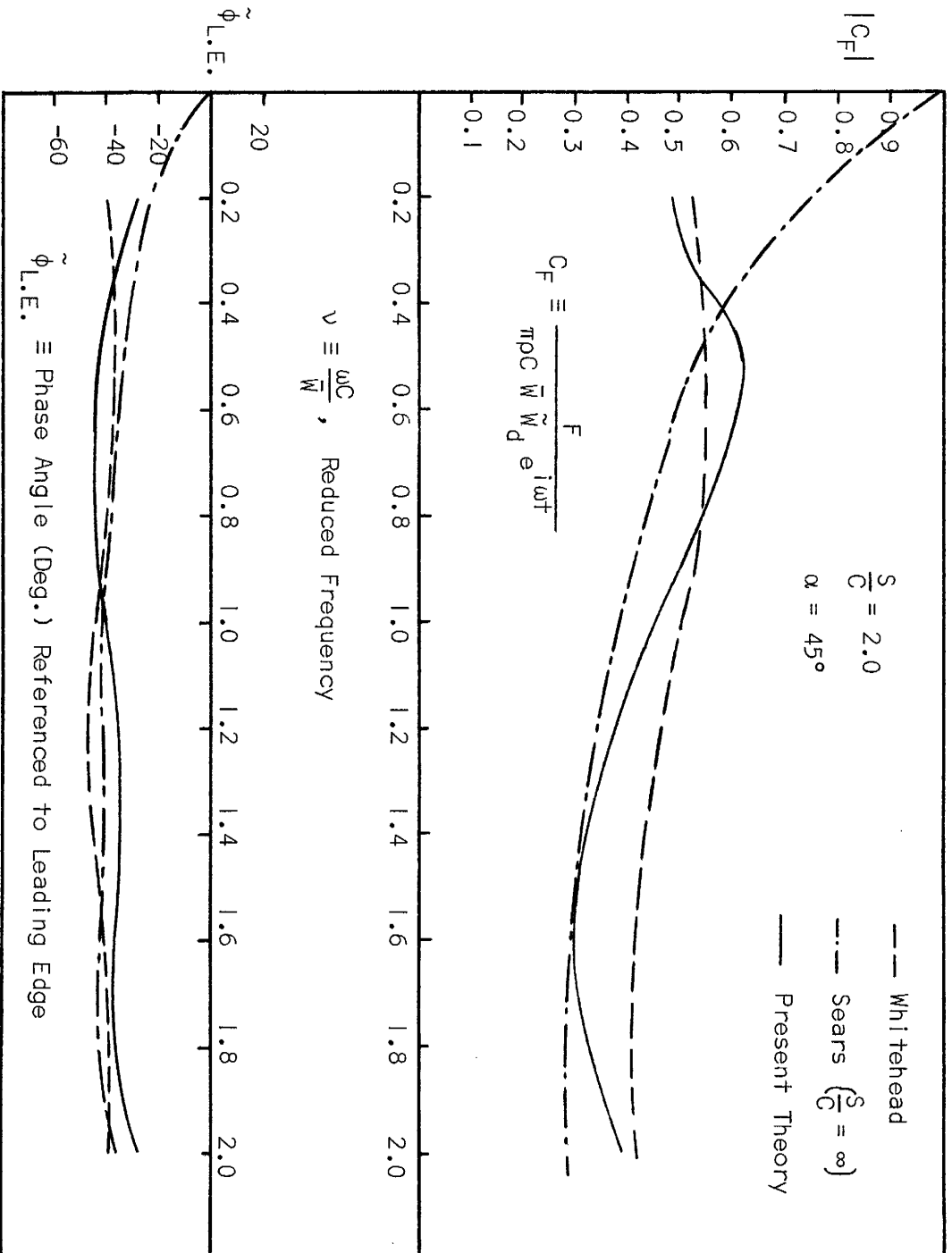


Figure 12. Comparison of predicted two-dimensional unsteady lift.

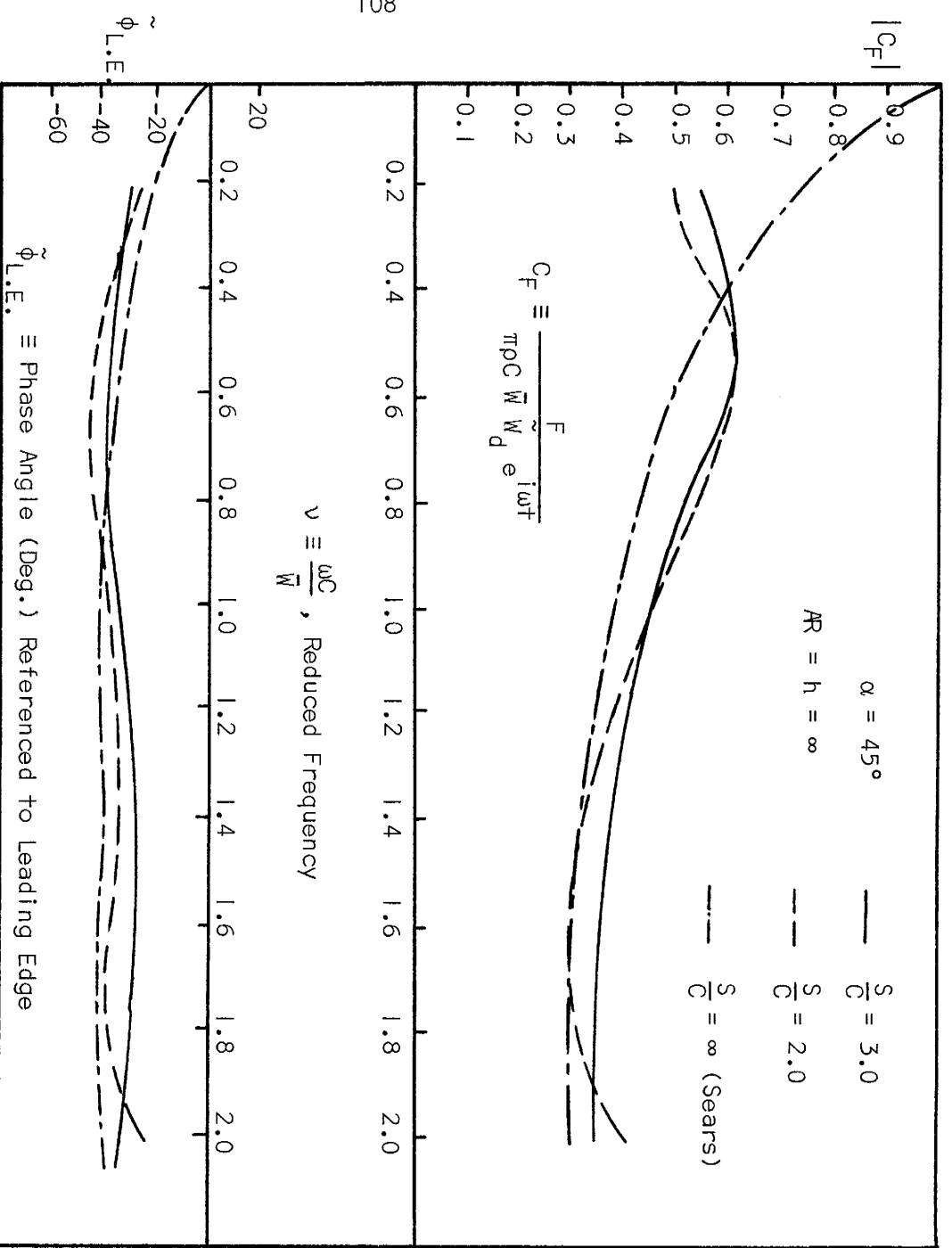


Figure 13. Comparison of predicted two-dimensional unsteady lift.

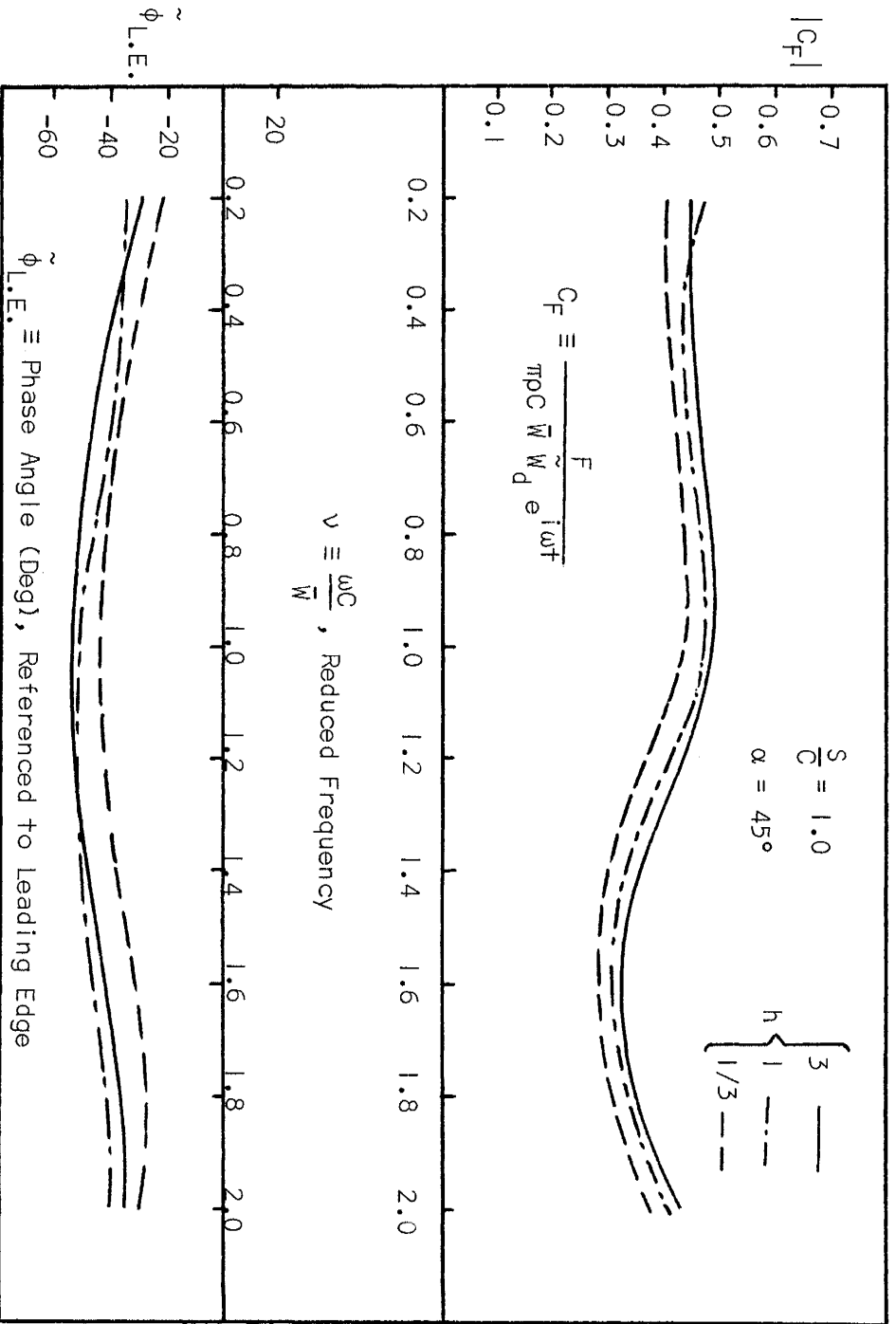


Figure 14. Comparison of predicted unsteady lift at different aspect ratios.

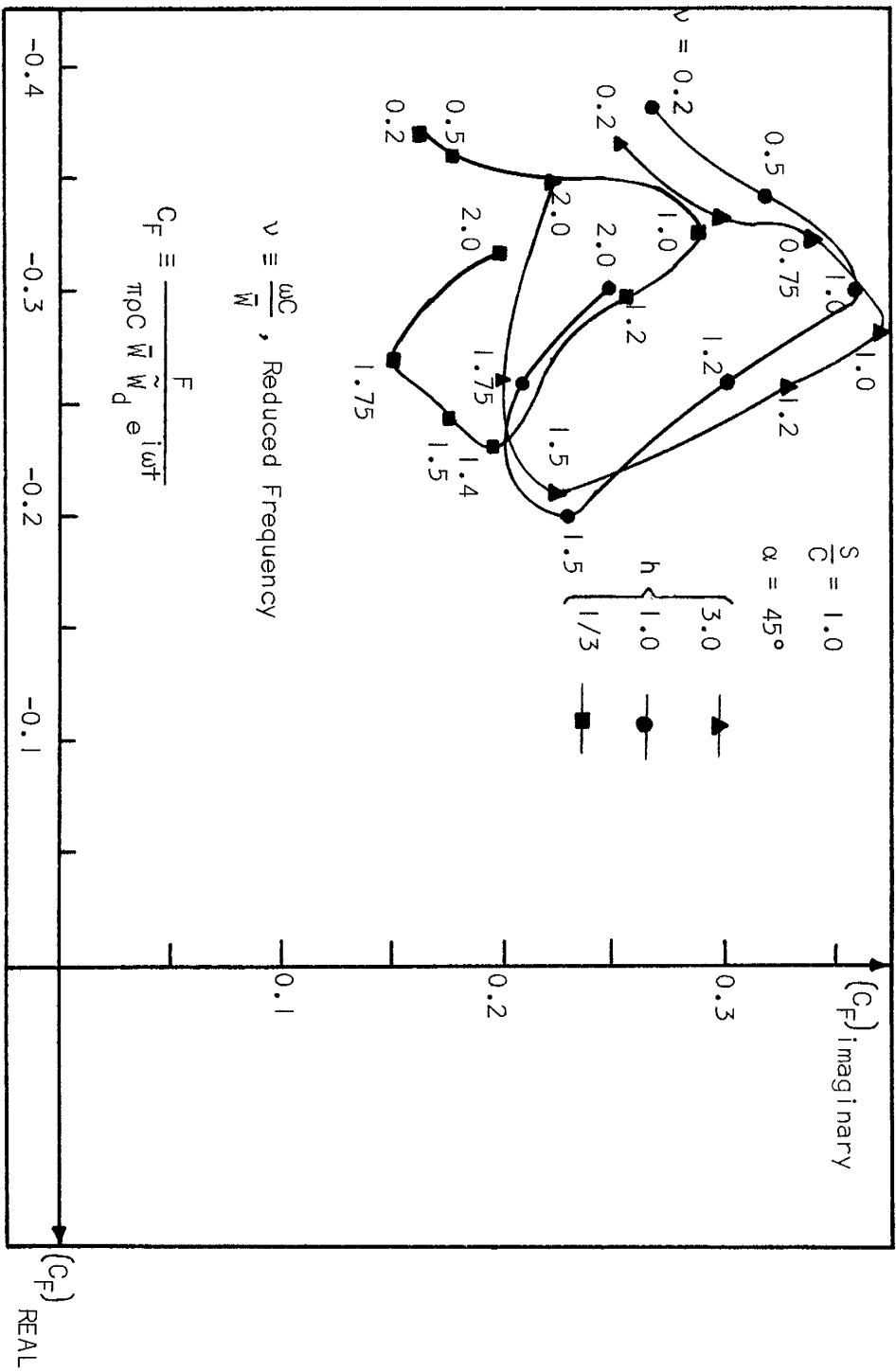


Figure 15. Phase-diagram of the unsteady blade response for different aspect ratios.

REFERENCES

1. Wagner, H., "Dynamischer Auftrieb von Tragflügeln," Zeitschr. f. Angew. Math. u. Mech., Bd. 5, page 17, 1925.
2. Glauert, H., "The Force and Moment on an Oscillating Aerofoil," British A.R.C., R&M No. 1242, 1929.
3. Theodorsen, T., "General Theory of Aerodynamic Instability and Mechanism of Flutter," NACA Tech. Rep., No. 496, 1935.
4. Küssner, H.G., "Zusammenfassender Bericht über den instationären Auftrieb von Flügeln," Luftfahrtforschung, Bd. 13, page 410, 1936.
5. von Kármán, Th., and Sears, W.R., "Airfoil Theory for Non-Uniform Motion," J. of Aero. Sci., 5, 10, pp. 379-390, August 1938.
6. Sears, W.R., "Some Aspects of Non-Stationary Airfoil Theory and its Practical Application," J. of Aero. Sci., 8, 3, pp. 104-108, Jan., 1941.
7. Kemp, N.H., and Sears, W.R., "Aerodynamic Interference Between Moving Blade Rows," J. of Aero. Sci., 20, 9, pp. 585-598, Sept., 1953.
8. Kemp, N.H., and Sears, W.R., "The Unsteady Forces Due to Viscous Wakes in Turbomachines," J. of Aero. Sci., 22, pp. 478-483, 1955.
9. Siverstein, A., Katzoff, S., and Bullivant, W.K., "Downwash and Wake Behind Plain and Flapped Airfoils," NACA Rep. 651, 1939.
10. Whitehead, D.S., "Vibration of Cascade Blades Treated by Actuator Disc Methods," Proc., Inst. of Mech. Eng., 173, 21, 1959.
11. Whitehead, D.S., "Force and Moment Coefficients for Vibrating Aerofoils in Cascade," Aero. Res. Council, R&M No. 3254, 1960.
12. Whitehead, D.S., "The Aerodynamics of Axial Compressor and Turbine Blade Vibration," Ph.D. Thesis, Cambridge University, 1957.
13. Lane, F. and Wang, C.T., "A Theoretical Investigation of the Flutter Characteristics of Compressor and Turbine Blade Systems," WADC Tech. Rep., pp. 54-499, 1954.
14. Lilley, G.M., "An Investigation of the Flexure-Torsion Flutter Characteristics of Airfoils in Cascade," Cranfield Aero. Col. Rep. No. 60, 1952.
15. Sisto, F., "Unsteady Aerodynamic Reactions on Airfoils in Cascades," J. of Aero. Sci., 22, pp. 297, 1955.



16. Eichelbrenner, E.A., "Application Numerique d'un Calcul D'Amortissement Aerodynamique des Vibrations D'Aubes de Compresseurs," *La Recherche Aeronautique*, No. 46, p. 7, 1955.
17. Horlock, J.H., "Unsteady Flow in Turbomachines," Presented at 3rd Australian Conf. on Hydraulics and Fluid Mechanics, Sidney, Australia, Nov., 1968.
18. Holmes, D.W., Private Communications, Reported by Horlock, Ref. 17 above.
19. Naumann, H., and Yeh, H., "Lift and Pressure Fluctuations of a Cambered Airfoil under Period Gusts and Applications in Turbomachinery," ASME Trans., J. of Eng. for Power, pp. 1-10, Jan., 1973.
20. Lane, F., and Friedman, M., "Theoretical Investigations of Subsonic Oscillatory Blade-Row Aerodynamics," NACA Tech. Note 4136, Feb. 1958.
21. Carta, F.O., Aerothermodynamics of Aircraft Gas Turbine Engines, Oates, Editor, Ch. 22, "Aeroelasticity and Unsteady Aerodynamics," pp. 22-1 to 22-54, 1978.
22. Bisplinghoff, R.L., Ashley, H., and Halfman, R.L., Aeroelasticity, Addison Wesley Pub. Co., Reading, MA, 1955.
23. Sears, W.R., "Contributions to the Airfoil Theory for Non-Uniform Motion," Proc. of 5th Int. Cong. on Applied Mechanics, pp. 483-487, 1938.
24. Chu, S., and Widnall, S.E., "Prediction of Unsteady Airloads for Oblique Blade-Gust Interaction in Compressible Flow," AIAA J, 12, 9, Sept. 1974.
25. Graham, J.M.R., "Lifting Surface Theory for the Problem of an Arbitrary Yawed Sinusoidal Gust Incident on a Thin Aerofoil in Incompressible Flow," Aero. Quarterly, 21, Pt. 2, pp. 182-198, May 1970.
26. Filotas, L.T., "Theory of Airfoil Response in a Gusty Atmosphere, Part I - Aerodynamic Transfer Functions," UTIAS Rep. 139, 1969.
27. Namba, M., "Three-Dimensional Analysis of Blade Force and Sound Generation for Annular Cascades in Distorted Flows," Dept. of Aero. Eng., Kyushu University, 1974.
28. Dean, R.C., "On the Necessity of Unsteady Flow in Fluid Machines," ASME, J. Basic Eng., pp. 24-28, March 1959.
29. Hawthorne, W.R., et al., "Non-Axisymmetric Flow Through and Annular Actuator Disc, Inlet Distortion Problem," ASME Paper No. 78-GT-80.

30. Temple, G., "Generalized Functions," Proc. R. Soc., pp. 175-190, 1955.
31. Lighthill, M.J., Introduction to Fourier Analysis and Generalized Functions," Cambridge Univ. Press, 1958.
32. McCune, J.E., "Three-Dimensional Inviscid Flow Through a Highly-Loaded Transonic Compressor Rotor," MIT GTL Rep. No. 126, Feb. 1976.
33. Chen, L.T., and McCune, J.E., "Comparison of Three-Dimensional Quasi-Linear Large Swirl Theory with Measured Outflow from a High-Work Compressor Rotor," MIT Gas Turbine Lab Rep. No. 128, Sept., 1975.
34. McCune, J.E., and Hawthorne, W.R., "The Effect of Trailing Vorticity on the Flow Through Highly Loaded Cascades," J. of Flu. Mech., 74, Part 4, pp. 721-740, 1976.
35. Tan, Choon Sooi, "Three-Dimensional Vorticity-Induced Flow Effects in Highly-Loaded Axial Compressors," Part I, and "Asymmetric Inlet Flows Through Axial Compressors," Part II, Ph.D. Thesis, MIT, 1978.
36. Adebayo, A.O., "Three-Dimensional Beltrami Flow Through a Highly-Loaded Axial Compressor Rotor Inducing Arbitrary Swirl," Ph.D. Thesis, MIT, 1978.
37. Cheng, W.K., "Uniform Inlet Three-Dimensional Transonic Beltrami Flow Through a Ducted Fan," MIT, GTL Rep. No. 130, May 1977.
38. Hawthorne, W.R., "Flow Through Moving Cascades of Lifting Lines with Fluctuating Lift," J. of Mech. Eng. Sci., 15, 1, 1973.
39. Darwin, C., "Note on Hydrodynamics," Proc. Cambridge Phil. Soc., 49 pp. 242-254, 1953.
40. Lighthill, M.J., "Drift," J. Flu. Mech., 1, pp. 31-53, 1956; note also "Corregenda to Drift," J. Flu. Mech., 2, pp. 311-312, 1957.
41. Hawthorne, W.R., "On the Theory of Shear Flow," MIT GTL Rep. No. 88, 1966.
42. Greitzer, E.M., Private Communication.
43. Horlock, J.H., et al., "The Response of Turbomachine Blades to Low Frequency Inlet Distortions," Trans. ASME J. Eng. for Power, 99, 2, pp. 195-203, 1977.
44. Kerrebrock, J.L., Private Communication.
45. Mikolajczak, A.A., "The Practical Importance of Unsteady Flows," Proc. AGARD Conf. on Unsteady Phenomena in Turbomachinery, Sept. 1975.

46. Kerrebrock, J.L., "Small Disturbances in Turbomachine Annuli with Swirl," AIAA J., 15, 6, pp. 794-803, June 1977; also MIT GTL Rep. No. 125, 1975.
47. Lamb, H., Hydrodynamics, 6th Ed., Cambridge University Press, 1932.
48. Hawthorne, W.R., "Engineering Aspects," Ch. 1, Research Frontiers in Fluid Dynamics, R.T. Seeger and G. Temple Eds, Interscience, NY, 1965.